Borders in the developing avian diencephalon.

Larsen, Camilla

BORDERS IN THE DEVELOPING AVIAN DIENCEPHALON

Camilla Larsen

Thesis for the degree of Doctor of Philosophy

Department of Developmental Neurobiology
King's College

ABSTRACT

The vertebrate diencephalon is composed of three functionally distinct regions, the synencephalon, the dorsal thalamus and the ventral thalamus. The embryonic diencephalon is believed to be patterned through the progressive subdivision into neuromeres (Bergquist and Kallen, 1954; Vaage, 1969; Keyser, 1972) that are segmentally arranged (Rubenstein et al., 1994, Figdor and Stern, 1993). However the number and sequence of neuromeric subdivision is a subject of disagreement in the literature. Based on morphology, gene expression, the appearance of a boundary specific phenotype and cell lineage restriction, results presented in this thesis show that the avian diencephalon becomes progressively subdivided into four distinct domains.

This involves the division of the diencephalon into the synencephalon and the parencephalon at HH 16. The synencephalon exhibit true neuromeric morphology and this is associated with neuromeric specific gene expression and the appearance of a boundary specific phenotype. Whereas these persist in the midbrain-synencephalic boundary, along with cell lineage restriction, they are transient at the synencephalic-parencephalic boundary, which does not exhibit cell lineage restriction. The physical subdivision of the parencephalon into the ventral and dorsal thalamus from HH 19 is linked with the formation of the interparencephalic boundary, the zli. This is correlated with the appearance of a boundary specific phenotype within the zli and initiation of expression of *Gbx2* and *Dlx2*.

The zli is formed from a broad "wedge" shaped compartment characterized by the absence of *Lunatic Fringe* (*L-fng*) expression. This compartment narrows from HH 12 to HH 19 and corresponds to the zli. At HH 22 the synencephalon becomes divided into two domains, distinguished by differential gene expression and tissue morphology. This subdivision is not associated with boundary formation or cell lineage restriction. Together these results indicate that the diencephalon becomes patterned through the progressive formation of separate domains, which generate distinct patterning units.

Acknowledgement

I would like to thank Prof. Andrew Lumsden for giving me the opportunity to work in his lab and for the financial support, which has allowed me to do this PhD. I would also like to thank Luis Puelles for inviting me to his lab and teaching me diencephalic neuroanatomy.

I am grateful to Dr Lori Zeltser for her day to day supervision, and to Dr Stefan Jungbluth for all his help. I would also like to thank the entire Lumsden Lab for their support.

Finally I thank my parents and Steve Hayes for their support and love.

Table of Contents

Table of Figures

CHAPTER I

Introduction

" Segmentation is serial repetition of embryonic rudiments in successive levels of regular spacing"

Rugh (1948)

The vertebrate central nervous system (CNS) is a highly complex structure composed of a large number of different cell types that connect distant regions and integrate information from the entire body. During embryogenesis, the spatial and temporal development of neuronal phenotypes must be tightly coordinated in order to generate functional neuronal networks. The embryonic diencephalon forms inter alia the adult thalamus, the main integration centre of the brain. Although it has been studied for more than a century, the complexity of the diencephalon and its physical inaccessibility during development is matched by the lack of information concerning the mechanisms regulating its formation. I have analysed the developing avian diencephalon using a combination of histological, cellular and molecular techniques. The chick system is ideal for these approaches because the embryo is accessible throughout development, allowing in vivo manipulation following long-term survival.

1.1 Pattern Formation

1.1.1 Chick Development.

The embryonic chick brain begins as a neural plate, which starts to fold into a hollow tube at HH8 (Hamburger and Hamilton, 1951). Within the enlargement of the cephalic portion three primary vesicles are formed, corresponding to the primordia of the major brain regions. The most posterior vesicle is that of the hindbrain or rhombencephalon, which develops into the isthmus, pons and medulla. The midbrain, or mesencephalic vesicle, is situated anterior to the hindbrain and develops into the optic tectum, tecmentum and associated structures. The most anterior vesicle is that of the forebrain

or prosencephalon, which is later subdivided into the secondary prosencephalon and diencephalon. The secondary prosencephalon includes telencephalic structures such as the striatum and ectostriatum, as well as the basal ganglia and hypothalamus, whereas the diencephalon primarily forms the thalamus, epithalamus and pretectum. The mesodermally derived notochord lies ventral to the ectodermally derived neural tube from its most posterior point and ends anteriorly beneath the diencephalon. The area overlying the notochord is called epichordal whereas the remainder of the anterior neural tube is considered prechordal.

The first neuromeres can be distinguished within the primary brain vesicles at approximately HH9. Neuromeres were first described by Von Baer (1828) and appear externally as bulges of neuroepithelium delineated by grooves, and internally as troughs delineated by ridges. These are most clearly marked within the hindbrain where subdivision into eight neuromeres is crucial to patterning in the region.(Lumsden and Keynes, 1989) In contrast, the mesencephalic vesicle is not further subdivided during development. Within the prosencephalon, subdivision into the secondary prosencephalon and diencephalon marks the formation of the first two neuromeres, termed prosomeres, which are further divided as development proceeds. The precise prosomeric boundaries and their role in regionalisation of the forebrain have been debated for over a century.

In understanding the events involved in patterning the vertebrate body, considerable attention has been directed towards invertebrate systems, such as *Drosophila melanogaster*. The extensive array of genetic tools developed for the *Drosophila* system has facilitated the elucidation of numerous molecular pathways involved in patterning.

1.1.2 Segmentation of *Drosophila*

During *Drosophila* development, cell fates are determined according to their position along the anterior-posterior (A-P) axis and morphogenic signals secreted from organising centres. Positional information is provided by complex interactions between segmentation genes and homeotic genes, which progressively divide the larva into fields of non-mixing cell populations that are then independently determined to form the structures of the adult fly. In *Drosophila*, cells are initially allocated into fourteen

patterning units termed parasegments that are out of phase with the morphological constrictions of the adult segments. Thus, a particular segment contains the anterior and posterior parts of neighboring parasegments (Garcia-Bellido and Moscoso del Pradio, 1979).

The allocation of cells into parasegments is directed by the alternating expression of the pair-rule genes even-skipped (*eve*) and fushi tarazu (*ftz*) in stripes along the A-P axis, with each band of expression corresponding to a parasegment (Small et al., 1991; Stanojevic et al., 1989). *Eve* and *ftz* in turn activate the transcription of the segment polarity gene *engrailed* (*en*) at the anterior margin of each stripe, so that each parasegment contains a band of *en*-expressing and non expressing cells (Martinez-Arias and Lawrence, 1985)(see figure 1A). Single cell labeling has shown that *en* positive cells and their clonal descendents are unable to mix with *en* negative cells, and therefore each parasegment is divided into an anterior and posterior compartment. This lack of cell mixing is probably the result of differential affinities, which cause cells with similar surface properties to preferentially adhere and sort out from those with different properties (Lawrence and Struhl, 1996). The larva is considered a segmented structure because of the repeated pattern of *eve* and *ftz* and *en* expression in the anterior and posterior compartments of each parasegment.

Diversification of each parasegment is primarily controlled by the action of homeotic genes belonging to the HOM-C complex (see figure 1A). The anterior limit of expression of each gene is fixed at a different parasegmental boundary along the A-P axis and specification of each parasegment is controlled by the interaction between the homeotic genes expressed at a particular position (Lawrence and Morata, 1994). Both the A-P patterning function and genomic organisation of homeotic genes has been conserved in the vertebrate Hox genes. Cell fates are not only determined according to which parasegment they belong, but also by positional information within the parasegment itself. *en* expressing cells produce a short-range inducer called hedgehog (hh), which diffuses across the parasegmental boundary and activates the expression of *wingless* (wg) in *en* negative cells immediately anterior to the boundary (Ingham, 1993). Wg is likely a long-range morphogen, which diffuses through the neighbouring anterior and posterior compartments to establish a morphogenic gradient (see figure 1B). The parasegmental boundary is thus a signaling centre, which provides information to the

cells about their position within the parasegment. Responding cells then have the ability to assess the direction and slope of the morphogen gradient.

Signaling centres play an important role in patterning the *Drosophila* imaginal disc, but unlike the parasegment, the disc is not segmented but composed of an anterior and posterior compartment. As for the situation in the parasegments, the posterior compartment expresses *en,* whereas cells within the anterior compartment do not. hh is similarly produced by *en* expressing cells and acts as a short-range inducer (Tabata et al., 1992), diffusing across the boundary into the anterior compartment. In the anterior compartment, hh will activate the expression of decapentaplegic (dpp), a member of the transforming growth factor β family (Basler and Struhl, 1994; Tabata and Kornberg, 1994), which acts as a long-range morphogen (Zecca et al., 1995).

Drosophila research has yielded several fundamental principles in development that have been conserved throughout evolution. First, the allocation of cells into compartments ensures that a group of cells are unable to mix with their neighbours, and therefore stay together during subsequent patterning events. This allows a unit of cells to be locally modified differently from the neighboring group of cells, and provides an opportunity for signaling molecules to be used in different scenarios within different compartments. Second, the reiterated or segmental organisation of compartments enables the efficient use of basic signaling mechanisms to simultaneously provide similar information at multiple sites. This minimizes the number of essential genes needed for proper development and thus promotes evolutionary diversity. Third, signaling centres that pattern adjacent tissues through long-range morphogens, provide positional information to compartments that have their A-P identity determined by Hox gene. Thus the sequence of events that seems to be essential for generating an adult fly is first to generated compartments so that individual groups of cells stay together to make a particular part of the body. Once a cell belongs to a compartment it will be informed by the expression of homeotic genes what part of the body the compartment will generate, for instance an abdominal segment. Finally positional signals within the compartment will influence the type of abdominal structure formed.

Both signaling centres and segmentation play important roles in regionalisation of the vertebrate embryo as well. The role of organisers in patterning along the D-V axis of the

CNS is well documented, but is beyond the scope of this discussion. The best-studied example of segmentation in the vertebrate is in the hindbrain, whereas organising centres likely provide most of the patterning information in the telencephalon and mesencephalon.

1.1.3 Segmentation of the Hindbrain

Neuronal nuclei in the adult hindbrain are organised in a columnar fashion (Marin and Puelles, 1995), whereas the developing hindbrain is divided into a series of transverse neuromeres, termed rhombomeres (Lumsden and Keynes 1989). The neuromeric subdivision is gradual, initiated at HH 9- by the formation of the boundary between rhombomeres 5 and 6 and ultimately divides the hindbrain into eight rhombomeres by HH 12. Fraser *et al.* (Fraser et al., 1990) have shown that rhombomeres are units of cell lineage restriction. Thus, clonal descendants of a cell injected with fluorescent dye before boundary formation were found in two adjoining rhombomeres, whereas labeling after boundary formation resulted in clonal descendents being confined to a single rhombomere. These clones were often aligned along the rhombomere boundary, spreading laterally along the boundary without crossing into the neighboring compartment. Furthermore they were able to mix with non-labeled cells, which indicates that cells can mingle within the neuroepithelium. Interestingly the lack of cell mixing persists until at least E5, after rhombomere morphology has disappeared and only postmitotic cells spread into adjacent territories within the marginal zones (Wingate and Lumsden, 1996).

An intrinsic immiscibility between rhombomeres underlies the lack of cell mixing, so that cells from an even numbered rhombomere sort out from cells from an odd numbered rhombomere. This has been demonstrated in studies where cells from an even/odd rhombomere transplanted next to a like rhombomere will mix with this cell population. Cells from an odd rhombomere grafted next to an even rhombomere, however, will not mix with the neighboring cell population, and vice versa. Similar results are also seen when only small pieces of tissue from odd numbered rhombomeres are grafted in an even numbered one and vice versa (Guthrie et al., 1993). Furthermore, when rhombomere boundaries are ablated a new boundary often regenerates (Guthrie and Lumsden, 1991). Cell aggregation cultures have shown that cells from odd

Figure 1

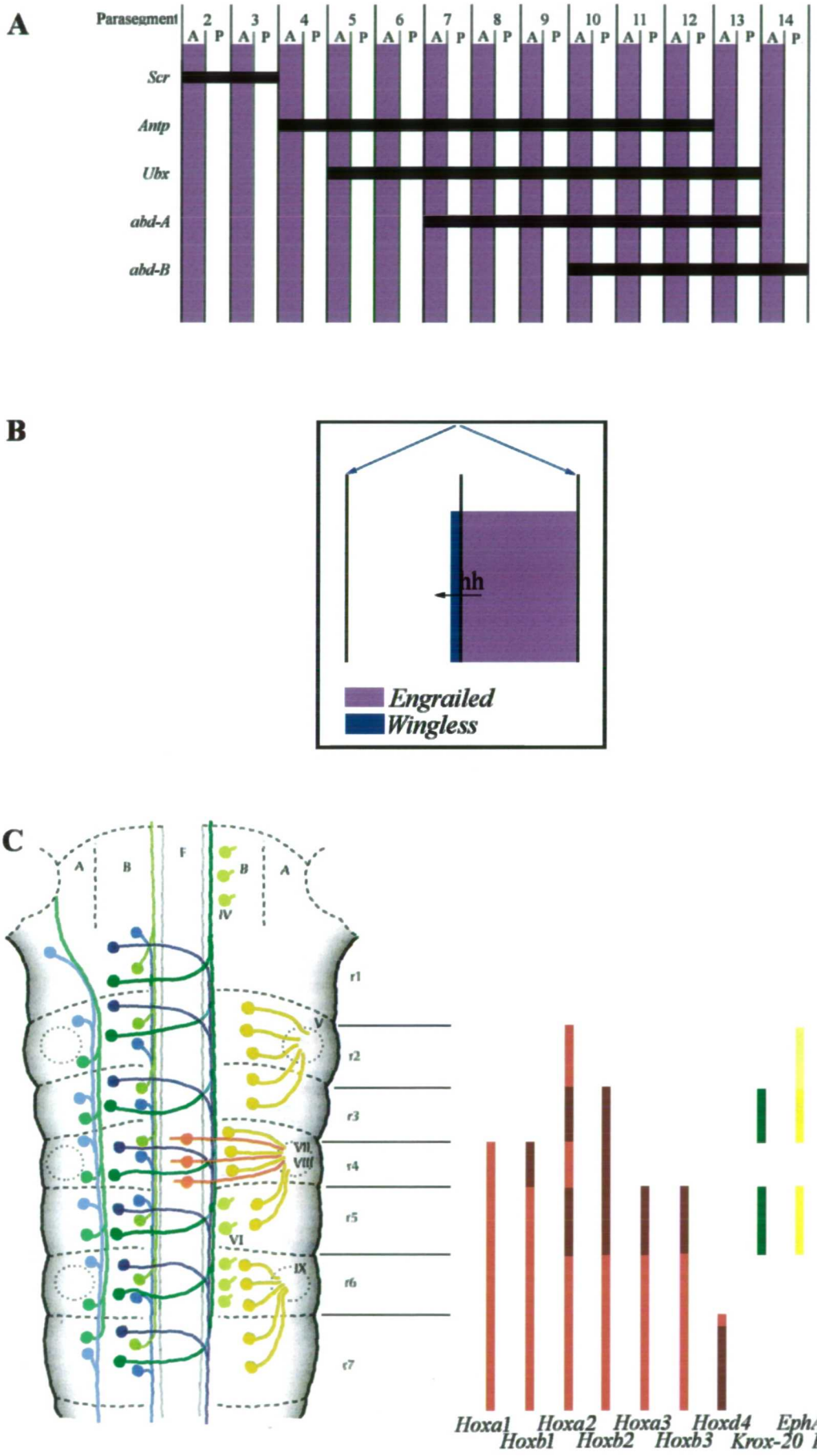
A
Parasegment
2 3 4 5 6 7 8 9 10 11 12 13 14
A P
Scr
Antp
Ubx
abd-A
abd-B
B
hh
Engrailed
Wingless
C
A
B
F
B
A
IV
V
VII
VIII
VI
IX
r1
r2
r3
r4
r5
r6
r7
Hoxa1
Hoxb1
Hoxa2
Hoxb2
Hoxa3
Hoxb3
Hoxd4
Krox-20
EphA4
EphB3
EphrinB2

rhombomeres segregate from cells from even rhombomeres, whereas cells from an even rhombomere mix with cells from other even numbered rhombomeres (Wizenmann and Lumsden, 1997).

Rhombomeres are thus similar to *Drosophila* parasegments in that they are a series of compartments with alternating cell affinities, but genes homologous to the pair rule genes have not been identified in the vertebrate hindbrain. However, the zinc-finger gene *Krox-20* may have a similar function to the pair-rule genes and is expressed in the prospective rhombomere 3/5 territory well before rhombomere morphology appears (Wilkinson et al., 1989). It regulates Hox gene expression in r3/5 *in vivo* and *in vitro* (Schneider Maunoury et al., 1993; Sham et al., 1993). The inability of cells to mix is likely regulated by a set of Eph-like receptor tyrosine kinases and their ligands, which are expressed in a complimentary manner in alternating rhombomeres (see figure 1C). Expression of a dominant negative form of one of these receptors *Sek1,* leads to expansion of *Krox-20* expression, probably because of the loss of inter-rhombomeric boundaries (Xu et al., 1995; Xu et al., 1999). This suggests that these molecules may convey the differential adhesion properties of rhombomeres.

Another similarity to *Drosophila* is that the hindbrain neuromeric compartments are segmented. However, in the hindbrain two different types of compartments are repeated in an alternating manner, generating a pattern of two-segment periodicity. This is confirmed on a neuronal level with the differentiation of both reticular and motor neurons. Reticular neurons initially appear at HH11-12 within even-numbered rhombomeres, whereas differentiation is not initiated in the odd-numbered rhombomeres until a stage later. Nuclear groups of motor neurons are formed by pairs of rhombomeres, but differentiation is initiated in even-numbered rhombomeres, which also contain the exit point for the nerve root (Lumsden and keynes 1989)(see figure 1C).

The two-segment periodicity is also seen at a molecular level, notably by the expression of the vertebrate homologues of the *Drosophila* Hox genes. Within the hindbrain, the anterior limits of anterior Hox genes generally correlate with rhombomere boundaries with a two-segment repeat (Wilkinson et al., 1989)(see figure 1C). An exemption to this rule is *Hoxb1*, which is expressed only in rhombomere 4, and *Hoxb2* with an anterior

expression limit at the r2/r3 boundary. Furthermore *Hoxa2*, which is expressed up to r1/r2 boundary, has increased expression in r3 and r5. Like its *Drosophila* counterpart, the Hox complex is involved in the specification of segment identity in vertebrates (Bell et al., 1999; Krumlauf et al., 1993).

Based on his extensive studies of hindbrain segmentation, Andrew Lumsden proposed four sets of criteria that a structure must meet to be considered segmented. First, the physical organisation of the segments should correspond to an underlying reiterated pattern of cellular and molecular differentiation. Second, subdivision must either be preceded by or produce a segmental pattern of cellular differentiation. Third, the segments should be units of cell lineage restriction. Finally, the expression of developmental genes should correspond to the segmental pattern.

Segment-polarity genes or A-P organising activities have not been identified in the hindbrain and the rhombomere boundaries are therefore probably not involved in setting up positional information. However, they may have acquired another function, which is guiding axons within the hindbrain neuroepithelium, and this function is accompanied by a change in phenotype of boundary cells.

1.1.4 Rhombomere Boundaries

Rhombomere boundaries are structurally quite different from the rhombomeres themselves and may represent a third type of cell population in the hindbrain. The first indication that cells within rhombomere boundaries are different is seen as early as HH 10, when their interkinetic nuclear migration is disrupted. Cells within the neuroepithelium normally divide at the ventricular surface followed by extension towards the pial surface, leaving end feet attached within the inner limiting membrane. After cells have extended to the pial surface, they enter S-phase and during G_2 retreat their pial end foot again as they round up towards the ventricular surface for another cell division. Bromodeoxyuridine (BrDU) pulse labeling has, however, shown that boundary cells enter S-phase while they are close to the ventricular surface, which could suggest that boundary cells remain at the ventricular surface throughout the entire cell cycle (Guthrie et al., 1991).

Shortly after neurogenesis is initiated the boundaries becomes increasingly populated with axons that follow the boundary ridge as far as the floor-plate, where many growth cones turn and join the medial longitudinal pathway (Lumsden and Keynes 1989). It has been suggested that rhombomere boundaries provide an environment that encourages axon growth, since a number of molecules involved in axon guidance are expressed there. From HH 14 onwards, extracellular spaces become larger at the rhombomere boundaries (Heyman et al., 1993; Lumsden and Keynes, 1989). Around this time both *Fgf-3* (Mahmood et al., 1995) and *PLZF* expression (Cook et al., 1995) are localized to boundary cells. This is followed at HH 16 and 17 with a decrease in the expression of *Hoxb1* and *Krox-20,* whereas *Pax6* is preferentially expressed within these cells (Heyman et all, 1995). In addition, at HH 16 specific immunostaining of the extracellular matrix proteins laminin (Lumsden and Keynes, 1989) and Chondroitin Sulphate Proteoglycan (CSPG) (Heyman et all, 1995) is found at the boundary. Interestingly, when new boundaries form after grafting, CSPG is specifically localised to regenerating as well as ectopic boundaries (Heyman et all, 1995).

At approximately HH 16/17, a number of adhesive molecules, in particular, Ng-CAM (Lumsden and Keynes 1989) and peanut agglutinin (Layer and Alber, 1990) are expressed within the boundaries, whereas the highly sialylated form of N-CAM is expressed exclusively within the rhombomeres (Lumsden and Keynes, 1989). The latter is less adhesive, which suggests that boundary cells are more adhesive than their rhombomeric neighbours. Later at around HH 19 boundary cells express Vimentin (Heyman et al., 1995), which has been associated with glial structures in chick (Tapscott et al., 1981). This is accompanied by a change in morphology of the boundary cells, which becomes characteristic of radial glial cells with their end feet at the ventricular and pial surfaces. Furthermore, radial glia are known to produce CSPG (Faissner et al., 1994) and Muller glial cells have binding sites for peanut agglutinin (Arregui et al., 1992), and both molecules are found in boundaries. It is thus possible that some boundary cells adopt a radial glial identity and provide a pathway for axonal tracts. This is supported by the fact that the expression of Ng-CAM on axons is associated with fasciculation as well as binding to glial cells (Grumet, 1992).

The hindbrain is similar to the *Drosophila* system in that segmentation, compartmentalisation and Hox gene expression are fundamental to patterning. By

generating compartments in which cell movement is restricted, the system ensures that each repeated pattern can acquire a unique identity through the action of homeotic genes. Due to the apparent absence of vertebrate homologues to the segment-polarity genes in the hindbrain, it has been suggested that evolutionary changes leading to vertebrates and insects have developed independently (Lumsden and Krumlauf, 1996; Wilkinson and Krumlauf, 1990). Since A-P organisers are not required for rhombomere patterning, it is possible that once a cell is specified to become a particular neuron, it has sufficient information to direct it to its correct destination. Patterning by signaling centres is observed in other parts of the CNS, namely at the midbrain-hindbrain boundary and at the anterior end of the embryo.

1.1.5 Midbrain-Hindbrain Boundary

The midbrain consists of the optic tectum and associated grisia in the alar plate and several nuclei (such as the substantia nigra and the nucleus of the oculomotor nerve) in the basal plate. The rostral hindbrain will form the isthmus and cerebellum. The development of the midbrain and the rostral hindbrain has been the focus of intense investigations in recent years, which have revealed that a signaling centre/organiser located at the boundary between the two primordia may be responsible for patterning of both tissues.

Classical neuroanatomical studies defined the boundary between the midbrain and hindbrain to be at the constriction between the two vesicles. However, fate mapping studies demonstrated that the isthmus and rostral part of the cerebellum are derived from cells located on both sides of this constriction (Le Douarin and Renaud, 1969; Martinez and Alvarado-Mallart, 1989). The caudal limit of *Otx2* expression, a vertebrate homologue of the *Drosophila orthodenticle* gene, delineates the true boundary between the two regions. *Otx2* is expressed throughout the forebrain and midbrain from early stages, but does not meet the midbrain/hindbrain constriction until HH17 (Millet et all, 1996). A series of chick/quail grafting experiments demonstrated that the isthmus and some cerebellar tissue are derived from the *Otx2* negative part of the posterior midbrain vesicle (Millet et al., 1996). The posterior boundary of prospective midbrain does not coincide with the midbrain-hindbrain constriction early in development, unlike the situation in the hindbrain, where rhombomeres are

delineated by morphological constrictions. Later in development, the *Otx2* expression boundary, midbrain anlage and morphological constriction are aligned.

Grafting studies have revealed that the caudal part of the midbrain vesicle, the isthmic region, has a polarizing effect on the neighboring tissue. When the midbrain without the isthmocerebellar region is inverted, the grafted tissue adopts the phenotype of its new A-P position; for example, the grisium tectalis is converted to a tectal fate. Inversion of midbrain containing the isthmocerebellar region enables the tissue to maintain its original fate. More importantly, this type of graft transforms the neighboring caudal diencephalon into a caudal midbrain/isthmic phenotype (Alvarado-Mallart et al., 1990; Marin and Puelles, 1994); similar to that seen when just the midbrain/hindbrain constriction is grafted into posterior diencephalon (Bally-Cuif et al, 1992).

Both types of manipulations are followed by a rearrangement of the expression of *En2*, which is normally expressed strongly at the midbrain /hindbrain boundary and decreases gradually on both sides (Bally-Cuif et al., 1992; Martinez and Alvarado-Mallart, 1990). These experiments demonstrate that the isthmus contains an organiser involved in patterning of the midbrain and cerebellum. They also show that the caudal part of the diencephalon is competent to respond to these signals and can be repatterned upon confrontation with the organiser. Another interesting aspect of this system is that *En* expression seems to be involved in the actual positional information established by the organizer, as opposed to its function as a segment polarity in *Drosophila*. When *En1* is misexpressed throughout the midbrain vesicle, the rostral part of the tectum adopts a caudal phenotype (Logan et al., 1996).

Otx2 and *Gbx2* could function as selector genes in this system. A null mutation in the *Otx2* gene in mice results in loss of forebrain and midbrain structures and in severe phenotypes, also rhombomeres 1 and 2 (Acampora et al., 1997; Matsuo et al., 1995). Mis-expression of *Otx2* in the rostral hindbrain under the control of the *en* promoter in transgenic mice, on the other hand, shifts the organiser caudally and some of the rostral cerebellar tissue is lost (Broccoli et al., 1999), indicating that the boundary of *Otx2* expression plays a role in positioning the organiser. The positioning of the organizer may also be through the action of *Gbx2*, which is expressed throughout the anterior hindbrain up to the midbrain-hindbrain boundary. Loss of *Gbx2* function results in a

disruption of isthmic signaling and produces a caudal expansion of the *Otx2* expression domain (Wassarman et al., 1997). Transplantation of caudal diencephalon into the midbrain-hindbrain constriction or more posterior regions, apposes *Gbx2* positive and *Otx2* positive domains, resulting in repression of *Otx2* close to the *Gbx2* domain followed by upregulation of *Gbx2* in that part of the graft. This in turn, will sometimes induce the expression of organizer molecules associated with midbrain-hindbrain cytodifferentiation (Hidalgo-Sanchez et al., 1999). Furthermore misexpression of *Gbx2* in the caudal *Otx2* domain under the *wnt1* promoter, results in a rostral shift of *Otx2* and associated formation of a normal organiser, indicating that *Gbx2* may function in positioning the *Otx2* border (Millet et al., 1999). These experiments indicate that the positioning of the *Otx2/Gbx2* boundary is the primary event in the establishment of a signaling centre at the isthmus.

Two known signaling molecules, Wnt1 and Fgf8, are expressed in the boundary region. At neural plate stages, *Wnt1* is expressed in the presumptive midbrain whereas *Fgf8* is expressed throughout the isthmo-cerebellar region. After neural tube closure, the expression patterns of both genes are restricted to adjacent transverse rings of the neural tube, where *Wnt1* is expressed within the midbrain and *Fgf8* is expressed in a complementary manner within the presumptive cerebellar region (Mahmood et al., 1995; McMahon et al., 1992). Fgf8-soaked beads can mimic the effect of the organiser when ectopically implanted in competent tissue. Thus Fgf8 beads in the posterior diencephalon can transform neighboring tissue to an isthmic-midbrain phenotype (Crossley et al., 1996). In the midbrain the beads sometimes induce an ectopic organizer, as evidenced by upregulation of *En2*, *Fgf8* and *Wnt1*. Fgf8 may be involved in the repression of *Otx2*, since *Otx2* is repressed close to the implanted bead (Martinez et al., 1999).

The expression of *Wnt1* at the midbrain-hindbrain boundary is likely controlled to a certain degree by Otx2 as well as Fgf8 (Rhinn et al., 1999). A null mutation in the *Wnt1* gene results in deletion of the midbrain and affects the development of the cerebellum (McMahon and Bradley, 1990; McMahon et al., 1992). The cerebellar phenotype may reflect a secondary effect due to the loss of *En1* and *2* expression, which is maintained by Wnt1 (Danielian and McMahon, 1996).

Patterning of the midbrain and rostral hindbrain is achieved primarily through the activity of compartment selector genes in establishing a signaling centre analogous to the parasegment boundary. In contrast to the *Drosophila* system, which requires the action of the segment polarity gene (*en*) on the posterior side of the boundary, formation of the isthmic organizer depends on the interaction between *Gbx2* and *Otx2*. It is possible that Fgf8 functions as a short-range inducer, which diffuses across the boundary and turns on the long-range morphogen Wnt 1. The resulting Wnt1 gradient turns on *En*, which is probably involved in patterning the tissues.

1.1.6 Anterior Organising Centre

Recent studies in mice and zebrafish suggest that an organising centre at the anterior end of the embryo is involved in regionalisation of the telencephalon. The anterior neural ridge (ANR) is defined as the structure between the anterior neural plate and the adjacent non-neuronal ectoderm, and is characterized by the expression of *Fgf8*. In mice the ANR is required for induction and/or maintenance of the telencephalon-specific marker *BF1* (Shimamura and Rubenstein, 1997). Inactivation of *BF1* results in a deletion of ventral telencephalic molecular markers and morphological structures (Xuan et al., 1995). Houart et al. identified a group of cells at the anterior end of the zebrafish neural plate (row 1 cells) involved in forebrain patterning. Ablation of these cells results in widespread cell death within the forebrain and abolishes the expression of forebrain specific markers. Transplantation of these cells more posteriorly, on the other hand, produces ectopic activation of forebrain markers (Houart et al., 1998). These results suggest that the telencephalon is at least in part patterned through signals secreted from a local organiser. The involvement of FGF8 in this system is reminiscent of the isthmic organising centre, which patterns adjacent unsegmented tissue.

The *Drosophila* system has been invaluable to research in vertebrates for providing several paradigms for patterning mechanisms and identifying molecular components of these pathways. A-P patterning within each part of the CNS appears to depend on a different combination of these patterning paradigms. Compartmentalisation, segmentation and Hox gene expression are essential to development of the hindbrain. In contrast, compartment selector genes and an associated signaling centre function in

midbrain and cerebellar regions. Whilst less is known about telencephalic patterning, it is probable that an anterior organiser is involved. The focus of this project is the characterisation of compartments and boundaries in the developing diencephalon.

1.2 Diencephalon

1.2.1 Anatomy and Function

When considering patterning units within the diencephalon, it is important to consider the adult anatomy, since individual structures may be patterned independently. During development, the diencephalon is the caudal-most part of the forebrain, situated between the midbrain and telencephalon. As development proceeds and the walls of the neural tube meet, the telencephalic vesicle enlarges considerably, and eventually comes to surround the diencephalon, leaving the latter as an egg shaped structure, located medially at the base of the brain. Due to the vast morphogenic movements within the forebrain, the developing avian diencephalon resembles little that of its adult structure.

During development four separate diencephalic primordia can be easily recognised. The most caudal of these is the synencephalon or pretectum, which will form the adult pretectal nuclei and associated posterior commissure. Adjacent and rostral to this is the dorsal thalamus, which will become the adult thalamus. Separating the dorsal thalamus from the adjacent ventral thalamus, which forms the nucleus geniculatum and associated nuclei, is the zona limitans intrathalamica (zli), the precursor of the external medullary layer. Finally the dorsally situated epithalamus forms the epiphysis and habenular complex, and will not be discussed here (Jones 1995). Early in development, the morphology of these primordia resembles that of neuromeres (see figure 2A), but as development proceeds the diencephalic ventricular relief changes considerably. Thus, shortly before the fusion of the ventricular surface, the posterior commissure and dorsal thalamus appear as large bulges of neuroepithelium, whereas the rest of the pretectum and ventral thalamus forms narrow grooves, partly hidden by the bulging of the dorsal thalamus and posterior commissure.

In general each group of nuclei within the pretectum or dorsal/ventral thalamus is responsible for independent sensory pathways and large variations in nuclei

thalamus (Butler, 1994). The mammalian thalamus contains between 15 to 17 nuclei and exhibits a large variation in connectivity, whereas the avian thalamus is somewhat simpler in organisation. It is beyond the scope of this introduction to describe the functional organisation of the mammalian diencephalon, (Macchi et al., 1996; Sherman and Guillery, 1996), and only the best characterized avian nuclei will be considered here. Anatomical studies have been complicated by the extensive difference in nomenclature and therefore the terminology of De Castro et al. (1998) and Rendhal (1924) has been adopted for simplicity. For an overview of diencephalic anatomy see figure 2B.

Pretectum

The pretectal nuclei are divided into three groups, the commissural, juxtacommissural and precommisural and are primarily involved in the communication between the retina and the optic tectum or cerebellum. The commissural nuclei are the main retinorecipients within the pretectum, but also the nucleus ectomammillaris within the juxtacommissural area and nucleus superficialis sinencephali in the precommissural area receive some retinal input as well (Gamlin and Cohen, 1988), and they all project to the optic tectum primarely (Brecha and Karten, 1979). However, retinal input may also be projected to the cerebellum via the juxtacommissural and precommissural nuclei formation (De Castro et al., 1998; Gamlin and Cohen, 1988; Gamlin and Cohen, 1988). The pretectum also receives somatosensory input through the paleostriatal complex, thought to be the avian counterpart of the mammalian basal ganglia. In the pretectum the paleostriatal complex projects almost exclusively to the juxtacommisurral nuclei spiriformus lateralis, which in turn projects to the optic tectum (Karten and Dubbeldam, 1973). The basal ganglia in birds as well as in mammals, are involved in the neuronal control of motor function and their projection to the spiriform lateralis indicates that the basal ganglia exerts its influences on motor function via the tectal pathway (Reiner et al., 1982). Spiriform lateralis also receives afferents from dorsal column nuclei (Wild, 1992), and the rostral part of the Wulst (Wild, 1987) both of which are somatosensory pathways.

Figure 2

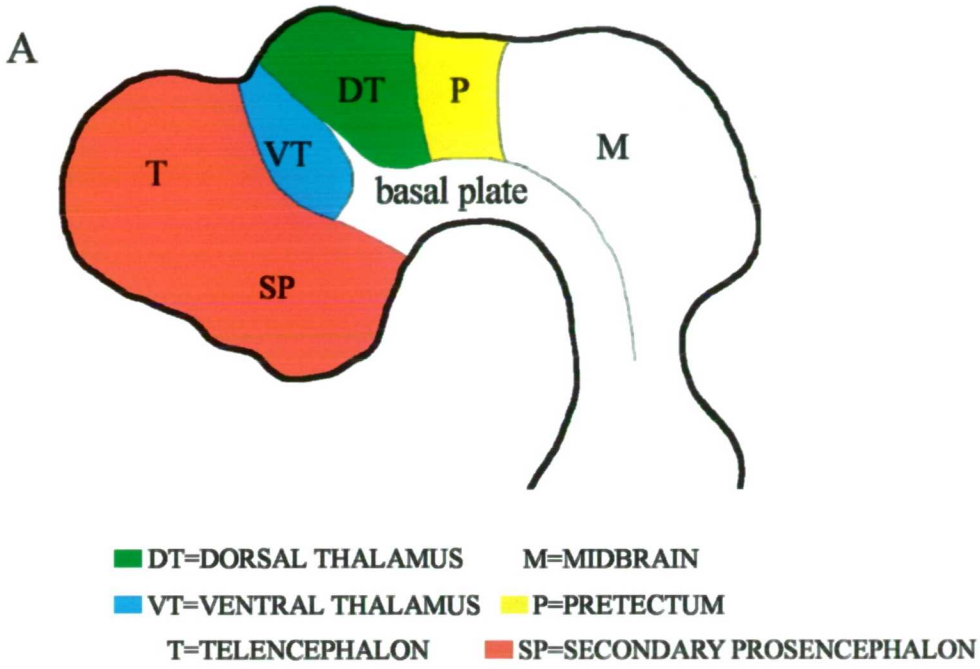
A
DT
P
M
VT
T
basal plate
SP
DT=DORSAL THALAMUS
M=MIDBRAIN
VT=VENTRAL THALAMUS
P=PRETECTUM
T=TELENCEPHALON
SP=SECONDARY PROSENCEPHALON

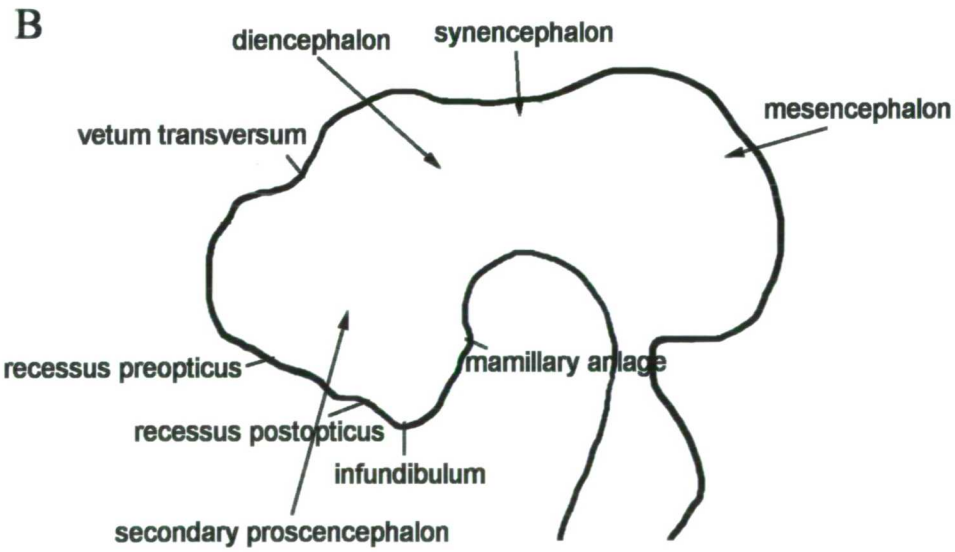
B
diencephalon
synencephalon
mesencephalon
vetum transversum
recessus preopticus
mamillary anlage
recessus postopticus
infundibulum
secondary proscencephalon

Figure 2

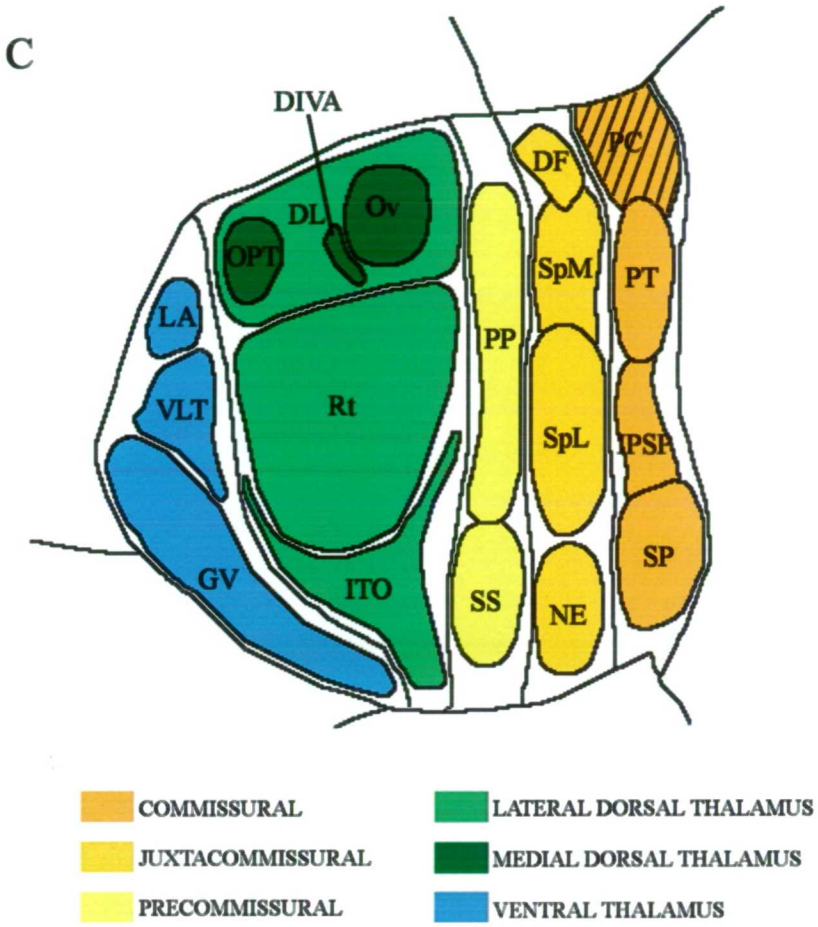

DF	nucleus dorsofrontalis
DIVA	nucleus dorsalis intermedius ventralis anterior
DL	nucleus dorsolateralis
GV	nucleus geniculatum
IPSP	nucleus tractus interstitiopretectosubpretectalis
ITO	nucleus interstitialis tracti optici
LA	nucleus lateralis anterior
NE	nucleus pretectalis externus
OPT	nucleus opticus principalis thalami
Ov	nucleus ovoidalis
Pc	posterior commissure
PP	principal precommissural nucleus
PT	principal pretectal nucleus
Rt	nucleus rotundus
SpL	nucleus spiriformis lateralis
SpM	nucleus spiriformis medialis
SP	nucleus subpretectalis
SS	nucleus superficialis sinencephali
VLT	nucleus ventrolateralis thalami

Dorsal Thalamus

The dorsal thalamus is the major integration and relay centre of the brain, and its main function is to convey visual, auditory and somatosensory input to the cortex. In mammals it is also involved in modifying these signals, and can control to some degree the information relayed to the cortex from prethalamic structures. More importantly, it receives a substantial number of afferents from the cortex and is thus thought to monitor outputs from one cortical area and send this information to other parts of the cortex (Guillery, 1995). Little evidence for this has been found in the avian system, although a few nuclei do receive afferents from anterior forebrain structures.

The visual system is one of the best-studied sensory pathways in the avian CNS, and the main route of communication from the retina to the telencephalon is via the tectofugal pathway, which connects to the thalamic nucleus rotundus (NR), en route to the telencephalon (Karten and Revzin 1966). There are three principal sources of afferents to the NR; from the optic tectum, from the commissural nuclei of the pretectum and from the reticular formation. These afferents project onto defined subregions of the NR, which in turn projects to the ectostriatum and striatum (Hodos and Karten, 1970; Watanabe et al., 1985). Retinal input also reaches the telencephalon via a thalamofugal pathway. A group of nuclei, collectively termed the nucleus opticus principalis thalami, receives direct input from the retina and in turn project to the visual Wulst, situated at the dorsal aspect of the cerebral hemisphere (Karten et al., 1973). Auditory input from the torus semicicularis is relayed via the nucleus ovoidalis (Bonke et al., 1979), which also receives some somatosensory input from the nucleus intercollicularis, both of which are in the midbrain. The latter nucleus in turn projects to an area of the dorsal ventricular ridge known as field L, as well as to the striatum (Bonke et al., 1979).

The main somatosensory relay structure is thought to be the nucleus dorsalis intermedius ventralis anterior (DIVA) (Korzeniewska and Gunturkun, 1990), but somatosensory inputs are also received by nucleus dorsolateralis posterior via the paleostriatum (D'Andrea et al., 1989; Delius and Bennetto, 1972). However this nucleus can also respond to a range of visual and auditory input (Korzeniewska, 1987), and projects to the striatum (Wild, 1987; Wild, 1987) and ectostriatum (Watanabe et al., 1985). In contrast the thalamic nucleus interstitialis tracti optici (ITO), is not a

telencephalic relay nucleus, receiving afferents directly from the retina and projecting to the optic tectum (Martinez et al., 1991).

Ventral Thalamus

In mammals the ventral thalamic nuclei are different to the dorsal thalamic nuclei in one fundamental aspect; they do not project to the cortex, but instead receive afferents from both the thalamus and the cortex and project to the thalamus with GABAergic inhibitory signals (Guillery, 1995). Three main nuclei make up the avian ventral thalamus, the nucleus geniculatum pars ventrale (GV), nucleus ventrolateralis thalami (VLT) and nucleus lateralis anterior (LA). Like their mammalian counterparts, they are heavily involved in retinal communication, but interestingly through the thalamofugal pathway. Both LA and GV receive afferents from this pathway (Karten and Revzin 1966, Karten et al., 1973), and efferents from the visual Wulst returns to GV, which in turn projects to the thalamus (Karten and Revzin, 1966). This suggests that the thalamofugal pathway is involved in modulating the visual input to the tectofugal pathway (Karten et al., 1973), which is one of the few examples in chick of communication from the telencephalon to the thalamus.

Fibre Tracts

During development, a number of major fibre tracts are formed within the diencephalon and are generally thought to project in the boundaries between the different primordia. The first tract to form in the avian diencephalon is the medial longitudinal fasciculus (mlf) around HH 12-13, extending from the caudal diencephalon rostrally (Puelles, 1987; Chedotal et all, 1995). Within this fibre tract, axons from neurons, which constitute the interstitial nucleus of Cajal, run exclusively within the basal plate along the alar plate. This tract has also been identified in mouse, where it first appears at E9.5 (Easter et al., 1993). The appearance of the second tract within the diencephalon is obvious from HH 19 onwards and corresponds to the posterior commissure (Chedotal et al., 1995). This tract projects dorso-ventrally and extends throughout the posterior commissural part of the pretectum. In mouse this tract is visible from E10.5 (Mastick and Easter Jr, 1996). Also at around HH19 the first axons appear in the zli. In mouse this tract corresponds to the mammillothalamic tract projecting from hypothalamus, but

this tract has not yet been identified in chick. Interestingly this tract does not seem to exist in zebrafish either (Macdonald et al., 1994). Finally from HH20, the habenulo-peduncular tract is formed, and is populated by axons from the lateral habenular nucleus (Chedotal et al., 1995).

From the anatomical description, it is clear that each structure within the diencephalon has a related but distinct function. They all relay information, but each operates at a different part of the relay chain. Both the pretectum and the dorsal thalamus relay sensory input, but the pretectum projects to the midbrain, whereas the thalamus relays inputs to the telencephalon. The function of the ventral thalamus on the other hand, is to relay telencephalic communication. It is thus possible that each primordium is patterned independently during development, and several classical neuroanatomists have tried to explain this on the basis of neuromery. These theories are based on the formation of sulci and ridges on the ventricular surface as well as histology and fibre tract formation. It has been proposed that the diencephalon can be divided into either a series of transverse neuromeres and/or longitudinal domains and these notions form the basis of the neuromeric models that are used today.

1.2.2 Neuromeric Models Based on Morphology

Throughout the twentieth century a number of prominent neuroanatomists studied the forebrain in different species, with the ultimate aim of establishing structural homology between species. It is important to stress that the existence of neuromeres and their morphological appearance within different species, first described by Von Baer, was widely accepted in the early days of forebrain research. The main subject of controversy in the field has been whether these neuromeres are fundamental to the development of the adult morphology or simply a secondary transient feature. Thus, if the structure of the adult nuclei could be shown to be the result of neuromeric organisation, it could be used as basis for homology, whereas if neuromeres were considered of no importance, other morphological features had to be used. The outcome of these opposing views would in turn result in very different models of forebrain subdivision.

The disagreement among authors has been partly accentuated by the use of different criteria and experimental methods, which would fall into four categories; adult

topological position of nuclei, origination during development, fibre connection and cytoarchitecture. Within each study the emphasis has always been placed on one of these criteria, sometimes supported by another, and this has limited the analysis by the authors to certain aspects of morphology. For example Palmgreen (1921) wrote; " If it can be proved that two nuclei are formed from the same position of a segment, they are homologous". Since a large number of neuroanatomists were concerned with the organisation of the CNS, it is not possible to present every single opinion and paper published, and instead I will discuss work of those authors who established each of the principle models within the field (for models see figure 3).

Charles Hill

Hill was one of the earliest neuroanatomists in this field and, being a student of Johnston, was chiefly concerned with identifying neuromeres across different species. In 1899, Hill published a comparative embryological study based on morphological undulation of the neuroepithelium and histology, which recognized the appearance of neuromeres during both chick and trout development. In his study Hill agrees with his predecessors that the neuromeres are metameric segments that resemble each other irrespective of their location within the forebrain, midbrain or hindbrain. Hill divides the salmon forebrain into three segments, which he claims are maintained throughout development. His first segment encompasses the front of the brain and ends ventrally just in front of the optic nerve in the area of the preoptic recess. His second transverse segment contains the infundibulum, with a posterior border starting dorsally at the velum transversum and ending just caudally to the infundibulum (for anatomical references see figure 2C). His third segment stretches caudally and contains the posterior commissure; a structure he claims divides the forebrain and midbrain.

In early chick, he identifies the same number and location of segments as in the salmon (see figure 3A). At later stages of development, however the segments in the forebrain and midbrain disappear, a phenomenon he explains is due to the rapid expansion and growth of the forebrain vesicles. Instead, he identifies two constrictions within the forebrain, one that divides the secondary prosencephalon (telencephalon and hypothalamus) and the diencephalon and one that divides the diencephalon into two parts. Since these constrictions appear so much later in development and are preceded

by segmentation, he finds it "very improbable that the two sets have the same morphological value" (Hill 1899). Due to the similarity between species in the number and arrangement of segments, Hill affirms that these must be homologous. Hill thus identified a neuromeric organisation within the forebrain, which he believed to be fundamental to all species and therefore important to the pattern of adult structures. However, since these subdivision are only recognizable very early in development, several anatomists most notably C. Judson Herrick, did not believe that they were relevant to adult morphology.

C. Judson Herrick.

Herrick considered neuromeres to be transient and of no importance to adult structure and consequently neither to homology. Due to the limitation of techniques at that time, neurogenesis and nuclei formation could not be identified until later in development, and he thus believed that the morphology of the neuroepithelium at later stages was the only basis for forebrain division (Herrick, 1910). To Herrick, interconnection between different parts of the brains was as important as the structures themselves and could therefore not be ignored when considering functional organisation and homology between species. His work on the amphibian brain yielded a completely different model that proposed by Hill, in which Herrick claims that the forebrain is divided into four longitudinal domains, extending through the diencephalon and the telencephalon, with each domain functionally connected by fibre tracts (see figure 3B). For example, he found that the straital part of the telencephalon is allied with the ventral thalamus and the dorsal thalamus is connected with the piriform area.

In this way he divided the diencephalon into a ventrally located column containing the hypothalamus, on top of this the ventral thalamus formed a column, followed by a dorsal thalamic column and finally the epiphysial column. In his model the synencephalon was not recognized as an individual structure but rather its separate nuclei were assigned to different columnar domains. He based this on fibre tracts but more importantly on the appearance of ventricular sulci, which he observed running longitudinally through the entire brain structure. These sulci were named sulcus diencephalicus dorsalis, medius and ventralis, and divided each of the columns. In 1893, His had already divided the brain into a basal and alar part separated by the sulcus

limitans, but since disagreement existed concerning where this sulcus ended, His' model had not been widely accepted. Herrick did not disregard the sulcus limitans, but claimed that the sulcus diencephalicus medius is an extension of this and that the sulcus limitans ends at the optic recess.

Herrick's model predicted that nuclear homology could be drawn on the basis of their location within a particular column, but the subdivision of these columns was based on sulci, which made the sulci the criteria for homology. However as other papers were published with different views and as Herrick's own studies developed in the following years, he himself came to realize that he could not find the support for the functional connection between the telencephalon and the diencephalon that he had proposed (Herrick C.J., 1933). Although Herrick does not propose an alternative model he does emphasize that connectivity, histology and embryology should be considered in interpreting forebrain organisation. Although Herrick changed his opinion on the columnar model, several neuroembryologists followed and supported this model, notably Margaret Gilbert and Hartwig Kuhlenbeck.

Hartwig Kuhlenbeck

From 1924 to 1947, Kuhlenbeck investigated the development of the forebrain in a large number of species and found that Herrick's basic columnar theory could be applied as a general model for diencephalic subdivision (Kuhlenbeck 1937, reviewed in Kuhlenbeck H., 1948). Through his extensive studies he noted that the columnar arrangement of the diencephalon found in lower vertebrates could be applied to reptiles, birds and mammals as well. However in higher vertebrates, longitudinal zones are only transitory and disappear later in development to form separate fields. Homology between the different vertebrate classes should thus be sought in their relationship to the zonal subdivisions, which he states are columns of cell masses forming units of cytoarchitecture. These are separated by constrictions, devoid of cells where fibres tend to grow, and which may correspond to sulci (Kuhlenbeck 1936).

Kuhlenbeck thus used slightly different criteria to Herrick, since he believed that the homologous units are the cell masses within each column and not the ventricular sulci. Thus he states in his paper of 1948 " It must be understood, however, that the spatial

relationship of the cellular zonal pattern within the wall of the neural tube is the primary feature, while the sulci are a secondary feature". The chicken diencephalon is strikingly similar to the reptilian diencephalon, both in longitudinal subdivisions, growth rate, and nuclei formation (Kuhlenbeck 1937), thus enabling the author to draw direct homology between the different nuclei of the reptilian and chick diencephalon. In the 1948 paper he also gives a very clear account of the columnar model which he proposes. Thus his caudal diencephalic boundary is just posterior to the posterior commissure, whereas the rostral boundary is dorsal to the velum transversum extending along the hemispheric vesicle to lamina terminalis (see figure 3C).

Ventral to the sulcus diencephalicus ventralis is the hypothalamic zonal domain, which extends to the tegmental cell cord in the mid-diencephalon. Dorsal to this is the ventral thalamic longitudinal domain, which extends caudally from the tel-diencephalic boundary and rostral to the tegmental cell cord. It is separated from the dorsal thalamic zonal domain by the sulcus diencephalicus medius, which extends from the tel-diencephalic boundary, corresponding to the foramen of Monroi, and back to the diencephalic-mesencephalic boundary. Finally the most dorsally situated columnar zone is that of the epithalamus, which extends from somewhere caudal to the velum transversum and ends by the epiphysis.

Interestingly Kuhlenbeck does acknowledge the presence of an early subdivision of the diencephalon into a synencephalic (pretectal) and parencephalic (dorsal thalamus and ventral thalamus) domain, but since these predate the longitudinal zones and are only transient, they are not considered as proper subdivisions. The important aspects of Kuhlenbeck's study are twofold. First, he extended the columnar model to a range of species, thereby validating Herrick's prediction on nuclei homology. Second, he emphasises that the ventricular relief cannot be used as a criterion for homology, but only as a guide. This was also the opinion of Harry Bergquist and Bengt Kallen, although they came to this conclusion from a very different angle.

Harry Bergquist and Bengt Kallen.

From the late 1940's through the 1950's, the Swedish school of neuroanatomists,

represented by Bergquist and Kallen, published a series of papers on the development of the vertebrate CNS. Although the prevalent neuromeric theory was that of the Herrick-Kuhlenbeck columnar model, both Kallen and Bergquist believed that neuromeres were central to homology. They were able to identify neuromeres early in development and trace them in adult morphology, and they discovered that neuromeres were areas of increased proliferative activity. On the basis of mitotic counts, Kallen demonstrated that the centres of the neuromeric furrow were crowded with mitotic cells, and this happened simultaneously with a decrease in mitosis at the ventricular ridges (Kallen, 1952a). This generated a proliferation centre within each neuromere, which appeared in waves corresponding to the appearance and disappearance of neuromeric morphology. By arresting mitosis he was able to show that the bulges of the neuromeres were a direct result of the increase in cell division at the centre (Kallen, 1953).

Kallen and Lindskog showed that the changing appearance of neuromeric morphology corresponded to two successive waves of segmentation; the first corresponding to proneuromeres, the next to neuromeres (1953). This is followed by the generation of transverse bands of migration areas, corresponding to units of migrating cells, and this constitutes the third wave of proliferation (Kallen, 1952b). More than one band of migration can be identified from one neuromere, and more than one neuromere can be identified from one proneuromere (Bergquist and Kallen, 1953a,b).

It is important to note that Bergquist and Kallen considered the neuromeric morphology as a secondary event, a result of proliferation, which is the primary and important feature. The finding that the increased rate in proliferation came in three phases, led them to propose that each phase is independent from the other and it is only the spatial relationship between them that links them together (Kallen, 1954, 1955). Therefore neuromeres cannot just develop from one fixed centre, but must be the result of the changes in mitotic activity within the neural tube (Bergquist and Kallen 1954).

Bergquist termed these migration areas *grundgebeite*, and since the cells migrated as units, he hypothesised that the adult structures are derived from these primary regions. He and Kallen found the neuromeric arrangements to be the same in all species of vertebrates (Bergquist, 1952; Kallen, 1955), and Bergquist thus deduced that an adult structure which derives from one particular migration area is homologous between

species regardless of their later position, interconnectivity and structure (Bergquist, 1954). This was in accordance with Kallen's opinion on homology, which he states in 1951 as " if it can be proved that two nuclei in different species develop from the same anlage and in a similar way, they most be looked upon as homologous". To Kallen only the migration and the grouping of cells takes part in the formation of nuclei, and therefore only this part of the process can be considered in establishing homology. Since cytoarchitecture and fibre tract organisation reflects the differentiation of the cells in the nuclei these events only mirror its function, and he does not consider functionality as a criterion for homology (Kallen, 1953).

In their joint paper (Bergquist and Kallen, 1954) they propose a model, which is the accumulation of data from their different studies, and which shows that the diencephalon is divided into three transverse migration bands (see figure 3D). One corresponds to the pretectum, one to the dorsal thalamus and one roughly to the ventral thalamus. These are preceded early in development by two proneuromeres, one corresponding to the diencephalon and one partly to diencephalon and partly to the secondary prosencephalon. They disappear and are succeeded by a number of neuromeres. Proneuromere 1 gives rise to one diencephalic and one telencephalic neuromere and proneuromere 2 gives rise to two diencephalic neuromeres. From these 4 neuromeres 5 migration bands are generated, where the ventral part of migration band 1 and 2 is the hypothalamus, which they consider part of the diencephalon. Shortly after the initiation of migration, the forebrain is also subdivided into longitudinal domains, dividing each migration band into smaller units of cells.

They do not see the forebrain as being divided into distinct brain vesicles, since the evaginations of the neuroepithelium are of no morphological value, and therefore cannot be used to identify a border between the telencephalon and diencephalon. The result of their model is a brain divided into squares of migration areas forming the different nuclei. The sequential occurrence of proliferation was later confirmed by Bergquist (1957) based on mitotic counts. At the end of the 1950's it had thus appeared through Bergquist and Kallen's work on many species, that neuromeres are linked with adult morphology, and although they are secondary events, they are the morphological manifestation of proliferation which results in migration and which in turn produces in nucleus formation.

Richard E Coggeshall.

Although Bergquist and Kallen had deduced that neuromeres correlated with migration areas, they had not been able to follow these directly to adult form. Furthermore at this time the Herrick-Kuhlenbeck model was considered by many to be the correct interpretation for forebrain subdivision. This led to two opposing views in the field, one of Bergquist and Kallen and one of Herrick and Kuhlenbeck. In his work on albino rats published in 1964, Coggshall attempted to follow the appearance of neuromeres into adult anatomy, and thereby be able to resolve the disagreement within the literature. The Coggeshall study is important because he was the first to direct his attention to the neuromeres themselves, and his work was really the first to show a link between neuromeres and the later developing sulci, a relationship already hypothesized by Bergquist and Kallen.

Coggshall (1964) identified two diencephalic neuromeres early in development, delineated by ridges, which are later populated by axon tracts (see figure 3E). One ridge is the zli, which forms the external medullary lamina dividing the dorsal thalamus and the telencephalon. The other ridge divides the dorsal thalamus and the pretectum, and forms the habenulo-peduncular tract. Finally, the posterior commissure delineates the pretectal bulge, and separates the diencephalon from the midbrain. He followed these into late development and found that they are continuous with the grooves of the various sulci proposed by Herrick. Interestingly his conclusion from this was that the transverse neuromeres now become longitudinal and therefore the caudal most neuromere, which through his description should be the synencephalon, now becomes the epithalamus. His first neuromere develops into the ventral thalamus, hypothalamus and telencephalon, and his second becomes the dorsal thalamus. Coggeshall thus accepted the basic columnar model of Herrick and did not agree with the model of Bergquist and Kallen, since he cannot find precursors of the adult nuclei early in development. Coggshall found a more plausible explanation for neuromeric bulges within the neuroepithelium. He believed that bulges are points of relative weakness, maybe due to proliferation, and that the ridges are points of relative strength. Due to the pressure of spinal fluid within the neural tube the weaker areas are pushed out to form bulges. In this scenario, the appearance of fibre tracts in the ridges is possible because

axons will tend to grow along a source of strong support. Although the conclusions that Coggeshall drew from his investigations are not entirely correct, he did recognise that the morphogenic movements leading to the columnar model represent the initial subdivision into neuromeric bulges.

Vaage

The confusion in the literature regarding the actual number of neuromeres led Vaage to investigate the morphogenic appearance of neuromeres in the chick CNS (Vaage, 1968). He concluded that the disagreement was not a result of variations in the species studied, but was due to the variation in embryonic age between the different studies. Therefore, he performed a detailed analysis of neuromeric morphology on successive stages of chick embryos from neural tube closure to E 5. Vaage was concerned with the development of the entire brain structure, in particular the rhombencephalon. However, only his findings on diencephalic development will be discussed here.

Using live embryos, as well as wax plate reconstructions of fixed and sectioned material, he confirmed that neuromeres are readily recognisable within the chick neural tube. He found that neuromeres were progressively subdivided through development, thereby explaining the confusion within the literature. The appearance of longitudinal sulci later in development is independent of the transverse neuromeres and run diagonally to these. According to his observation neuromeres precede nerve formation and are identical in all brain regions and should therefore be considered segments. Vaage disagreed with Bergquist and Kallen concerning their waves of neuromery as well as the Herrick-Kuhlenbeck model, which he interpreted as a late-occurring longitudinal subdivision.

According to Vaage, the chick diencephalon is divided into four neuromeres. At the most posterior end the diencephalon is divided from the mesencephalon just caudal to the posterior commissure. As early as HH 12 he divided the diencephalon into two neuromeres identical to the synencephalon (pretectum) and the parencephalon (thalamus). The subdivision of the parencephalon into an anterior (VT) and a posterior (DT) neuromere takes place at HH 14, and is followed at HH 17 by the subdivision of the synencephalon into two neuromeres. The importance of Vaage's study is thus

twofold. First, he was the first to propose the step-wise subdivision of neuromeres. Second, he identifies two neuromeres within the synencephalon, thus dividing the diencephalon into four neuromeres, which are later obstructed by morphogenic movements.

Keyser

The existence of a strong debate in this field led Keyser to publish a paper in 1972 on the development of the Chinese hamster, where he tried to test the validity of each of the different models. He was of the opinion that it was the limited use of different techniques in previous studies that had led to the discrepancies, since individual studies only examined a few aspects of development. In his study he used all the different criteria presented by other authors, concentrating on the embryonic morphology per se rather than the question of resulting homology.

Keyser thus used a number of different techniques, looking at various embryological features in detail throughout development. First, he examined the appearance of grooves and ridges on the ventricular wall and from that he affirmed the presence of neuromeres that persist until later stages. He also agreed with Vaage that distinctions between proneuromeres and neuromeres, as proposed by Bergquist and Kallen could not be made. He was in agreement with Hill and Johnston on the fact that the telencephalic diencephalic constriction runs from the velum transversum in a ring shape fashion to meet the ventral midline just caudal to infundibilum in between that and the mammillary anlage. He found that from E11-12.5 the forebrain is divided into three neuromeres, the parencephalon becomes divided into an anterior and posterior part, pars dorsalis thalami and pars ventralis thalami, flanked caudally by the synencephalic neuromere (see figure 3G). The interneuromeric boundary between the two parencephalic regions is the zli, and the boundary between the parencephalon and synencephalon is the ridge later inhabited by the habenular tract.

These neuromeres develop into a number of progressively differentiating areas within the caudal part of the parencephalon, and he agreed with Bergquist that the interneuromeric ridges have a lower rate of proliferation than the neuromeres. Because the ventricular relief changes considerably later in development, the interneuromeric

ridges disappear and the neuromeres start to bulge due to increased proliferation. Therefore, the ridges now become sulci, where some of the sulci are remnants of interneuromeric boundaries (such as the sulcus diencephalicus medius which corresponds to the zli), whereas some are not. He therefore deduced that sulci must be secondary histogenic events, due to the bulging of the neuroepithelium.

From his analysis of matrix growth he described a caudorostral and basodorsal gradient of neurogenesis. Within the early developing diencephalon he saw a progressive matrix development at the interneuromeric borders as well as the basal plate, and only later was this followed by neuromeric bulging. The advanced state of the basal plate, compared to the alar plate, was also confirmed on the basis of histology, and he agreed with Bergquist and Kallen's sets of ventral and dorsal migration areas.

Although Keyser did not venture into the field of anatomical homology, he did consider fibre tracts as a criterion for subdivision. This was based on his findings that certain fibre tracts such as the posterior commissure develop in an interneuromeric boundary and therefore continue the subdivision of the brain later in development after ridges have disappeared. He therefore deduced that subdivisions must be important in fibre formation. Keyser's work was thus important since he looked methodically at development from as many different angles as were available to him. Importantly he verified the existence of neuromeres as important morphological units in accordance with both Bergquist and Kallen and Vaage, being stable structures and thereby casting considerable doubt on the columnar model.

Luis Puelles

As a result of technical advances that allowed new level of analysis, Puelles published his first paper on forebrain subdivision 1987 (Puelles et al., 1987). With the advent of modern staining techniques, Puelles developed a model for chick diencephalic organisation on the basis of acetylcholinesterase (AChE) expression, which is one of the earliest markers of neural differentiation. He showed that there is a mosaic pattern of neuronal differentiation from HH13 onwards within the basal part of the diencephalon. This pattern of neurogenesis does not follow a gradient as had been proposed earlier by Keyser and others, but develops as patches of cells within each neuromere. The matrix at the interneuromeric boundaries exhibits scarce or no neurogenesis, which is in

contrast to Keyser and Herrick who found increased activity at the boundary. Puelles ascribes this discrepancy to the limitations of the techniques they used. He thus confirmed the findings of Bergquist and Kallen that the basal plate is subdivided into areas of differentiation as opposed to a continuous band of differentiated cells.

The most important point from this paper (Puelles et al, 1987) is the temporal and spatial correlation between the initiation of neurogenesis and neuromeric divisions. Since the basal plate matures first, Puelles divided the brain into longitudinal columns, but not on the basis of ventricular sulci or adult nuclei structures, as proposed by Herrick and Kuhlenbeck. He argues that subdivision of the brain on the basis of sulci is questionable since some of Herrick's and Kuhlenbeck's longitudinal boundaries seen in coronal sections actually correspond to transverse limits. Thus Puelles commented, "The authors are evidently oblivious of the changing relations of the arbitrary coronal section plane with the curving axis of the prosencephalon along the course of development". His results also support previous assertions by Vaage and Keyser, that neuromeric formations do not come in waves as hypothesized by Bergquist and Kallen, but are a permanent feature during development. On this he comments, "Taking all this into consideration, one may state that, whereas our provisional theoretic grasp of neuromorphogenetic processes may squirm and change noticeably within our minds, Nature, as expressed in the actual neural tube preparations, manifest a rather well-ordered, topologically invariant course of events leading to the increase of static effects known as *Brain structure*, the unraveling of which is our ultimate morphological purpose".

From his analysis of neurogenesis, Puelles described the progressive subdivision of the diencephalon and put forward his version of a neuromeric model. Early in development there is a division between the epichordal and prechordal parts of the neural tube, separating the diencephalon and secondary prosencephalon. The diencephalon becomes subdivided into the synencephalon (pretectum) and parencephalon (dorsal and ventral thalamus), where the latter subsequently splits into posterior (dorsal thalamus) and anterior parencephali (ventral thalamus). On the basis of his staining, he cannot divide the telencephalon into neuromeres but does in later publications in the context of gene expression domains.

In his 1987 paper Puelles showed that neurogenesis is correlated with neuromeric morphology and that these two events evolve in parallel. He then reinterpreted the data from the many studies in this field in the context of his own model. What is apparent from the description above is that whether the forebrain is divided into columns or transverse domains, all studies recognised the same primordia as independent; the ventral thalamus, the dorsal thalamus and the pretectum. However dividing them into transverse domains would imply that they are segmentally arranged, and therefore must be a repetition of some common theme. Puelles regarded them as segmented since he saw a repetition of neurogenetic centres within the basal plate of each neuromere, but unlike segmentation in the hindbrain this repetition is not alternating.

1.2.3 Neuromeric Models based on Gene Expression and Cell Lineage Restriction

Luis Puelles and John Rubenstein.

In subsequent years Puelles and John Rubenstein provided further support for this neurogenic model on the basis of gene expression patterns, which correspond to neuromeric boundaries. Additional research identified more genes that appeared to obey the proposed neuromeric borders. In 1993 Bulfone et al. (Bulfone et al., 1993) compared the expression of the developmental genes *Dlx1*, *Dlx2*, *Gbx2* and *Wnt3* in mouse and showed that these genes demarcate complimentary transverse and longitudinal domains within the mouse forebrain. *Dlx1* and *2* are homologous to the *Drosophila* gene *distal-less*, and members of a growing family of *Dlx* transcription factors (Price, 1993). *Dlx1* and *2* transcripts are found throughout the ventral thalamic neuromere, (P3 according to the author's nomenclature), where *Dlx2* is expressed exclusively in undifferentiated cells (Porteus et al., 1994). They both demarcate the boundary between P3 and P2 (dorsal thalamus), which is the zli.

The expression of *Gbx2* and *Wnt3* was found in the P2 domain. Wnt-3 is a member of the WNT growth factor family (Roelink et al., 1992), which is homologous to *Drosophila wingless* genes. The domain of *Wnt3* expression confirmed previous expression studies (Salinas and Nusse, 1992), which had shown that it is expressed before the morphological appearance of the presumptive dorsal thalamic neuromere. Bulfone et al. further showed that *Wnt3* transcripts are found in the P1 (pretectum) as

well. The expression of *Wnt3* both in the dorsal thalamus and pretectum follows a general D-V gradient where the strongest expression is close to the dorsal midline and completely absent from the basal parts. The expression of *Gbx2* on the other hand, clearly demarcates the entire alar part of P2, delineating the boundaries with P3 and P1. These expression patterns appeared to be consistent with the neuromeric "model" of Puelles.

In a review article in 1994, Puelles and Rubenstein proposed the "prosomeric model", in which they represent the forebrain in six subdivisions, called prosomeres, three diencephalic, described above, and three secondary prosencephalic. Within the latter the hypothalamus constitutes the ventral part and the telencephalon the dorsal part. These authors also divided both the diencephalon and the secondary prosencephalon into four longitudinal domains analogous to the roof, alar, basal and floor plate (Rubenstein et al., 1994). The subdivisions are based on the expression of *Sonic hedgehog* (*Shh*), *Nkx2.1* and *-2.2*, *Otx* and *Emx* genes (see fig. 3 I). *Nkx 2.1* and *-2.2* are homeobox genes and likely downstream targets of SHH signaling (Barth and Wilson, 1995).

Both *Shh* and *Nkx2.1,-2.2* are expressed continuously within the basal part of the forebrain in non-overlapping complimentary domains. They delineate the boundary between the basal and alar plate, apart from the basal part of P5 (the tuberal hypothalamus), which does not express *Shh*. Furthermore *Shh* expression extends along the zli from HH 16 onwards, and *Nkx 2.2* maintains its complementary expression domain on the dorsal side of the *Shh* domain (Shimamura et al., 1995). *Nkx 2.1* is expressed throughout the basal plate both within the diencephalon and secondary prosencephalon (Rubenstein et al., 1994).

The expression patterns of *Emx1* and *-2* and *Otx1* and *-2* were offered as further support for the prosomeric model. *Emx* is the vertebrate homologue of *Drosophila empty spiracles*, and *Otx* is homologous to *orthodenticle*. Both *Drosophila* genes are expressed in the head and their targeted disruption results in deletion of head structures (Hirth et al., 1995). In vertebrates, both *Emx* and *Otx* are expressed in nested domains within the developing forebrain. *Otx2* is expressed throughout the forebrain and midbrain, whereas the dorso-caudal boundary of *Otx1* is within the midbrain. *Emx2* is expressed in the ventral thalamus, delineating the zli and extends anterior to span a

large dorsal domain within the telencephalon, whereas *Emx-1* is expressed exclusively in a small domain at the dorsal midline within the telencephalon (Boncinelli et al., 1993). As for its *Drosophila* counterparts, disruption of *Otx2* gene function results in deletion of most anterior brain structures (Matsuo et al., 1995). The Puelles prosomeric model (1987) is supported by both cellular and molecular criteria and allocates the main three primordia within the diencephalon into separate neuromeres. However some aspects of this model were challenged by a different analysis of diencephalic development, based on a different combination of techniques.

Michael Figdor and Claudio Stern

On the basis of morphology, gene expression and cell lineage restriction analysis Figdor and Stern claimed that the diencephalon is divided into four neuromeric compartments designated D1-D4. D1 and D2 correspond to the ventral and dorsal thalamus respectively, whereas D3 is the anterior part of the pretectum and separate from the posterior part (D4). They base their model on the topography of the ventricular surface as assessed by scanning electron microscopy (SEM) and staining with AChE and peanut agglutinin.

Figdor and Stern observed close similarities to the morphological and molecular characteristics of the developing hindbrain, and thus propose that the diencephalon is a segmented structure. Like the hindbrain the neuromeric subdivision of the diencephalon is progressive, where the ridge between the midbrain-D4 (posterior pretectum) appears first at HH12 followed by the formation of the zli dividing D1 and D2 (ventral and dorsal thalamus, respectively) at HH 14. At HH15 the boundary between the telencephalon and diencephalon is formed, followed at HH 16 by the interpretectal boundary and at HH17 by the boundary between the D3 (anterior pretectum) and D2. The localisation of both AChE and peanut agglutinin at HH 24 indicates that the neuromeres are arranged in an alternating segmental pattern, being strongly expressed in even-numbered neuromeres. The pattern of neurogenesis does not correspond to that described by Luis Puelles, possibly due to the different stages of development analysed in the different papers. The boundaries were later populated with axon tracts, thus resembling the hindbrain boundaries. The mammillothalamic tract forms along the zli, and the habinulo-interpedencular tract runs along the P3-P2 boundary. The boundary

between P3 and P4 is the site of the anterior border of the posterior commissure and the midbrain-P4 boundary contains the posterior border of the posterior commissure. Finally, cell lineage restriction experiments suggests that clonal descendants from a cell injected before boundary formation at HH10, could be found in adjacent neuromeres, but respected the boundary if injected after boundary formation at HH 17. Irrespective of stage of injection clones were large and able to mix with non-labeled cells. In some cases, clones generated from cells injected after boundary formation spanned the entire neuromere.

Figdor and Stern (1993) also utilized various gene expression patterns to support their neuromeric model. The expression pattern of the paired-box transcription factor, *Pax*6, is particularly important to support their claim that the pretectum is divided into two neuromeres. It is expressed early throughout the diencephalon but becomes restricted to the ventral thalamus and posterior commissure later in development (Chalepakis et al., 1993). In the ventral thalamus the expression of *Pax*6 borders the zli, and transcripts are found exclusively in the internal germinative layer. The expression within the pretectum delineates the posterior commissure, the posterior compartment of the pretectum (Stoykova and Gruss, 1994). Loss of *Pax*6 function results in a deletion of the midbrain-pretectal boundary, resulting in the posterior commissure being severely reduced (Mastick et al., 1997), and ventral thalamic nuclei fail to form (Stoykova et al., 1996). Furthermore in zebrafish pioneering axons have been proposed to navigate along the boundaries of *Pax6* expression in the diencephalon (Macdonald et al., 1994).

In summary, Figdor and Stern's neuromeric model is distinct from its predecessors in that it proposes that the diencephalon is divided into four neuromeres that are segmentally arranged in with an alternating periodicity. Using uniquely-tagged replication incompetent viruses to analyse clonal descendents, Golden and Cepko (Golden and Cepko, 1996) demonstrated that cell lineage restriction is lost at later stages of development.

1.2.4 Other Genes Correlated with Neuromeric Models

In recent years the expression of a growing number of developmental genes have been correlated with both the longitudinal and transverse subdivisions of the prosomeric

model. In chick *Brx1*, a homeobox-containing gene, is expressed in the basal part of the diencephalon and extends along the zli. Expression is first seen within the basal plate at HH 18, but does not extend along the zli until HH 20, when its expression is restricted to the lateral pial side of the ventricular zone of the zli (Kitamura et al., 1997). Similar expression patterns are observed with the murine homologues of the *Drosophila single-minded* gene, *Sim-1* and *Sim-2* (Ema et al., 1996; Fan et al., 1996). The expression of the rat tyrosine phosphatase gene is restricted to the dorsal thalamus at E19 (Sahin et al., 1995), whereas murine *Promyelocyte Leukemia Zing Finger* (*PLZF*) gene transcripts are found in the anterior part of the pretectum and alar part of dorsal thalamus at E 12.5 (Avantaggiato et al., 1995).

The *chicken ovalbumin upstream promoter-transcription factors* (*COUP-TF*) I and II are expressed as early as E 10.5 in mouse, throughout the ventral and dorsal thalamus, but at E 14.5, COUP-TF II expression is lost in dorsal thalamus (Qiu et al., 1994). *R-Cadherin*, a member of the Cadherin family of cell-surface glycoproteins is strongly expressed in the ventral thalamus, where it delineates the zli, and in the caudal aspect in the pretectum from E 12.5 in mouse (Ganzler and Redies, 1995). *In vitro* aggregation studies have shown that *R-Cadherin* positive cells do not mix with *R-Cadherin* negative cells. However cells are able to mix when *R-Cadherin* is inhibited, suggesting that it is involved in setting up differential adhesion between neuromeres (Matsunami and Takeichi, 1995).

1.3 Definition of Problem

Although it has been studied for more than a century, the neuromeric organisation of the diencephalon is still debated. The three major questions are: How many neuromeres are in the diencephalon? Is the diencephalon segmented? If so, are the segments arranged with alternating periodicity like the hindbrain?

If the organisation of the diencephalon and hindbrain are analogous, one would predict an alternating pattern of neurogenesis as well as the pair-wise expression of segment specification genes. This would imply a common neuronal structure repeated in each pair of neuromeres, setting up a basic plan for neuronal development. Genes functioning in a similar way to the Hox genes in the hindbrain would then independently specify these neuronal structures. This type of segmentation would involve the alternating

expression of cell adhesion molecules, setting up the segmental compartments similar to the periodic segmentation found in the hindbrain. We may also expect that boundary regions behave similarly, being areas for preferential growth of axons and expressing molecules that encourage growth cone entry.

If however we accept the prosomeric model of Puelles and Rubenstein, we may expect segmentation to be a repetition of a common theme within each segment. This would include the repetition of neurogenesis in a similar pattern within each segment, and segment specification would require the expression of genes within each segment, independently from one another. We would still expect the formation of compartments, since cell lineage restriction seems to be essential for patterning independent cell units. Both modern models are consistent with the existence of unique boundary morphology, since boundaries arise at the interface between two compartments. This morphology may still be similar to that found in the hindbrain since axon tracts are found at the boundary between some of the neuromeres within the diencephalon.

In designing my project, I hypothesized that if particular boundary morphology can be identified within all of the boundaries, then the subdivision of the pretectum could be more accurately assessed. However, before such an analysis could be undertaken it was important to carry out an independent evaluation of the spatial and temporal appearance of these boundary regions. This was done using scanning electron microscopy (SEM), histology and a detailed analysis of neurogenesis. Once these were established each boundary region was analysed using some of the techniques previously applied in the hindbrain and a panel of markers similar to those found in the hindbrain. This includes cell division labeling with BrdU, immunocytochemistry and glial labeling, as well as transmission electron microscopy (TEM). An extensive gene expression analysis was also performed to find additional early markers for the different neuromeres. In the context of the results obtained from this analysis a cell lineage experiment was done in combination with molecular markers to evaluate the presence of one or two compartments within the pretectum.

Figure 3

A

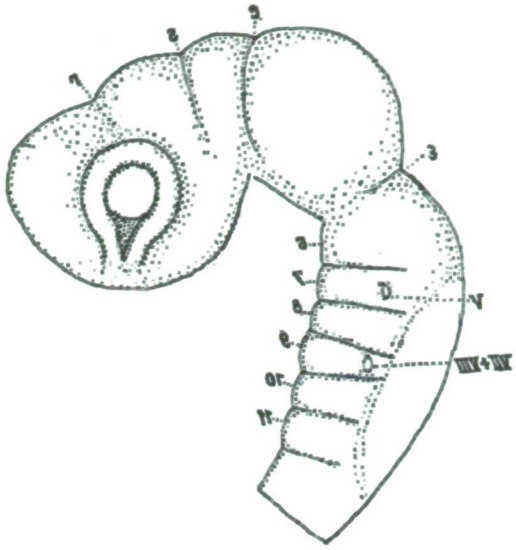

Charles Hill 1899

A*

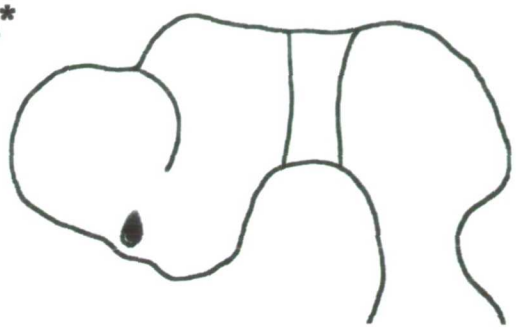

B

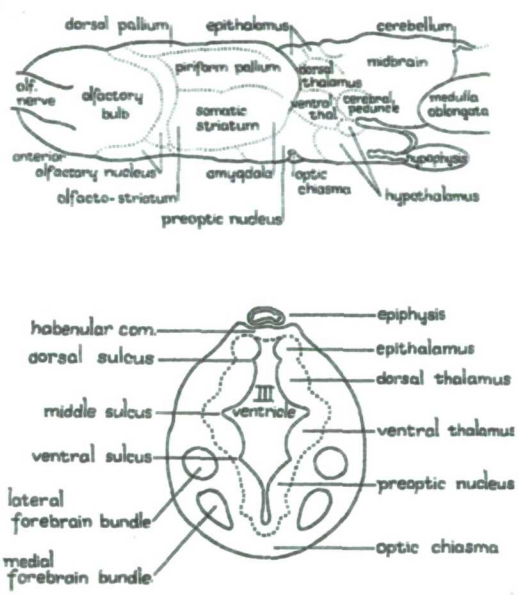

B*

C. Judson Herrick 1933

C

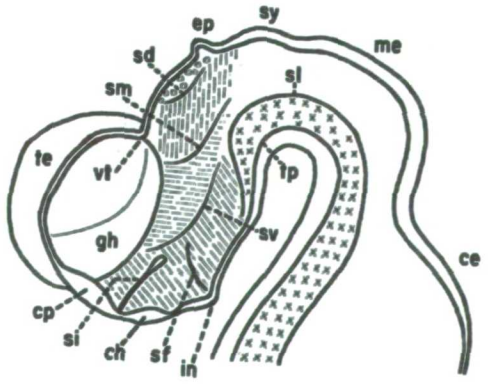

Hartwig Kuhlenbeck 1948

C*

Figure 3

D

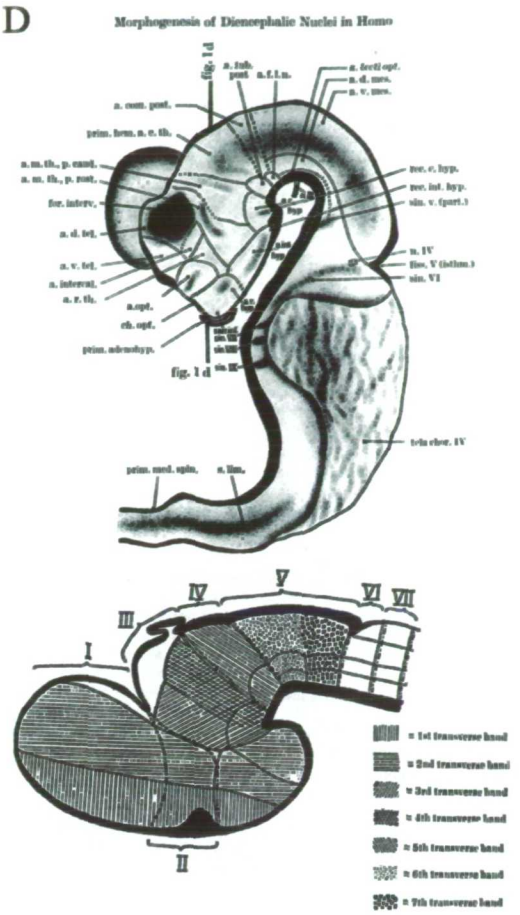

D*

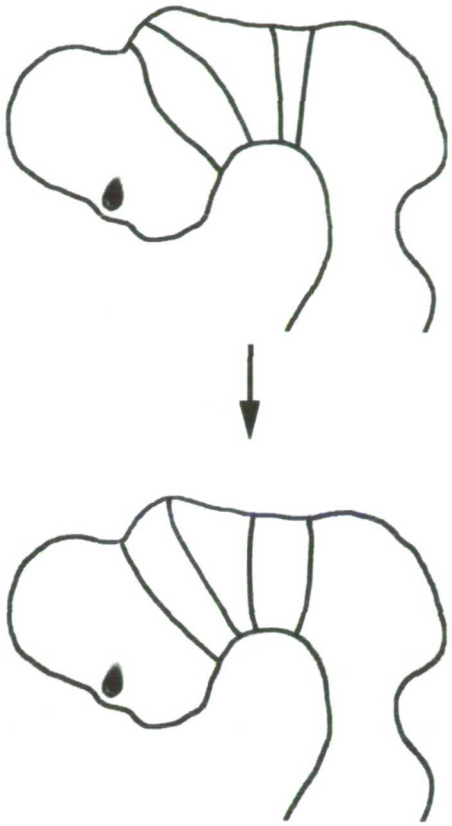

Harry Bergquest and Bengt Kallen 1954

E

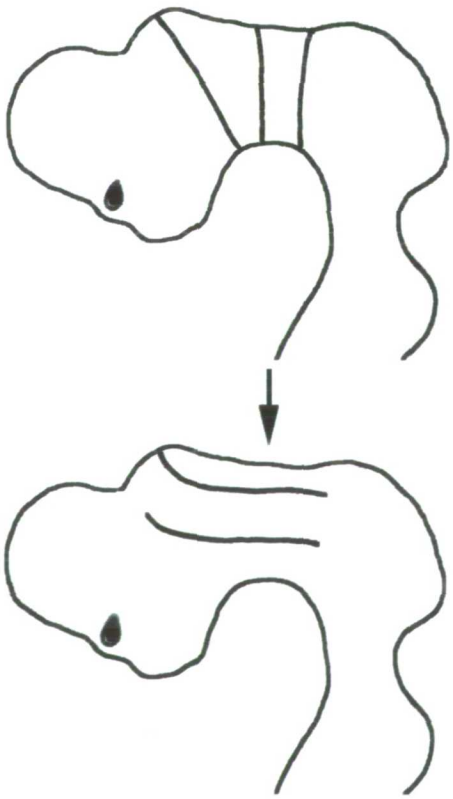

Richard E. Coggshall 1964

Figure 3

F

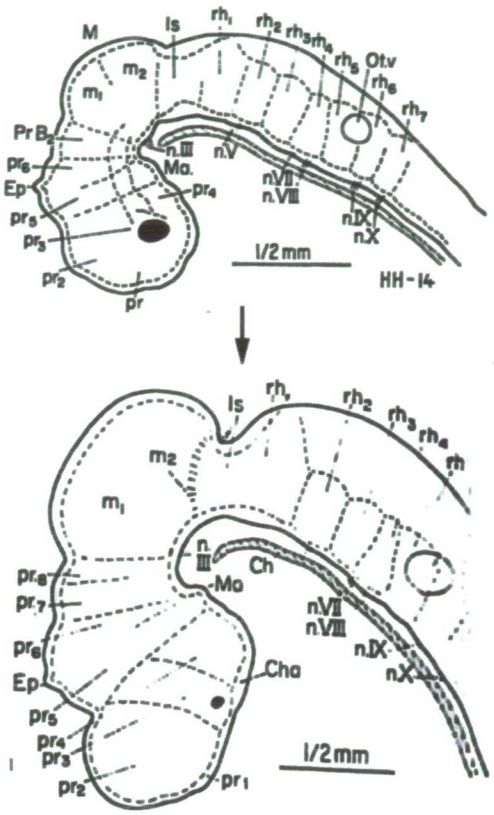

F*

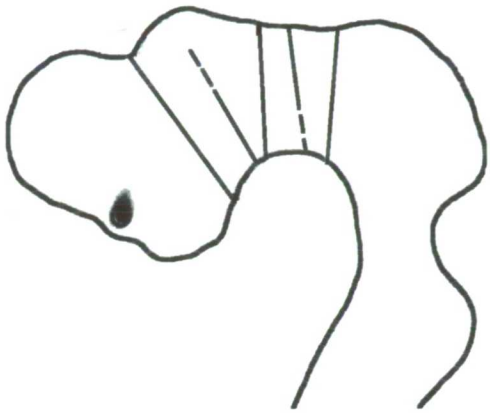

S. Vaage 1968

G

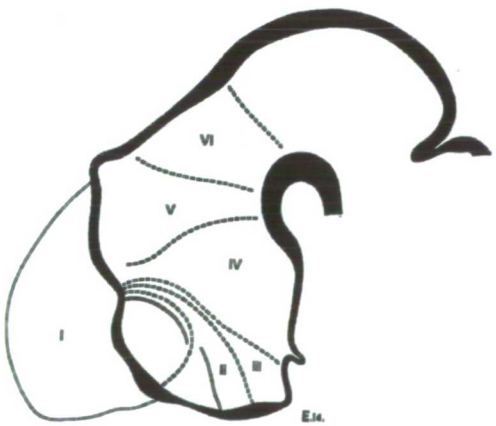

G*

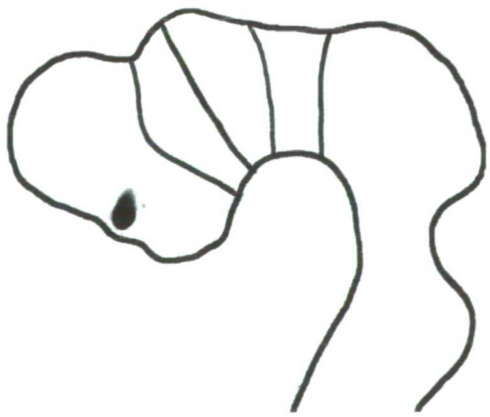

A. Keyser 1972

Figure 3

H

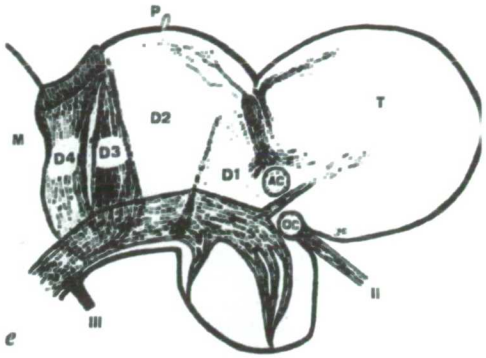

H*

Michael Figdor and Claudio Stern 1

I

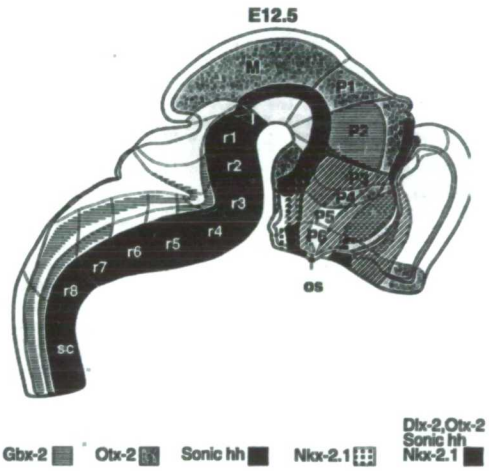

I*

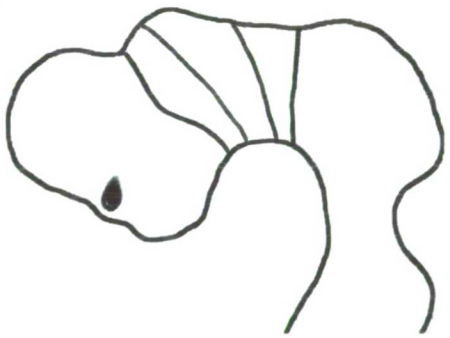

John Rubenstein and Luis Puelles 1994

CHAPTER 2

Materials and Methods

2.1 Chick Embryos

2.1.1 Incubation

Fertilised eggs (Rhode Island Red) were delivered weekly and stored at room temperature until incubation. Eggs were incubated with its long axis horizontal at 39-40°C in 40-50% humidity, enabling the developing embryo to lie at an accessible position within the egg. Length of incubation varied depending on desired developmental stage, which was determined according to the known tables of Hamburger and Hamilton (1951).

2.1.2 Preparation of eggs for *in vivo* manipulation

To clear the surface of minimal contaminants eggs were spayed with 70% ethanol and allowed to dry. Using an egg-pricker the egg was pierced at the blunt end and a small hole was made on the top of the egg with a blunt pair of forceps. 1-2 ml of albumin was removed from the pierced end with 21 gauge needle attached to a 10 ml syringe, thus lowering the embryo from the shell. The top hole was covered with a piece of sellotape and a window of about 1.5 cm in diameter was cut, exposing the underlying embryo for manipulation.

Approximately 100 µl of sterile Howard's ringer containing a 1:100 dilution of penicillin/treptomycin/fungizone (AAM, Gibco) was added to the egg, to prevent bacterial and fungal infection. In order to improve the visual outlines of the embryo, a small volume of India ink (Pelikan Fount) was injected into the sub-blastodermal space, using a 1ml syringe with a 27 gauge needle. To allow direct access to the embryo, the viteline membrane was removed from the area of interest.

After manipulation a few drops of Howard's ringer was added and the egg was closed with thick black tape placed over the window. Eggs were incubated until they reached the appropriate developmental stage.

2.1.3 Harvesting and fixation

Eggs were cracked into a flat dish, keeping the yolk intact. Manipulated embryos were removed through the original window in the egg. The embryo and surrounding tissue were removed using a small pair of scissors, rinsed quickly in Howard's ringer and fixed in 4% PFA for 12-24 hours at 4 °C.

2.2 Vibratome Sections

2.2.1 Preparation and embedding

Embryos were washed 3x20 min in PBS and were then transferred into embedding wells containing 20% gelatine in PBS, prewarmed to 55 °C, and allowed to settle for 30 min. in a 55 °C waterbath. The angle of the embryo was adjusted before allowing them to set at room temperature. Once the gelatine had set, embryos were incubated at 4 °C for 12 hours in an airtight chamber to prevent drying out. The blocks were trimmed using a razor blade leaving the minimum of gelatine around the embryo. Blocks were fixed in 4% PFA for minimum 2-4 days.

2.2.2 Sectioning

Embryos were cut on a vibratome (Leica VT 1000S) using disposable blades (General Scientific) in a metal tray with PBS. Typically, sections were cut at a 40-50 μm thickness and transferred straight on to subbed slides. Excess liquid was removed from the slides and they were allowed to semi dry on a warmplate, and then coverslipped with 80% glycerol in PBS. To prevent drying, the edges of the coverslip were sealed with nail polish.

2.3 Wax Sections

2.3.1 Preparation for wax embedding

After fixation embryos were taken through a series of 50% 70% 90% ethanol washes, (2x 30 min each), and then transferred into 100 % ethanol 3 x 1 hour. After dehydration embryos were transferred into histoclear and washed 3 x 45 min. Embryos were then transferred to molten wax (Sherwood) at 62°C, and incubated for 4 hours in molten wax , which was changed every hour. Embryos older than HH 30 were left overnight to allow for maximum penetration. After wax incubation the embryos were transferred to wells containing warm wax, orientated to the appropriate angel and allowed to set at room temperature.

2.3.2 Sectioning

A microtome (Leitz 1512) was used with disposable microtome blades (Faither). Blocks were trimmed, orientated at the appropriate angle and cut at a thickness of 10μm. Sections were then transferred onto subbed slides by placing on a layer of H_2O on the slides. The H_2O had been boiled for 10 min to minimise air content. After positioning the sections on the slide, the water was removed and they were allowed to dry on a warmplate (Hearken) at 37°C.

2.4 Frozen Section

Fixed embryos were washed 3 times in PBS and transferred to 30% glycerol in PBS, until they sank. They were cryoprotected by incubation in 80% glycerol in PBS for 12 hours at 4 °C and transferred to embedding wells containing O.C.T medium (Tissue Tek). They were incubated between 12-24 hours in O.C.T medium at 4 °C, and once orientated to the right angel for cutting, were frozen at -70 °C.
Blocks were melted onto warm metal stubs and allowed to freeze onto the stubs at -25 °C. They were cut at a temperature of -18-23 °C on a Cryostat (Bright model 5030), at a thickness of 25 μm. Cut sections were melted on to warm subbed slides and allowed to dry for 1 hour.

2.5 Nissl Stain

Nissl stains were performed on wax sectioned embryos only. All embryos were fixed in Bouin's solution for a minimum of 12 hours and length of incubation times throughout the staining procedure were similar regardless the stage of the embryo.

2.5.1 Staining

500 ml glass containers were used at all staining steps which can hold plastic racks of 20 slides. Dry sections were taken through a dehydration series by initially emersing into two washes of histoclear (National Diagnostics), followed by two washes in 100% IMS (Industrial Methylated Spirit) for 5 min. each. Sections were then immersed into single washes of 90%, 70% and 50% IMS (each 5 min.) and finally quickly washed in H_2O before immersing into Nissl stain for a 12 hour incubation at room temperature. This stain was prepared by heating to 60°C to allow maximum saturation of the solution.

The solution was then slowly cooled to room temperature and filtered through Watmann paper. After incubation, the sections were washed in H_2O and surplus stain was removed by quickly washing in 70% IMS containing 1N acetic acid until the stain remained only in cell membranes. Sections were then dehydrated in 90% IMS, followed by two washes of 100% IMS. Sections were then washes twice in histoclear, coverslipped using DPX, and allowed to dry at room temperature.

2.6 Scanning Electron Microscopy (SEM)

After harvesting, embryos were fixed in SEM fixative for 4 hours at 4°C and then washed in washing solution for 4 hours to 2 days at 4°C. They were then post fixed in 1% osmium tetroxide in Millonig's constant osmolarity phosphate buffer at 4°C for 90 min. They were then dehydrated through an acetone (Analar) series at room temperature for 10 min each step, (H_2O, 10%, 50%, 70% and 90%). This was followed by two washes in absolute acetone and 1 wash in absolute acetone that had been filtered dry. Embryos were then critical point dried in a Emscope CPD 750 critical point dryer, followed by mounting onto metal stubs with carbon conductive paint. The mounted

embryos were coated with a thin layer of gold using a sputter coater (model SC500), and were then viewed using a scanning electron microscope (S520).

2.7 Transmission Electron Microscopy (TEM)

2.7.1 Fixation and preparation for Resin embedding

Embryos were fixed, washed and postfixed as for S.E.M. This was followed by dehydration in 10% ethanol for 10 min., 70% ethanol for 30 min and finally 3x20 min. 100% ethanol washes. Embryos were then transferred to propylene oxide for 2x10 min., to aid impregnation of the resin. They were then transferred to a 1:1 mixture of propylene oxide and resin (TAAB premix medium resin) for 90 min, and subsequently incubated for 5 hours in pure resin. Embryos were transferred to embedding vials and left to set in resin for 6 hours.

2.7.2 Sectioning

Once the resin was hard, embryos were cut on a microtome using glass knives freshly prepared for each cutting. Orientation and dorsal-ventral position of sections were checked under the microscope by cutting semithin sections of 1µm thickness, which were transferred onto glass slides, allowed to dry on a hotplate at 60 °C and stained with 1% Toluidine Blue. When the appropriate orientation and position were achieved, the knife was changed to a diamond knife filled with filtered H_2O and ultrathin sections (0.1 µm) were cut on the automatic setting and collected on the water surface.

Usable sections had a gold-silver colouring, and once sufficient sections of this colour had been cut, a glass rod dipped in chloroform was passed over the sections. This stretches the section and prepares for collection on meshed grids. Grids were first coated in a 1.5% solution of Formvar resin and allowed to dry for 1 min. Section were collected from the water filled diamond knife onto the grids and placed face up onto Whatmann filter paper to dry.

2.7.3 Staining

Once sections were thoroughly dry they were stained in uranyl acetate for 12 minutes by immersing grids face up into the solution. Sections were rinsed by several washes, initially by pouring in distilled H_2O followed by dipping in 3 pots of distilled H_2O, 20 times each. Grids were then placed face downwards on drops of lead citrate solution and left for staining for 12 min, and washed as described. After drying the sections were transferred to gelatine capsules to prevent damage to the sections, and were not removed until viewed, with a transmission electron microscope (Hitachi H7000).

2.8 Whole-Mount Immunocytochemistry

Concentration of various primary and secondary antibodies used for immunocytochemisry are described in appendix 1. For all of the antibodies similar protocols were used apart from RMO 270. Unless otherwise stated, all washes were carried out in washing solution containing PBS 1% triton (sigma) and 1 % goat serum(GS).

Fixed embryos were washed twice in PBS, followed by a 10 min. in washing solution. They were then transferred into cryoprotection solution and left for 45 min. to settle. Embryos were then incubated twice at -20°C until just frozen, allowing the embryos to thaw and reach room temperature after each incubation. Fresh cryoprotection solution was added prior to each freeze incubation. After the last thawing embryos were washed 3 times in PBS, 1% triton, 5%GS and incubated for 12 hours in PBS 1% triton, 5%GS containing 0.1% H_2O_2. After incubation, embryos were washed 3 times in washing solution and incubated in the appropriate antibody for 4-5 days.

After antibody incubation embryos were washed 3 times in washing solution followed by 7 hourly washes in washing solution. The appropriate secondary antibody was added and left for 12 hours to bind. Then embryos were washed for 3x5 min followed by 3 hours in washing solution. Embryos were then washed for 2x20 min in PBS, 2x30 min in 0.1 M tris buffer pH 7.4, and incubated for 3 hours at room temperature in inactive DAB in 0.1 M Tris buffer pH 7.4. To activate the DAB reaction approximately 50µl of a 1:100 dilution of 30 % H_2O_2 was added to the remaining DAB solution, and the stain was allowed to react under constant rocking to allow access to all areas of the embryo. Typically, reaction times were about 2-5 min. Once the required staining intensity was

obtained, the embryos were washed quickly twice in tap water, followed by washing in PBS. Stained embryos were fixed in 4% PFA.

2.8.1 RMO-270

For staining with RMO-270 antibody, embryos were washed in 3xPBT and then taken through a series of 25%,50%,75% methanol in PBT. They were then washed twice in 100% methanol and left at -20°C for 12 hours in 100% methanol. After incubation embryos were rehydrated through 75%,50% and 25% methanol in PBT, followed by two washes in PBT. Embryos were then washed twice in PBS, 1% triton, 5%GS and incubated in PBS 1% triton, 5%GS containing 0.1% H_2O_2 for 12 hours. The remaining protocol was similar to the one described above.

2.9 Immunocytochemistry on Sections

Immunocytochemistry was performed on vibratome sections of embryos that had been fixed in 4% paraformaldehyde. All staining procedures were carried out in 48 well plates. Sections were transferred into PBS containing 1% triton, 5% GS and 0.1% H_2O_2 for 1 hour. Sections were then washed 3x10 min in PBS, 1% triton, 5% GS and incubated with 10% GS for two hours. The GS was removed and primary antibody added at the appropriate concentrations in PBS containing 10% GS and 1% triton, for 12 hours at 4 °C. Sections were washed 6x10 min in PBS with 1% triton, 1% GS. They were then incubated with PO-conj. secondary antibody at the appropriate concentration for 4 hours at room temperature. Sections were washed 3x10 min in PBS with 1% triton, 1% GS and quickly in PBS to remove excess triton and GS. Detection of antibodies was performed as for whole-mount immunocytochemistry.

2.10 *In-Situ* Hybridisation

2.10.1 Preparation and synthesis of probe

Approximately 10µg of plasmid DNA was linearised using 10 µl of restriction enzyme in 100 µl of appropriate buffer solution and incubated for 3 hours at 37 °C. Linearasation of plasmid DNA was confirmed by gel electrophoresis on a 1% agarose

gel with 1% ethidium bromide compared to uncut plasmid. Linearised DNA was purified by phenol/chloroform extraction and precipitated in 3 x volume 100% ethanol, 0.1 x volume 3 M sodium acetate (RNAse free) for 30 min at -20 °C. DNA was precipitated at 13 K for 15 min., and the resulting supernatant was removed and the pellet allowed to air dry. The pellet was then resuspended in 10 µl PEPC-H_2O.

For the transcription of probe, a reaction mixture of 1µg linearised DNA, 2µl appropriate RNA polymerase (Promega), 4 µl 5x transcription buffer (Promega), 4 µl 5x nucleotide mixture (digoxygen (DIG)or fluorscein (FITC) labelled) (Promega), 2 µl 100 nM DTT (Promega), 1 µl RNAse inhibitor (Promega), made up to 20 µl with DEPC-H_2O was used. The reaction was incubated at 37°C for 2 hours and then the DNA was digested for 15 min. using 1 µl DNase (RNAse free) and an additional 1 µl RNAse inhibitor added, to prevent RNA degradation.
RNA was precipitated by adding 3 x volume 100% Ethanol and 0.1 x volume 4M LiCl and incubated on ice between 15-30 min, followed by centrifugation at 13K for 15 min. The resulting pellet was dissolved in 100 µl H_2O to give an approximate concentration of 1 µg/µl. Probe synthesis was confirmed by gel electrophoresis as for DNA linearisation.

2.10.2 Hybridisation

Embryos were washed twice in DEPC-PBS and dehydrated to permeabalise membranes, through a methanol series of 25%, 50% and 75% methanol in DEPC-PBT, washed in 100 methanol twice and left in 100% methanol at -20 °C for at least 12 hours. To rehydrate, embryos were taken through 75%, 50%, 25% methanol in DEPC-PBT and washed twice in PBT. Embryos were bleached for 1 hour in PBT containing 6% H_2O_2 and then washed 3 times in PBT. To increase permeability embryos were taken trough 3x20 min washes of detergent solution and postfixed for 20 min in PFA containing 0.2% gluteraldehyde. To remove fixative, embryos were washed 3 times in PBT and transferred into hybridisation solution at 70 °C for a minimum of one hour. The appropriate probe was mixed to prewarmed hybridisation solution at a concentration of 10µg/1 ml and added to the embryos, followed by a 12 hour incubation at 70 °C.

After incubation embryos were washed 4x30 min with solution X at 70 °C and allowed to cool to room temperature in a 50/50 mixture of solution X and MABT. This was followed by 3 washes with MABT and any solution X left in embryos was removed by washing 2x30 min in MABT.

2.10.3 Immunocytochemistry

To block non specific binding, embryos were first incubated for 1 hour in MABT, 2% BBR followed by a 2 hour incubation in MABT, 2% BBR, 20% goat serum(GS). To this solution the antibody (AP-conj anti-dig or anti-Fitc) was added, at a concentration of 1:2000 and incubated for 12-36 hours at 4 °C. The embryos were washed 3 times in MABT followed by 7 hourly washes in MABT, followed by a overnight wash in MABT at room temperature. The AP-conj anti-dig antibody was detected by a mixture of NBT/BCIP. Initially embryos were washed 4x10 min in NTMT pH 9.5, followed by addition of reaction mixture containing 3.5 µl/ml NBT, 3.5 µl/ml BCIP in NTMT pH 9.5. Reactions were kept at room temperature in the dark until the stain was sufficiently developed or reaction mixture turned purple, at which point new reaction mixture was added.

After required staining intensity was achieved the reaction was stopped by washing in NTMT pH9.5 for 10 min., followed by 2 washes in PBT. Embryos were fixed to preserve stain in 4% PFA. Embryos with a AP-conj anti-fitc antibody were washed 4x10 min in NTMT pH 8 and then transferred into Fast Red (Sigma) until required stain intensity. Fast Red was made by dissolving 1 tablet of buffer in 1 ml of DEPC-H_20. Once the tablet was dissolved 1 tablet of Fast Red was dissolved and made up to 3 ml. with NTMT pH 8. Reaction was stopped as for the dig-labelled probe.

2.10.4 Double labeled *in-situ* hybridisation

The protocol for detection of a dig-labelled and a fitc-labelled probe in the same in-situ reaction is similar to the above described protocol apart from the following modifications. 1) Both probes are added together during the 12 hour incubation in hybridisation solution at 70 °C. 2) The dig labelled probe was detected first and to

ensure that alkaline phosphatase reaction is fully inactivated, embryos were post fixed for 12 hours after the detection of the dig-labelled probe. This was followed by the immunohistochemistry step described above with the final detection with Fast Red.

2.11 Bromodeoxyruidine (BrdU) Labeling

Embryos were prepared for *in vivo* labeling as described in 2.1 (Preparation of eggs for *in vivo* manipulation). To perform the labeling it was however not necessary to remove any overlying membranes, or inject with ink and due to the short survival period only Howard's Ringer was used. Unless otherwise stated, all stages of embryos were labeled for 30 min, each with 10 µl BrdU solution.

2.11.1 Labeling

Thin-wall single-barrel standard borosilicate glass capillaries (World Precision Instruments), were used to make micropipettes on a Flaming/Brown micropipette puller model p-87. For the injection, a mineral oil (Sigma) based injection system (Narishige IM-6) was used, which allowed full manual control of the injection. All injections were hand held to allow more flexibility when injecting.

For HH 12-16 embryos BrdU was injected just above the head beneath the viteline membrane. For HH 17-24 embryos BrdU was injected into a blood vessel with blood flowing in the direction of the embryo, thus carrying the BrdU quickly via the blood stream to the entire embryo. For embryos older than HH24, BrdU was injected straight into the third ventricle through the midbrain. Embryos between HH 30- HH 32 were also allowed to survive for 4 hours.

After incubation with BrdU embryos were killed quickly by removing from the egg into 4% PFA and fixed for 12 hours. After fixation, embryos were taken through the in-situ hybridisation and left to wash in PBT for 12 hours.

2.11.2 Immunocytochemestry

Embryos were incubated for 1 hour at room temperature in 2N HCl, to prepare the DNA for the antibody binding. They were washed 4 times in 0.2 M Tris pH 8.5, followed by 3x5 min washes in PBS. To prevent non specific binding they were incubated for 3 hours in PBS, 3% GS, 1% triton. To detect incorporated BrdU, embryos were incubated for 4 days at 4 °C in a 1:10 dilution of anti-BrdU antibody (Becton-Dickington) in PBS, 3% GS, 1% triton.

Embryos were washed 3 times in PBS, 1% triton, followed by 6 hours of hourly changes. They were incubated with a Cy3-conjugated secondary antibody for 18 hours in PBS, 1% triton at 4 °C. This was followed by several washes in PBS, 1% triton to ensure that unbound antibody was washed out. Embryos were post fixed and prepared for vibratome sectioning.

2.12 DiI Labeling of Glial Cells

Embryos at the appropriate stage were fixed for a minimum of 7 days. For this technique it is important to keep the embryos in fix for as much of the time as possible. Thus for the labeling procedure itself, embryos were kept in small wells containing 4% PFA. The micropipette and injection systems were similar to the one used for BrdU labelling.

For the injection 1 µl of a 6mg/ml DiI was added to 250 µl Howard's Ringer. This allows the DiI to form small crystals, where larger DiI crystals were prevented by vigorous votexing. To further ensure that crystals did not aggregate, a fresh solution of DiI in Ringer was made up before each injection. The needle was inserted through the midbrain into the third ventricle and approximately 10 µl of DiI was injected into embryos between HH14-22, and 20 µl into embryos between HH 24-28.
After injection embryos were incubated at room temperature for 5 days to allow full penetration of the DiI. They were then prepared for vibratome sectioning, as described above. However since some PFA should remain in the tissue to prevent dye spread, embryos were only washed a few times in PBS and left for no longer than 5 min in warm gelatine before they were allowed to set.

2.13 Dextran Labeling

Embryos were prepared for in vivo work as described in 2.1 (Preparation of eggs for *in vivo* manipulation) and allowed to survive for 48 hours before fixation.

2.13.1 Labeling

With a tungsten needle a small hole was cut through the mesenchyme and epithelium either just above the eye on the right side of the embryo (facing upwards), or in the most anterior dorsal part of the midbrain. This hole was large enough to allow the needle to pass through without touching any tissue.

Single-barrel standard borosilicate glass capillaries with filament were used for the injection, fixed in a holder on a metal rack. To label cells, an iontophoric technique was used, where dye is injected into the cells using an electric current. This was achieved by backfilling the needle, once loaded with dye, with 1M LiCl and inserted into a holder filled with 1M LiCl. The LiCl is in direct contact with a silver wire which was connected to the positive terminal of a 9 V. battery, when injection was required. To close the circuit, an electrical wire connected to the negative terminal of the battery, was inserted into the end of the egg, usually through the hole generated when the albumin was removed during preparation.

The dye-filled needle was manoeuvred through the hole in the embryo to touch the ventricular surface of the opposite side. Injection was achieved by touching the wire from the needle holder to the positive terminal for approximately 0.5-1 min. Injection was confirmed by using a fluorescence stereomicroscope which visualises the rhodamine-labelled dextrans.

2.13.2 *In-situ* hybridisation and immunocytochemistry

After incubation embryos were removed from the eggs and fixed for 12 hours. They were then hemisected and viewed on a Zeiss Axiophot to determine the site of labelling. *In-situ* hybridisation with the appropriate molecular marker was performed as described above.

After fixation embryos were washed three times in PBS and incubated for 2 hours in PBS 1% triton, 5% GS to prevent any non specific binding. A PO-conjugated streptavidin antibody (1:250) was used to detect the biotin-labelled dextran and incubated for 18 hours. Embryos were washed 3 times in PBS 1% triton, 1% GS followed by 3 hourly washes in PBS 1% triton, 1% GS. Embryos were then washed twice in PBS and transferred into inactive DAB in PBS. The detection was similar to that described for whole-mount immunocytochemistry. After fixation embryos were flatmounted and coverslipped and viewed under the Axiophot.

2.14 Double labeling with DiI and DiO

Embryos were prepared for in vivo work as described in 2.1.2 (Preparation of eggs for *in vivo* manipulation) and for injection as described in 2.13.1 (Labeling), apart from the following exception. To access the ventricular surface on the left side of the embyo (facing downwards) a small flap was cut with a tungsten needle above the eye. Injection with DiI was carried out as for injections with Dextrans. DiO was injected using a mineral oil (Sigma) based injection system (Narishige IM-6). After manipulation embryos were allowed to survive for 48 hours, and were then fixed in 4% paraformaldehyde for 12 hours. After fixation embryos were flatmounted and coverslipped and viewed under the Axiophot.

Chapter 3

Neuromeric division based on morphology

I used three main criteria to identify neuromeres within the diencephalon: gross morphology, neuroepithelial organisation and neurogenesis. The first criterion was neuromeric morphology, which has been defined as a bulge of neuroepithelium delineated by grooves, which internally appear as troughs delineated by ridges (Von Baer 1928). These structures were identified through the use of Scanning Electron Microscopy (SEM), which visualises the physical appearance of the ventricular surface both at low and high magnification. The second criterion was the organisation of the neuroepithelium itself, which should correspond to the neuromeric structure described above. The visualisation of the neuroepithelium was performed using straightforward staining techniques, in particular Nissl's, on sectioned material. This classical approach reveals the epithelial cell organisation with respect to cell clustering and shape as well as the thickness of the epithelium itself. The final criterion for neuromeric division was the spatial and temporal appearance of neurogenesis, where a neurogenic phenotype was identified through immunocytochemistry with a neurofilament specific antibody. Neurogenesis should initially be restricted to individual neuromeres and be separated from adjacent neuronal populations. The use of these three techniques enabled me to map the spatial and temporal neuromeric subdivision of the diencephalon and thereby predict the appearance of boundary regions between the neuromeres.

3.1 Colour coding

Throughout all of the results chapters the boundaries between the different neuromeres will be marked by a different coloured arrow. Thus, the boundary between the midbrain and the synencephalon is marked by a red arrow ➡, and the synencephalic-parencephalic boundary is marked by a yellow arrow⇨. The zli, the interparencephalic boundary between the dorsal and ventral thalamus, is marked by a blue arrow➡, and the boundary between the anterior and posterior part of the synencephalon is always marked by a purple arrow ➡.

Figure 4

HH14-

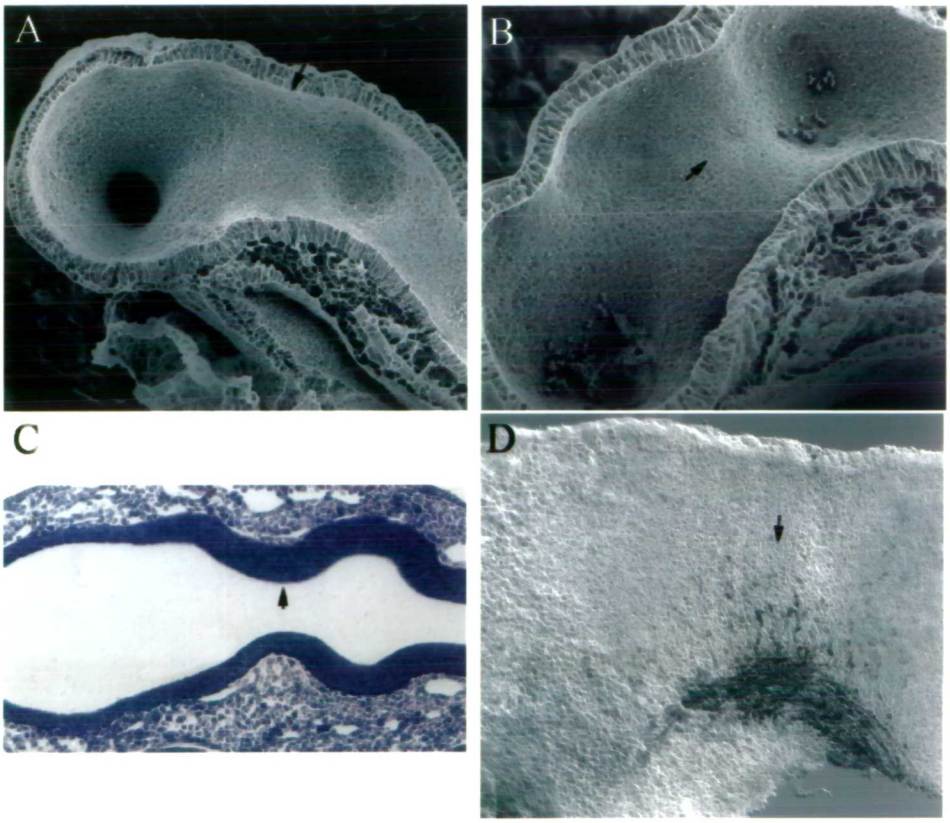

HH 18

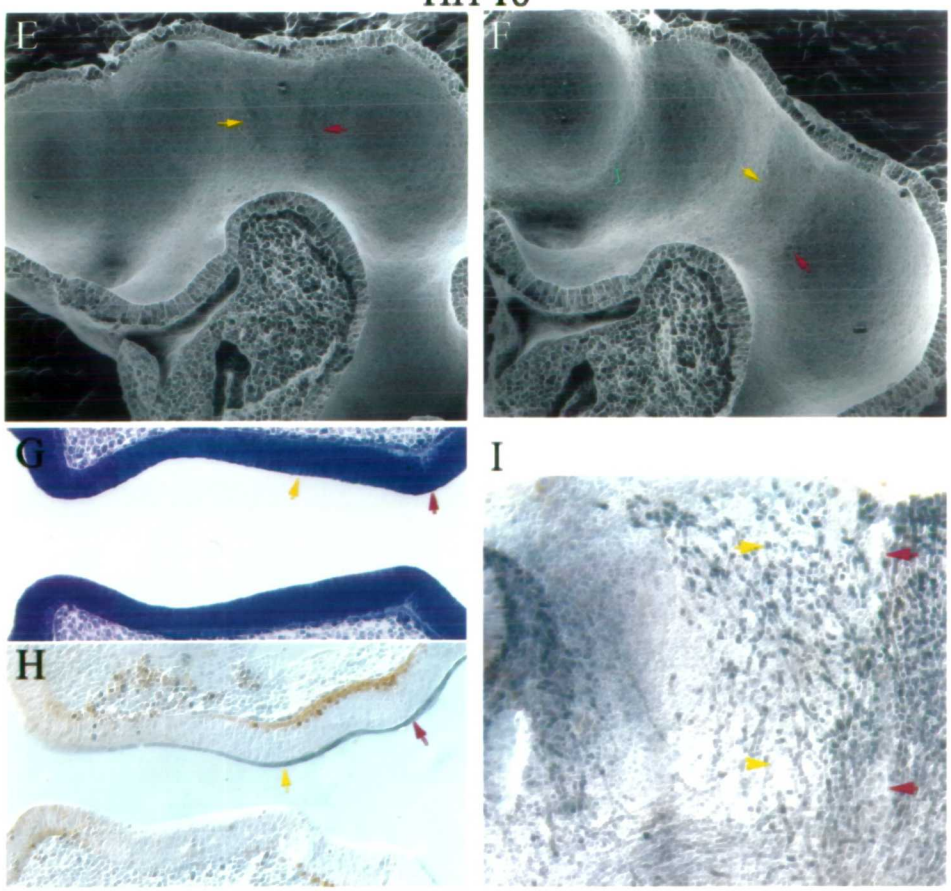

3.2 Dorso-Ventral division

The initial division within the neural tube occurs at HH14 in the dorso-ventral plane, prior to neuromere formation. The presumptive synencephalic neuromere has no apparent neuromeric structure yet, but appears as a bulge on the inside of the ventricular surface (Figs. 4A, B, C), with no apparent physical ridge between it and the rest of the diencephalon. The pattern of neurogenesis however, indicates that at this stage the neural tube is divided into a dorsal alar and a ventral basal component. This is contemporaneous with the formation of the medial longitudinal fasiculus (mlf) extending along the basal part of the brain (Fig. 4D). Within the alar plate a few neurons can be recognised ventrally (marked by a black arrow), whereas there is no staining in the dorsal aspect of the alar plate.

3.3 HH 16: Subdivision into Synencephalon and Parencephalon (yellow arrow)

The first neuromeric subdivision in the diencephalon is apparent at HH 16, when the synencephalon adopts a typical neuromeric morphology (Figs. 5A, B, C,). Its borders with the midbrain and parencephalon are marked by ridges that forms transverse lines extending from the dorsal midline and nearly to the ventral midline. In Figs. 5B, and C the ridge between the midbrain and synencephalon and the ridge between the synencephalon and the parencephalon, are easily recognised by their lighter colouring. This is compared to the darker areas within the neuromere and the parencephalon and midbrain, reflecting the concave nature of the latter. At this stage, the organisation of the neuroepithelium is pseudo-stratified and appears to be similar throughout the diencephalon (Fig. 5D). The angle of this section reveals the ridges on both sides of the synencephalon and demonstrates that there is little difference in the thickness of the neuroepithelium between the synencephalon and the parencephalon.

Within the synencephalon, neurofilament staining reveals that a few neurons and axons can now be identified at the dorsal aspect of the neural tube, presumably corresponding to the first neurons of the posterior commissure (Fig. 5E). These can readily be distinguished from the more posterior situated neurons within the midbrain, since the latter are closer to the dorsal midline. The ventrally situated group of neurons and axons within the alar plate appear to either originate from the mlf or send their axons into the

Figure 5

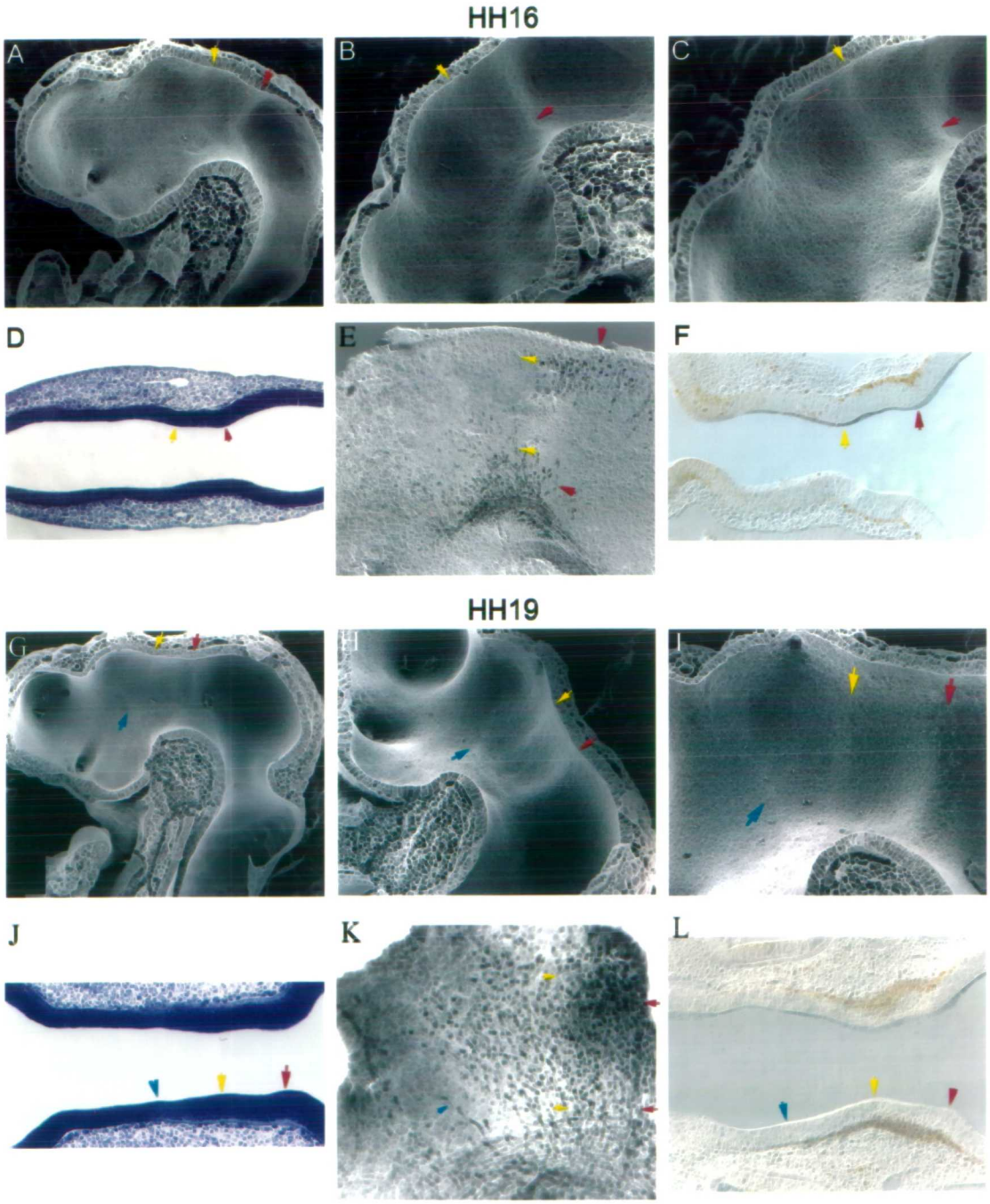

mlf (Fig. 5E). Although the adjacent parencephalic neuronal population seems continuous with the synencephalic group, there is a clear change in axonal trajectories, which seem to follow the curvature of the parencephalon (Fig. 5E). A few axons within the parencephalon appear to project along the boundary and turn 90 ° into the parencephalon. Similar to the synencephalic neuronal group, the axons from the parencephalic group of neurons also appear to originate or project to the mlf. However, unlike the synencephalon at this developmental stage, there are no neurons located at the dorsal aspect within the parencephalic portion of the diencephalon. This pattern of neurogenesis indicates that not only is there a ventral to dorsal gradient of neurogenesis, but also a caudo-rostral gradient, where the synencephalon is more advanced than the parencephalon. This is well illustrated in Fig. 5F, a neurofilament stained horizontal section taken from the ventral part of the diencephalon. This slightly oblique section shows a thicker and stronger staining within the synencephalon, and only little staining within the parencephalon.

3.4 HH 19: Subdivision of the parencephalon- the zona limitans intrathalamica (zli) (blue arrow)

The zli is the ridge that separates the parencephalon into the ventral and dorsal thalamic neuromeres. Unlike the ridges delineating the synencephalic neuromere, the zli extends gradually from the most ventral part of the alar plate towards the dorsal aspect of the alar plate. This gradual growth takes place over a period of stages beginning at HH 19 and is not fully extended until HH 26. Not only is there a ventral to dorsal extension of the zli, but it also expands as development proceeds so that initially the ventral part is considerably wider than the dorsal part. HH 19 is the first stage that the initial ventral ridge formation can be recognised by SEM, and it extends at an angle of approximately 45 ° compared to the ridge separating the dorsal thalamus and the synencephalon (Fig. 5G-H). As a result, the dorsal thalamus is in a shape of a triangle with a rounded top edge, illustrated in Fig. 5I. At this stage, the basal-alar division of the diencephalon is more obvious, since the ridges clearly do not meet the ventral midline but stop some distance away.

All three ridges are also visible in the horizontal Nissl stained section shown in Fig. 5J. This section is through a ventral position, which allows all three ridges to be visualised,

although only the most dorsal part of the zli is seen and is thus not that prominent. This figure also shows that the organisation of the neuroepithelium appears to be similar throughout the diencephalon. At the basal edge of the neuroepithelium there is a clearing of cells, which constitutes the marginal layer. This is where the axonal processes are located, and appear on these stained sections as pale purple. The axonal processes have come from neurons, which after migrating from the epithelial zone have settled in the mantle layer. The matrix layer or ventricular zone is the layer of proliferating cells, which appears darkly stained neuroepithelium. The marginal layer is observed in both the synencephalon and the dorsal thalamus, but is absent from the ventral thalamus. It is also possible to see that the cells within the dorsal thalamus are packed less tightly than their synencephalic counterparts, especially towards the lateral edges of the epithelium. Since this section is taken ventrally, it is not possible to see the clearing of cells within the ridge between the synencephalon and the midbrain, which is present in the section of a HH 18 embryo shown in Fig. 4G. This clearing of cells is clearly demonstrated in the section taken through the HH 18 embryo at a more ventral level. At this ridge the clearing of cells starts in the middle of the epithelium and meets the basal edges of the neuroepithelium (Fig. 4G).

At HH 19, neurogenesis has advanced considerably since HH 16, but a general ventral to dorsal gradient of maturation can still be recognised by neurofilament staining in Fig. 5K. The entire synencephalic neuromere is filled with neurons and axons, which are more tightly packed towards the dorsal part of the neuromere. Similar to the ventral part of the synencephalon, the neuronal population within the dorsal thalamus is sparse but even throughout this neuromere. Axonal trajectories within the dorsal thalamus seem to follow the forming zli.

This projection angle is also seen amongst neurons at the ventral part of the synencephalic neuromere, which project towards the dorsal thalamus but do not cross the synencephalic-parencephalic boundary. The anterior part of the dorsal thalamus towards the zli shows very little neurogenesis, and this is also the case for the posterior part of the ventral thalamus, which is almost devoid of neurons. Towards the anterior edge of the ventral thalamus, there is an evenly spaced neuronal population, both dorsally and ventrally. Fig. 5L shows that the marginal layer within the synencephalon is considerably thicker than that of the dorsal thalamus and that the thickness of the

neuroepithelium is larger at the posterior part of the dorsal thalamus compared to the anterior region.

3.5 HH 22: Subdivision of the Synencephalon (purple arrow)

The subdivision of the synencephalon can be recognised from HH 22 onwards, but it does not form a clear ridge shaped structure like the other neuromeric borders. Figs. 6A and C show that the posterior part of the synencephalon is bulging outwards compared to the anterior part. Adjacent to this bulge a ridge can be recognised as a small swelling of the tissue. It is only visible as a slight shadowing on the caudal slope of the ridge, which indicates that this ridge is considerably smaller than the others. It seems that the ridge that forms the boundary between the synencephalon and the dorsal thalamus is beginning to be become less detectable towards the middle of the neural tube. The dorsal part of the ridge is still visible in Fig. 6C and the ventral part can be seen in Fig 6B, but there is no obvious ridge formation between the two points. Fig. 6B also demonstrates that the zli has thickened considerably at its ventral aspect, forming a clear ridge extending dorsally but not reaching the dorsal midline (see Fig. 6A).

The reason for the bulging of the posterior part of the synencephalon becomes clear when looking at the Nissl stained serial sections shown in Fig. 6F and G. A dorsally situated section shows that the ventricular zone maintains the same thickness throughout the synencephalon, but a clearing of cells within the tissue is apparent within the posterior synencephalon (Fig. 6G). The clearing of cells forms a line corresponding to the location of the forming posterior commissure and may represent the location of the axons within this tract (marked by a black arrow). It also clearly divides the synencephalon into a posterior and an anterior part, where the latter does not appear to have an equally developed mantle layer. At the level of this section, the ridge between the synencephalon and dorsal thalamus is still recognisable although it has diminished in size compared to earlier stages. A more ventral situated section (Fig. 6F) shows that the neuroepithelium of the dorsal thalamus has enlarged and is slightly thicker than that of the synencephalon. The zli is easily identified by a clearing of cells within the ridge (Fig. 6F), similar to that seen at the boundary between the synencephalon and midbrain at HH 18. This clearing is particularly obvious towards the basal part of the epithelium, where it seems to join with the marginal layer. When comparing Fig 6F and G it is clear

Figure 6

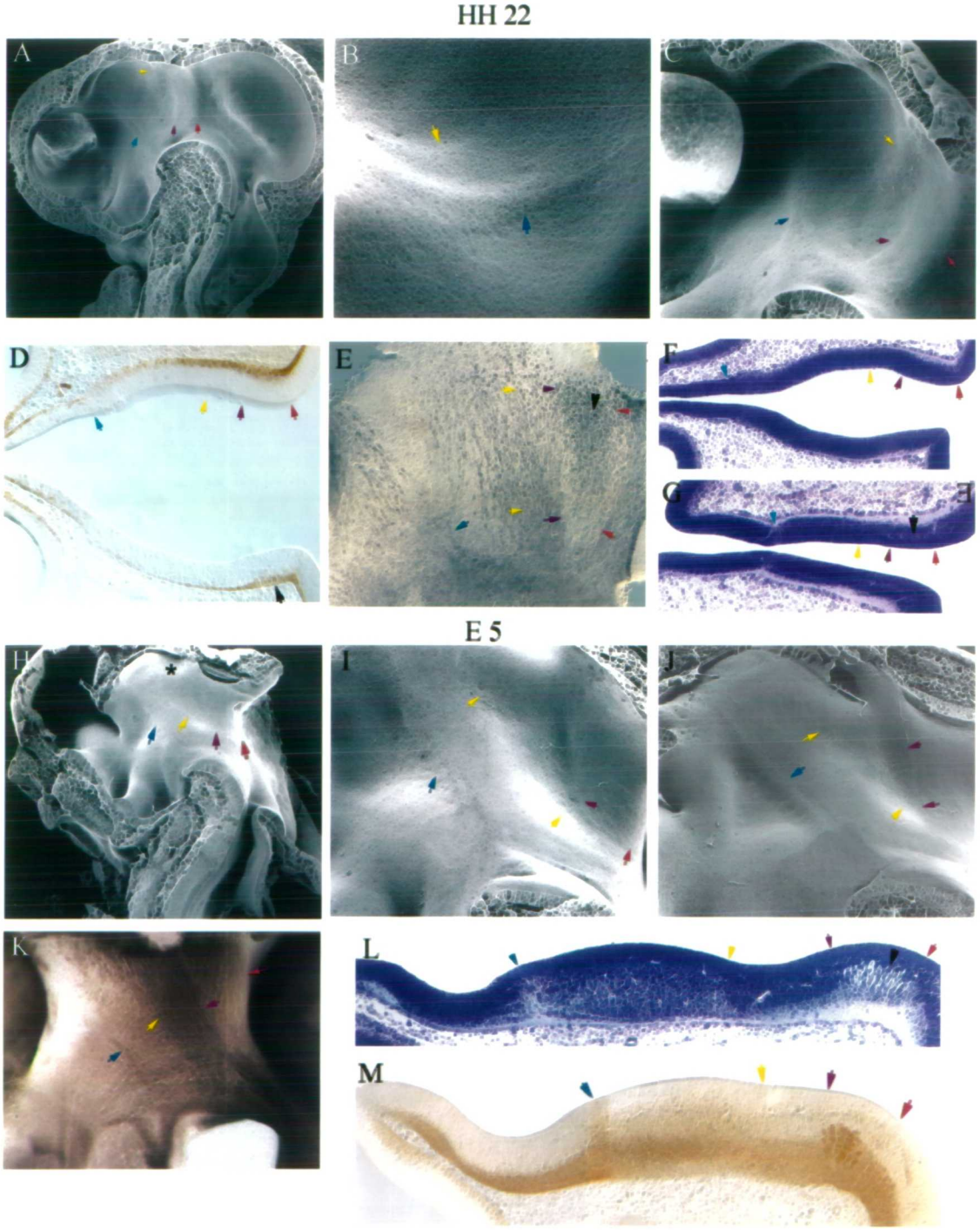

that the marginal layer is considerable thicker at ventral levels (Fig. 6G) compared to dorsal levels (Fig. 6F). The clearing of cells within the midbrain-synencephalic ridge is still noticeable in the dorsal section.

Fig. 6D and E demonstrate that the neuronal population expressing neurofilament within the posterior synencephalon has increased (marked by a black arrow). This neuronal group is wider at the dorsal aspect and appears to narrow towards the ventral part of the alar plate. Immediately adjacent and anterior to this population there is an area of lower staining which mirrors the shape of the posterior synencephalic neuronal population. Dorsally the boundary between the anterior and posterior part of the synencephalon is adjacent to the presumptive posterior commissure and does not include this area of low staining. However, in the ventral aspect, the posterior synencephalon does include this area and the boundary is just posterior to the high levels of staining seen within the anterior synencephalon.

Unlike the neurons in the posterior part of the synencephalon, the anterior synencephalic neuronal population seems to project towards the dorsal thalamus and furthermore may cross the boundary. Therefore, the boundary between the dorsal thalamus and the anterior synencephalon is difficult to identify, in particular in the ventral aspect, where the two neuronal populations are continuous. Accurate identification can only be achieved by noting the location of the ridge prior to flatmounting. In the dorsal aspect, neurons are evenly spaced between the anterior synencephalic and the dorsal thalamic neuromeres. The area around the zli is still fairly devoid of neurofilament staining, although the ventral thalamic neuronal population has extended caudally compared to HH 19. The neurofilament stained section shown in Fig. 6D shows the thickening of tissue containing neurons and axons within the marginal zone. Neurons within the marginal layer can now be detected in the ventral thalamus.

3.5 Morphological development up to E5

Between HH 22 and E5 the ventricular surface of the embryo changes considerably (Fig. 7F-J). At HH 24 the ridge between the dorsal thalamus and the synencephalon has disappeared and now looks like a swelling, which slopes towards the anterior part of the dorsal thalamus (Fig 7F). This is particularly clear on the Nissl stained section shown in

Figure 7

HH 21

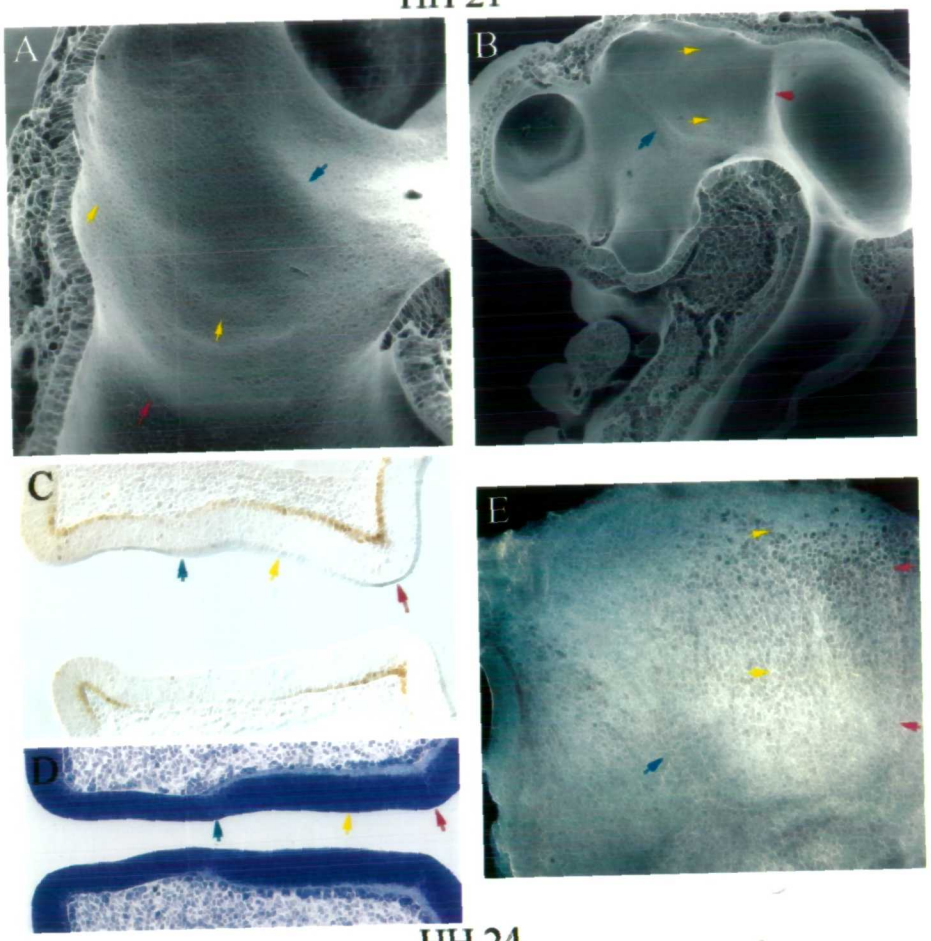

HH 24

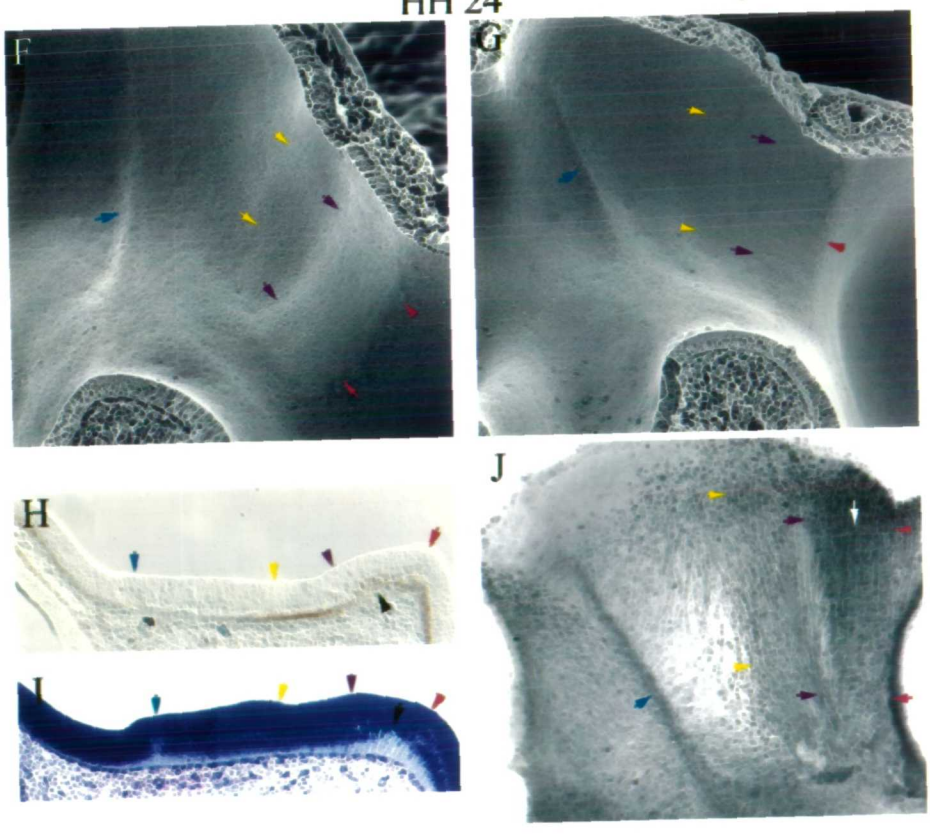

Figure 8

HH 26

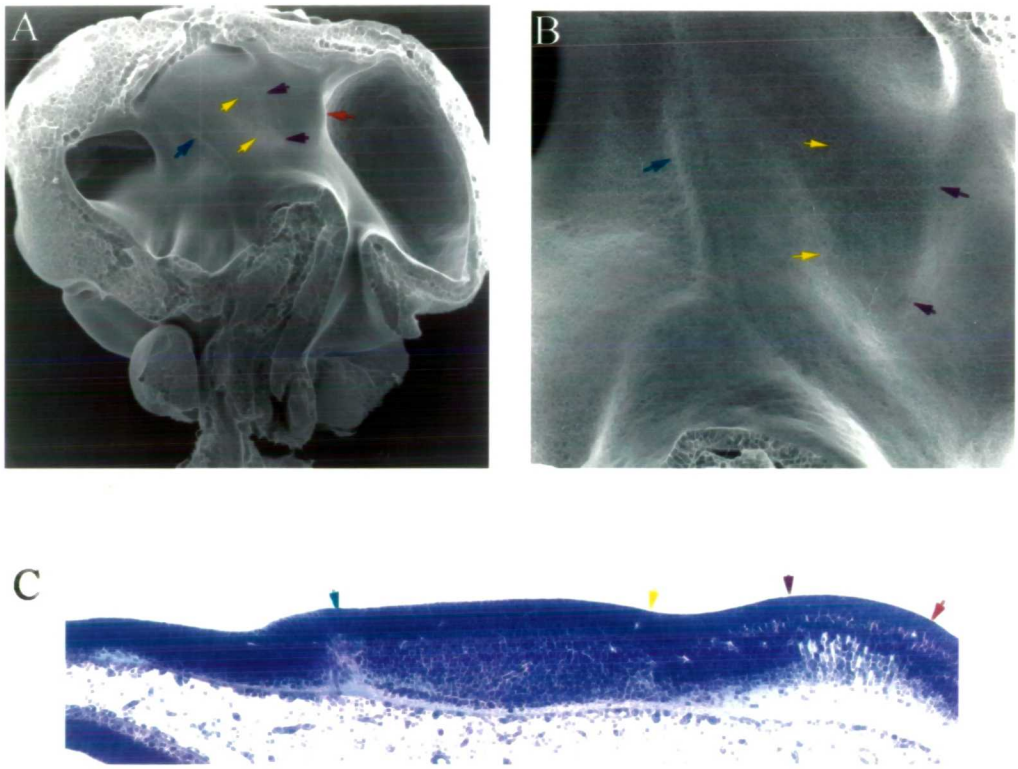

Fig 7I, which also shows the appearance of the posterior commissure (marked by a black arrow) at the caudal level of the synencephalon, within the marginal layer and the basal part of the mantle layer. The appearance of the posterior commissure is also visible in Fig. 7J, where the neurofilament stained axons and neurons of the posterior commissure are clearly separated from the more diffuse axons of the anterior synencephalon.

The axons of the posterior commissure can be clearly seen within the posterior part of the synencephalon, and the adjacent stripe of low staining is more obvious. In the extreme ventral part of the posterior synencephalon, a few neurons cross the boundary into the anterior part of the synencephalon (Fig. 7J). The anterior synencephalic neuronal group is more defined compared to earlier stages and a few axons extend into the dorsal thalamus. The neurons within the dorsal thalamus are still more sparsely packed compared to the two synencephalon neuronal populations, although the former are more clearly seen at the dorsal aspect compared to the ventral aspect. Strong staining is seen throughout the zli and it seems that axons project into the zli from both sides in particular from the ventral thalamus.

Between HH 24 and 26 the ventricular surface of the diencephalon changes considerably (see Figs. 8A-C). By E5 (Figs. 6H-J) all the ridges apart from the zli have disappeared, and instead the surface appears as a series of large grooves and bulges, resembling the ventricular sulci described in earlier literature. The posterior part of the synencephalon bulges considerably inwards into the lumen of the third ventricle, whereas the anterior part of the synencephalon is left as a large groove, now shaped like a triangle. The dorsal thalamus has changed its shape from that seen at HH 24 and appears as an elongated quadrant, which increases in width ventrally and is slightly narrower at the dorsal aspect. The angle of this quadrant corresponds to the zli, which is still 45 °. Within the extreme dorsal part of the dorsal thalamic neuromere there is a rounded region, marked with a star in Fig. 6H, that will later form the epithalamus. Note also that the zli has now thickened through out its entire length, protruding from the surface compared to the shallow triangular groove of the ventral thalamus.

Neurogenesis has advanced considerably and each neuromere appears to contain a separate sheet of projecting axons (Fig. 6K). The neuronal sheets of the anterior part of

the synencephalon and the dorsal thalamus project at the same angle, that of the zli, whereas the posterior synencephalic sheet does not. It appears that some of the neurons in the ventral part of the anterior synencephalon originate within the posterior synencephalon, and projects into the anterior synencephalon. Therefore, the pattern of neurogenesis does not fit the general morphology seen by SEM, indicating that the ventricular sulci seen at later stages of development do not exclusively reflect neuronal organisation.

The dorsal thalamus and anterior part of the synencephalon contain separate neuronal groups, where the latter group is more strongly stained. The staining within the zli is reduced compared to that of HH 24 and is now only visible within the ventral part, which is probably due to the relatively increased staining of both the dorsal and ventral thalamus. The explanation for the relatively increased staining within the anterior synencephalon compared to the dorsal thalamus is seen in a section through the neural tube stained with neurofilament specific antibody (Fig. 6M). Neurons extend further into the mantle layer and are more diffuse in the dorsal thalamus compared to the anterior synencephalon, where neurons are packed at a higher density closer to the basal wall of the neural tube. The posterior commissure can be seen in the posterior part of the synencephalon as groups of neurons and axons.

The differences between each neuromere within the diencephalon are recognised in the Nissl preparation seen in Fig. 6L. The ventricular and mantle layers can be distinguished, where the former appears as a tightly packed, heavily stained band of cells along the ventricular surface. The adjacent mantle layer is packed less densely and is considerably thicker than the ventricular layer at this stage. The posterior commissure spans most of the mantle layer of the posterior synencephalon, visible as faint axonal staining and a few scattered stained cells. The cells within the anterior part of the synencephalon, on the other hand, are more tightly packed throughout the majority of the mantle layer. Just rostral to the synencephalic-dorsal thalamic boundary there is a lighter packed area of cells, appearing as a triangle, compared to the rest of the dorsal thalamus which is evenly packed. The zli is still almost devoid of cells within the mantle region, whereas the ventricular layer is still evenly packed although thinner than the rest of the diencephalic ventricular region. Within the ventral thalamus, the cells are tightly packed and it is difficult to distinguish a separate mantle and ventricular layer.

Figure 9

A

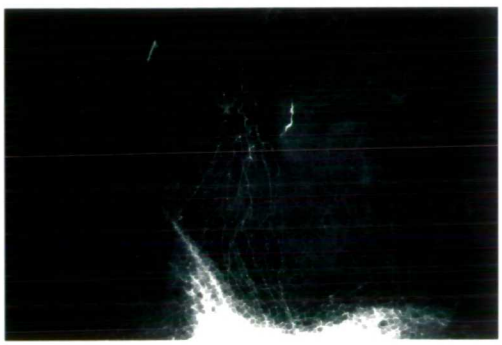

B

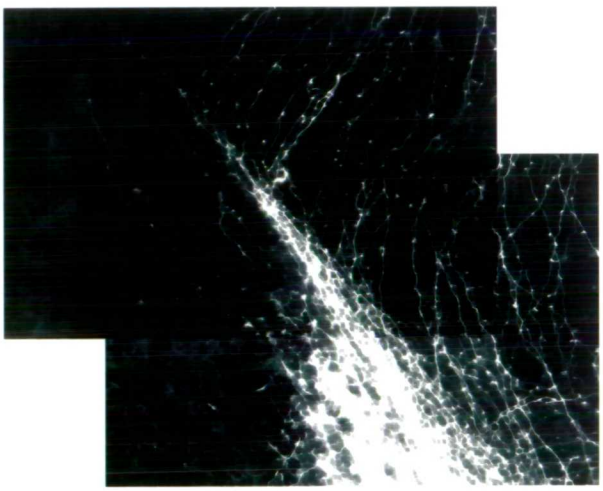

C

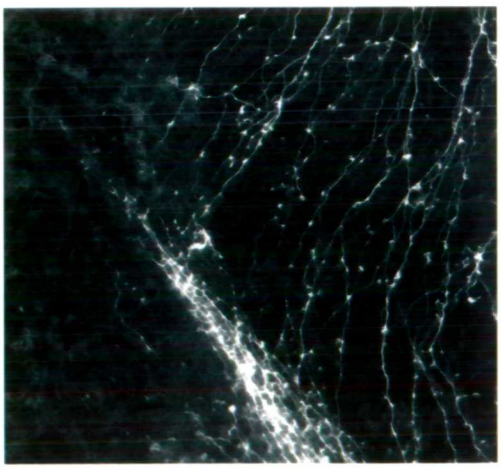

3.6 Projections along the zli

As previously described, the mammolothalamic tract or any other tract projecting within the zli has not been identified in chick. For this reason I looked for the origin of the neurofilament positive fibres seen within the zli by applying DiI dorsal and ventral to the ridge. When DiI is applied to the dorsal aspect of the zli, there is no transport of dye into the dorsal or the ventral thalamus (data not shown). Figs. 9A-C shows a tract tracing experiment in an E6 embryo, where DiI has been applied just below the zli within the basal plate. This DiI application has labeled axons within the zli and the dorsal thalamus (Fig. 9A), and since the cell bodies seem to be within the dorsal thalamus, the axons could originate from this structure. While some dorsal thalamic axons project directly to the basal plate, without following the zli, others seem to turn sharply upon meeting the zli and follow it ventrally (Figs. 9B and C).

This suggests that axons from the dorsal thalamus project ventrally, but if they encounter the zli, they will project along it toward the basal plate. This may explain the darker staining in the zli seen in Fig. 7J and Fig. 6K, which shows neurons projecting towards the zli within the dorsal thalamus. The former figure also shows that the axons within the ventral thalamus project in a similar manner, and in Fig. 8A labeled axons are seen extending into the ventral thalamus from the area where the DiI was applied. Some neurons and axons can also be identified further away as seen in Fig. 8B.

3.7 Morphology of the ventricular surface

SEM analysis revealed that the ventricular surface itself has changed within the anterior synencephalic and ventral thalamic grooves (Fig. 6B). High magnification (Figs. 10A and C) shows that the appearance of the ventral thalamus resembles clumps of cells protruding from the surface, which are not present on the surface of the dorsal thalamus (Figs. 10B and D). Also the surface of the ventral thalamus is more undulating than the dorsal thalamus, where the latter is relatively smooth.

In Transmission Electron Microscopy (TEM) studies, clumps of cells were not detected on the surface of the ventral thalamus (Fig. 10E). However, along the surface of this area cells send out extensions into the lumen (Fig. 10E). The surface of the dorsal

Figure 10

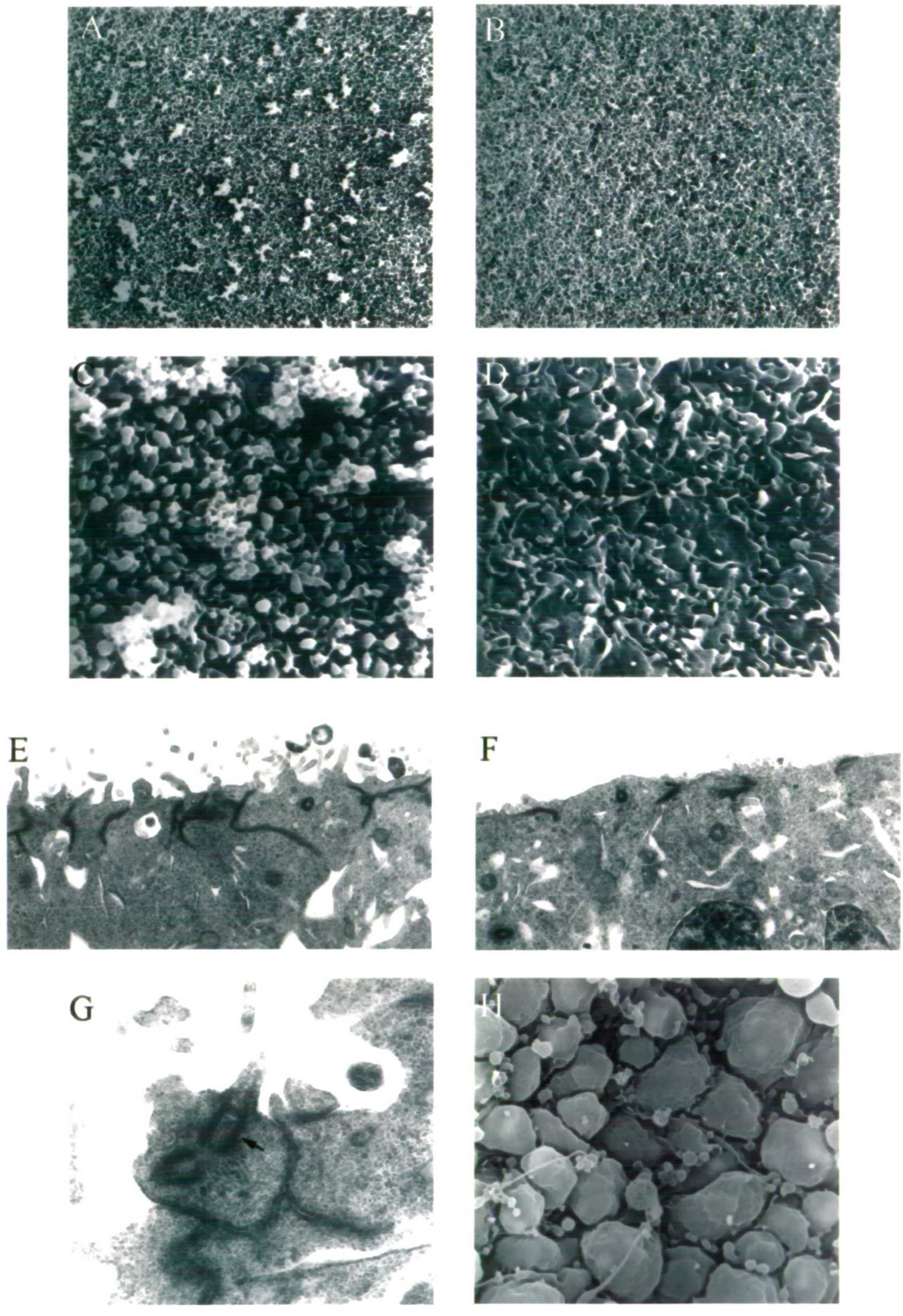

Figure 11

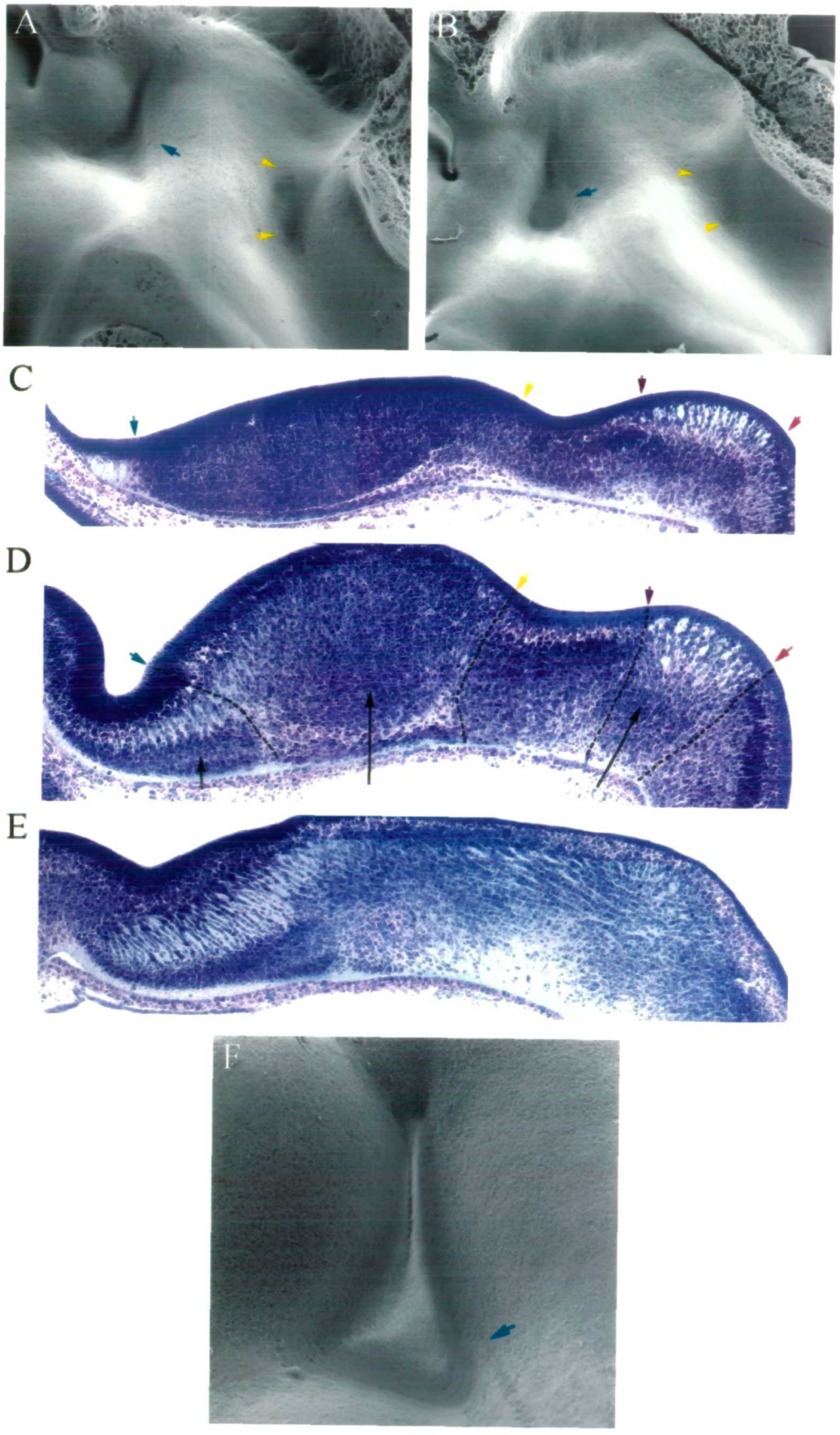

thalamus (Fig. 10F) is smooth, and cells aligning the ventricular surface exhibit a few small extensions into the lumen. The cells are linked by tight junctions, which are visible as dark staining with TEM. At the ventral thalamic surface there are more tight junctions than at the dorsal thalamic surface, and it appears that the part of the cells which faces the ventricular lumen is narrower than in the dorsal thalamus (compare Figs 10E and 10F). The tight junctions also extend further within the tissue, and it seems that some parts of the cells are completely surrounded by tight junctions. One of these extensions is seen at high magnification in Fig 10G, and it appears to contain rod shaped parts, where it extends from the surface of the cell. The ventricular surface earlier in development is rather different to that seen at E 5, which is clear when comparing Figs. 10B and H both taken at the same magnification. At earlier stages the part of the cell facing the lumen appears to be bigger and more rounded.

3.8 Morphological development at E 6.5

A day later in embryonic development the bulging of the thalamus and the posterior synencephalon is more clearly visible (Figs. 11A and B). The broad groove, which at E5 constituted the anterior part of the synencephalon, has almost disappeared due to the rapid growth and expansion of this area as well as the widening of the dorsal thalamus. Thus, the anterior part of the synencephalon now begins to bulge as nuclear formation is initiated in this region. The occlusion of the ventral thalamus is due to a rapid expansion of the telencephalon and the dorsal thalamus, which meet and fuse over the ventral thalamic domain at E 7 (Fig. 11F). This results in a lateral shift of the entire ventral thalamic domain, and this morphogenic feature is clearly demonstrated in the Nissl stained section shown in Fig. 11D. In dorsally situated Nissl stained sections, the dorsal thalamus is very broad, whereas the ventral thalamic neuromere is not visible. The clearing of cells within the zli is still visible at this level but is slightly obscured by the stria medularis axon tract adjacent and anterior.

At this stage, it is possible to identify the aggregation of the first nuclei, which are marked by black arrows in Fig. 11D. Within the ventral thalamus the characteristic shape of the nucleus geniculatum is visible at the lateral part of the mantle layer, and the large tightly packed cell mass within the dorsal thalamus is the nucleus rotundus. Within the synencephalon, the principal pretectal nucleus has started to form lateral to

the posterior commissure. The black dotted lines in this section mark the boundary between each neuromere. The section shown in Fig. 11E is taken ventrally from within the basal plate. The boundaries between each neuromere can no longer be identified and the entire posterior diencephalon appear to be continuous. Due to the angle of the section the ventral aspect of the ventral thalamus is included in this section.

3.9 Summary

(1) The avian diencephalon appears to be progressively subdivided into four domains during development, as illustrated in Fig. 12.
The first subdivision is apparent at HH 16, dividing the diencephalon into the synencephalon (S) and the parencephalon (PAR). This is associated with ridge formation at the parencephalic-synencephalic boundary (p-s), and the synencephalic-midbrain boundary (s-m). The second division is seen from HH 19 when a ridge forms at the ventral aspect of the zli (ZLI) dividing the parencephalon into the ventral thalamus (VT) and the dorsal thalamus (DT). The final division can be recognised at HH 22 when the synencephalon is divided into a posterior (Sp) and an anterior (Sa) part.
(2) The anterior synencephalon does not exhibit normal neuromeric morphology and neurons are seen to cross the intersynencephalic (i-s) boundary. However, at later stages of development the tissue is organised different within the anterior synencephalon compared to its neighbouring neuromeres.
(3) Between HH 24 and HH 26 the ridges between the dorsal thalamus and synencephalon, the anterior and posterior part of the synencephalon, as well as the between the synencephalon and the midbrain disappear. Only the zli remains.
(4) From HH 26 onwards the ventricular surface begins to form large bulges and grooves corresponding to the expansion of the synencephalon and the dorsal thalamus. This expansion continues until at least E7, when the ventral thalamic groove has been displaced and the anterior part of the synencephalon has expanded.
(5) Due to the progressive extension of the zli as well as the bulging of the dorsal thalamus at HH 26, the dorsal thalamus and the ventral thalamus never adopt a classic neuromeric phenotype.
(6) The axons appearing in the zli from HH 24 onwards seem to originate from the dorsal thalamus and some project via the zli towards the basal plate.

Figure 12

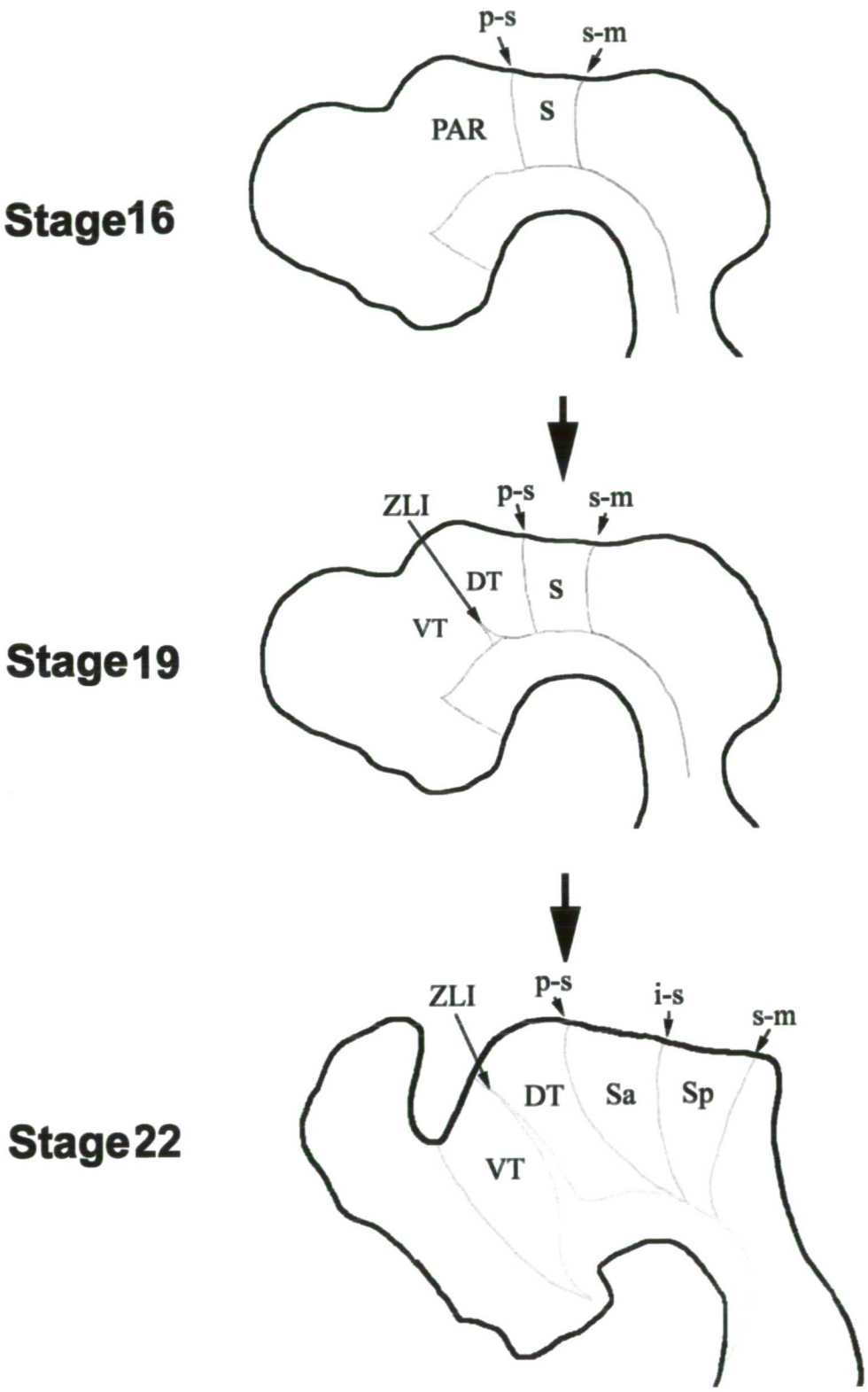
Stage16
p-s
s-m
PAR
S
Stage19
ZLI
p-s
s-m
DT
S
VT
Stage22
ZLI
p-s
i-s
s-m
DT
Sa
Sp
VT

Chapter 4

Neuromeric subdivision based on gene expression domains

As described previously, gene expression domains demarcate developmental compartments in several experimental systems, and initiation of expression is often correlated with the formation of these patterning units. This also appears to be the case for certain regions of the forebrain. Within the murine and avian diencephalon some genes are expressed exclusively within the dorsal and ventral thalamus respectively (see 1.2.3). However, genes whose expression domains demarcate the synencephalic neuromeres have not been reported. Furthermore, many of the gene expression studies carried out in vertebrates have concentrated on one or two stages of development and it is not clear from these studies when expression is initiated within the individual neuromeres. The onset of expression of these genes may not be correlated with the temporal subdivisions described in Chapter 3.

I performed a stage-by-stage *in situ* hybridization (ISH) analysis of the expression domains of genes reported to be expressed within specific diencephalic neuromeres, such as *Pax6*, *Dlx2*, *Gbx2* and *Wnt3*. These expression analyses were carried out to determine if the onset of gene expression correlated with the physical subdivisions identified previously and whether these genes demarcate specific subdivisions in chick, as in the mouse. Furthermore, the expression of a large number of other developmental genes was analysed to identify those, which might be exclusively expressed within the synencephalon or later within the anterior or posterior synencephalon. Although a genetic marker for the anterior synencephalon was not found, one gene; *Prox,* was shown to demarcate the synencephalon. Furthermore two other genes were shown to vary their expression levels within individual neuromeres; these were *Lunatic Fringe* (*L-fng*) and *NeuroM*.

4.1 Expression of *Pax6*

The expression pattern of the paired box gene *Pax6* (Chalepakis et al., 1993) is very

dynamic throughout development. Prior to the first neuromeric subdivision at HH 14, *Pax6* is expressed throughout the diencephalon with higher expression levels within the presumptive dorsal thalamic neuromere (Fig. 13A). The expression continues anteriorly into the presumptive ventral thalamus, where it gradually fades. Posteriorly, there is a sharp decrease in expression levels between the presumptive dorsal thalamus and the presumptive synencephalon at the dorsal aspect, whereas expression is still high in the ventral part of the presumptive synencephalon.

Throughout the diencephalon, the expression of *Pax6* never reaches the ventral midline but stops some distance away, presumably marking the division between the alar and basal plate. At HH 16 *Pax6* expression in the ventral part of the synencephalic neuromere has decreased, and is uniform within this neuromere (Fig. 13B). This expression domain is separated from the presumptive dorsal thalamic expression domain by a line of *Pax6* negative cells, which corresponds to the boundary between the synencephalon and the parencephalon. The level of expression within the presumptive ventral thalamus has increased and expanded anteriorly. There is a line of low expressing cells separating the dorsal and ventral thalamic domain, which corresponds to the morphological presumptive zli.

At HH 18, expression within the morphological presumptive zli has practically disappeared and *Pax6* now demarcates the posterior limit of the presumptive ventral thalamic domain (Fig. 13C). At this stage the expression of *Pax6* continues into the telencephalic vesicle, although this domain is separated dorsally from the presumptive ventral thalamic domain by a line of low expressing cells. The line of *Pax6* negative cells between the presumptive dorsal thalamus and the synencephalon has disappeared and the expression is now continuous. There is a strong expression domain at the extreme dorsal aspect of the presumptive dorsal thalamus, which probably corresponds to the forming epithalamus. At HH 20 the ventral and dorsal thalamic expression domains have begun to retract from the zli, in particular at the ventral aspect (Fig. 13D). Expressions within the dorsal thalamus and the synencephalic neuromere has faded considerably. Below the synencephalic domain, within the basal plate, a line of strong expression has appeared, which extends from the anterior to the posterior limit of the synencephalic neuromere.

Figure 13

Pax-6

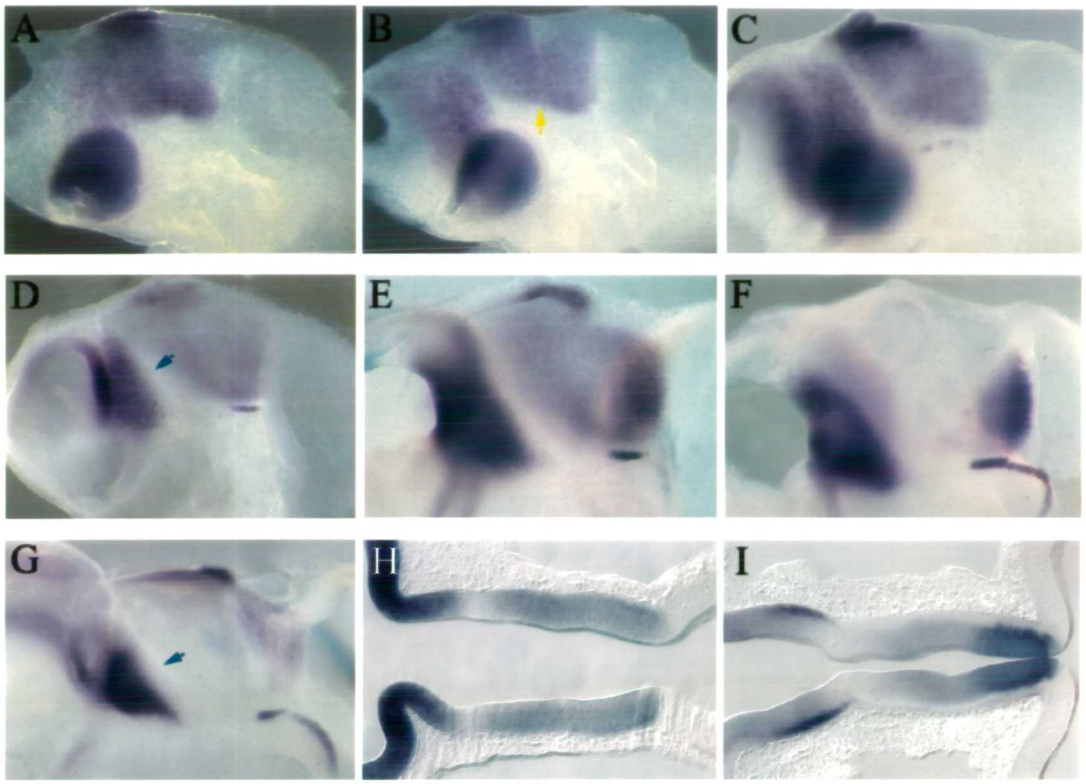

Dlx-2

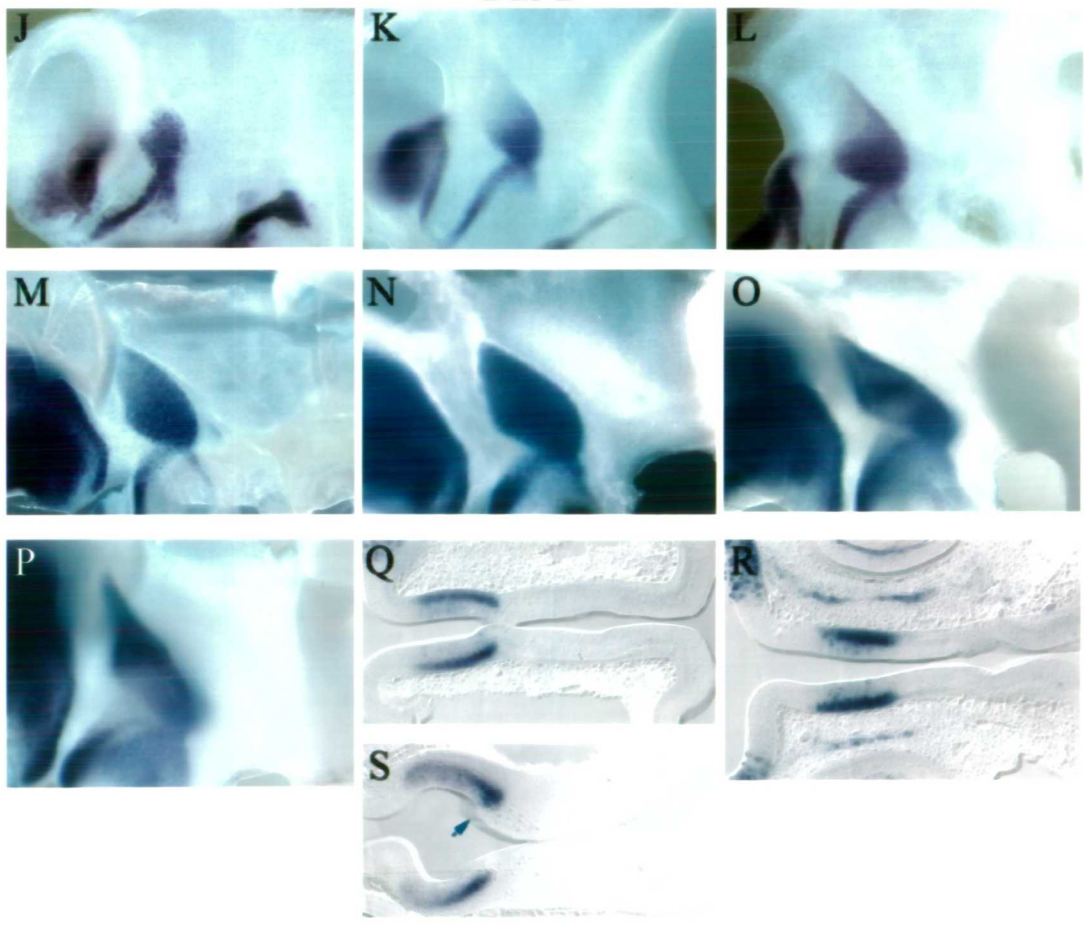

At HH 22 *Pax6* expression is upregulated within the dorsal thalamus and the posterior synencephalic neuromere (Fig. 13E), but does not continue up to the dorsal midline within the latter domain. In the dorsal thalamus, expression is stronger in the ventral aspect, as well as within the epithalamus. *Pax6* levels are comparatively lower in the dorsal part of the anterior synencephalic domain, but strong ventrally. Interestingly, this expression domain is triangular and resembles the shape of the anterior synencephalon determined by SEM at E 5 (compare Fig. 13E and Fig. 6I). The ventral thalamic expression domain now appears to be continuous with the telencephalic expression domain. At HH 24, the expression of *Pax6* has disappeared from the dorsal thalamus and anterior synencephalon, but still remains in most of the ventral thalamus (Fig. 13F). Strong expression is also seen within the posterior synencephalon, in particular at its posterior limit, whereas expression fades more anteriorly and is absent from its dorsal aspect. At E 5, the expression within the posterior synencephalon has expanded to include the dorsal part and appears to be localized to the axons of the posterior commissure (Fig. 13G). The expression in the ventral thalamus is still high, but has retracted rostrally from the zli.

In horizontal sections at HH 18, *Pax6* is expressed throughout the ventricular zone in proliferating cells (Fig. 13H). At HH 22, however, the expression within the ventral thalamus is stronger at the basal edges of the ventricular layer, and low more apically (Fig. 13I). This is also the case for the posterior synencephalic expression domain, although expression levels are comparatively higher in this area. Furthermore, the increased expression at the basal edges of the ventricular zone appears to extend into the forming mantle layer. There is a line of high expressing cells just rostral to the midbrain-diencephalic boundary spanning the ventricular layer. Throughout the diencephalon, the marginal layer is devoid of *Pax6* expression.

4.2 Expression of *Dlx2*

The only expression domain of the homeobox gene *Dlx2* (Price, 1993) in the diencephalon is within the ventral thalamus, where eventually it demarcates the whole neuromere. Expression is initially observed at HH 19 (data not shown) at the ventral-most part of the ventral thalamus, next to the zli. By HH 21 the expression extends dorsally and anteriorly along the zli (Fig. 13J). There is also a line of expression from

the ventral point of the *Dlx2* domain extending into the secondary prosencephalon. Over the next two days of development, the *Dlx2* expression domain moves dorsally and anteriorly to fill the entire ventral thalamus (Figs. 13K, L and M). This progressive expansion appears to be further advanced just rostral to the zli. By E 5.5, the expression reaches the most dorsal and anterior aspect of the ventral thalamus and thus demarcates the entire ventral thalamus from this stage onwards (Fig. 13N). Over time there is a gradual disappearance of expression within the ventral aspect, leaving a small triangular shaped domain in the dorsal part of the neuromere (Figs. 13O and P). Whether this reflects the movement of part of the ventral thalamus behind the dorsal thalamic and telencephalic bulges as described in chapter 3, or down regulation of expression is not clear. However, there is still low expression of *Dlx2* below the triangle at E 6.5, which could correspond to the ventral aspect of the forming nucleus geniculatum, which is present at this level (Fig. 11D).

Coronal sections of a HH 24 embryo reveal that *Dlx2* expression is confined primarily to the basal aspect of the ventricular zone and the mantle layer, although a few *Dlx2* positive cells can be seen further medially within the ventricular zone (Figs. 13Q and R). This may suggest that *Dlx2* is turned on in cells that are about to differentiate. The thickness of the expression domain increases at the ventral aspect of ventral thalamus (Fig. 13R) compared to a dorsal level (Fig. 13Q). At E 5 the *Dlx2* expression domain is confined predominantly within the mantle layer just lateral to the ventricular zone, whereas expression is low within the basal region of the mantle layer (Fig. 13S). It is clear from the sections at both stages that the posterior limit of *Dlx2* sharply demarcates the zli.

4.3 Expression of *Gbx2*

Gbx2, a homeobox gene that has previously been shown to mark the dorsal thalamus (Bulfone et al 1993), is first seen at HH 19 in the ventral aspect of this region. Initial expression is restricted to a small area of the ventral and rostral part of the dorsal thalamus, next to the zli (Fig. 14A). At HH 21, this domain expands caudally along the ventral aspect of the dorsal thalamus and dorsally it narrows towards the zli (Fig. 11B). By HH 24 the expression domain has extended further dorsally and clearly demarcates the anterior and posterior limit of the dorsal thalamus at its ventral aspect (Fig. 14C).

Figure 14

Gbx-2

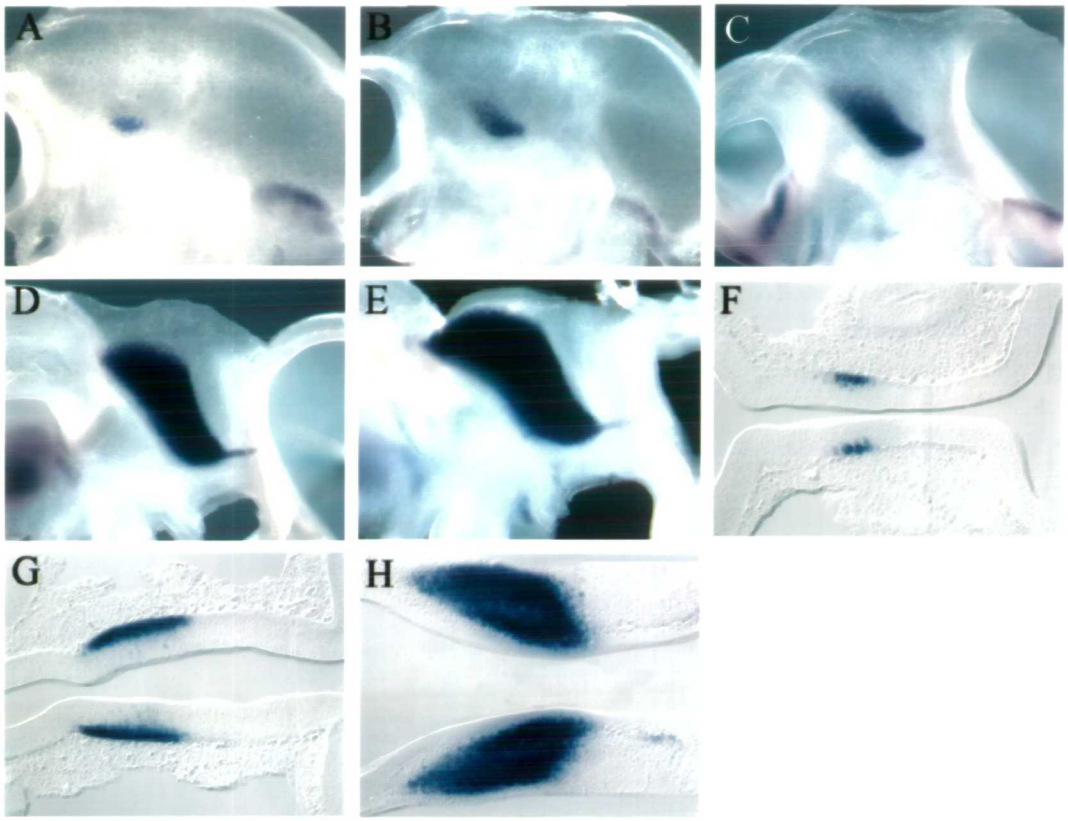

Lunatic Fringe

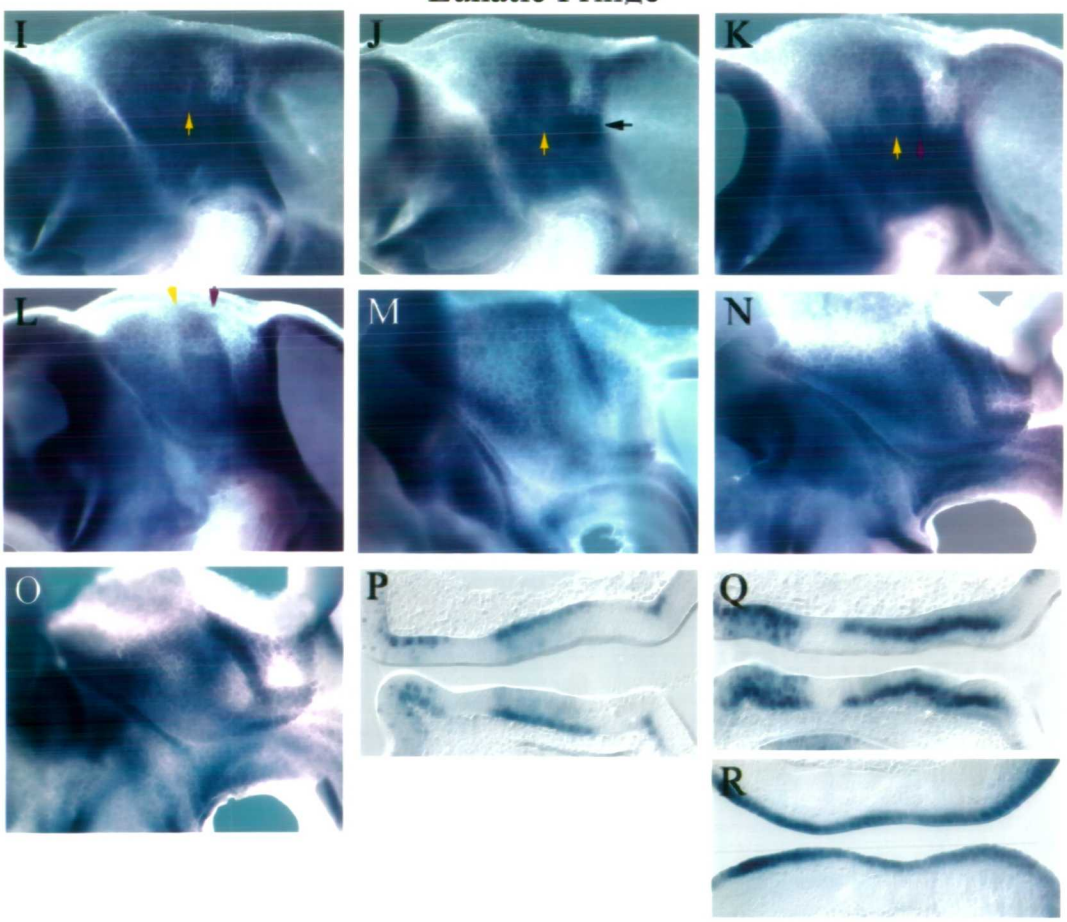

Gbx2 expression may be initiated at the zli, since expression is further advanced at the zli compared to that of the posterior aspect of the dorsal thalamus. The dorsal extension continues until E 5, when it reaches its dorsal limit close to the dorsal midline (Fig. 14E). Between HH 26 and E 5 as the dorsal thalamus grows and expands posteriorly, the expression domain of *Gbx2* expands as well. Similar to *Dlx2*, *Gbx2* seems to be confined primarily to the mantle layer at earlier stages, with a few *Gbx2* positive cells within the ventricular zone (Figs. 14F and G). However, by E 5, *Gbx2* expression is seen throughout most of the caudal mantle layer (Fig. 14H), whereas rostrally the expression domain narrows down towards the basal edges of the mantle layer and ends as a tip close to the zli. Therefore, the part of the mantle layer closest to the zli is devoid of *Gbx2* expression, whereas at caudal levels expression appears to extend into the basal part of the ventricular zone as well. Although the boundary of expression between the dorsal thalamus and the synencephalon is sharply defined, some *Gbx2* positive cells are seen within the anterior synencephalon.

4.4 Expression of *L-fng*

L-fng is a secreted molecule and a member of the *Fringe* gene family, associated with the Notch signaling pathway (Johnston et al., 1997). *L-fng* is expressed in the diencephalon from early development and its early onset will be described in detail in Chapter 7. However, from HH 19 onwards its expression begins to vary considerably between and within different neuromeres. At HH 19, *L-fng* is expressed throughout most of the diencephalon both within the basal and alar plate (Fig. 14I). However, it is absent from the zli and is downregulated in the dorsal aspect of the posterior synencephalon, apart from close to the dorsal midline, and in the ventral and anterior aspects. There appears to be a line of weakly expressing cells at the ventral aspect of the boundary between the dorsal thalamus and the synencephalon, as well as from the zli through the basal plate down to the ventral midline.

The line of low expressing cells at the dorsal thalamic-synencephalic boundary, appears to be broader at HH 20 (Fig. 14J). The expression seen at the extreme dorsal aspect of the posterior part of the synencephalon has almost disappeared and the synencephalon is nearly devoid of expression apart from the most ventral aspect. The zli still shows no expression of *L-fng*, and expression is downregulated within the dorsal aspect of the

anterior part of the dorsal thalamus as well as the ventral thalamus. This area of downregulation is square shaped and is delineated anteriorly by the telencephalic vesicle. *L-fng* expression in the remainder of the dorsal and ventral thalamus is comparatively strong.

At HH 22, the posterior synencephalon still shows no expression of *L-fng* apart from the ventral most parts, whereas expression is seen throughout most of the anterior synencephalon (Fig. 14K). There is no detectable expression within the dorsal thalamus, apart from the ventral most aspect, and there are low levels of expression within the extreme dorsal part of the ventral thalamus. A stage later, *L-fng* is upregulated within the dorsal and anterior aspects of the dorsal thalamus as well as the dorsal aspect of the ventral thalamus (Fig. 14L).

The upregulation within the dorsal thalamus extends in a broad domain along the zli at the same thickness as that seen of the *Gbx2* domain a stage later (Fig. 14C). The ventral part of the dorsal thalamic *L-fng* domain appears to be continuous ventrally with the expression in the anterior synencephalon, whereas a triangle of low expression can be seen at the dorsal aspect bordering the anterior synencephalon. Within the anterior synencephalon, expression is strong throughout the alar plate although it appears to become stronger at the boundary between the anterior and posterior synencephalon. Furthermore the strong expression detected at the ventral aspect of the alar plate throughout the synencephalon and dorsal thalamus has disappeared, and the expression level characteristic of each neuromere extends down to the division between the alar and basal plate.

At HH 26, *L-fng* expression has been downregulated throughout most of the dorsal thalamus and the anterior/posterior synencephalon (Fig. 14M). High levels of expression at this stage appear to be confined to the boundary between the dorsal thalamus and the anterior synencephalon and at the dorsal aspect of the boundary between the anterior and posterior synencephalon. There is also an area of high expression next to the zli within the dorsal part of the dorsal thalamus, whereas the expression within the ventral thalamus remains high. Interestingly the anterior slope of the zli now appears to express *L-fng* at high levels, whereas the posterior slope shows low level patchy expression.

At E 5 the expression levels again change, with expression returning to all neuromeres within the diencephalon (Fig. 14N). The dorsal most and ventral most aspect of the posterior synencephalon show strong expression leaving the middle part devoid of staining. The strong expression at the boundary between the anterior and posterior synencephalon has extended ventrally, and the anterior synencephalon shows decreased expression at the ventral aspect compared to the dorsal aspect. At this developmental stage, expression of *L-fng* has spread to the whole of the zli, whereas a line of lower expressing cells can now be seen adjacent and posterior to the zli. Further posterior from the zli within the dorsal thalamus expression is upregulated, whereas the ventral thalamus exhibits strong expression throughout.

At E 5.5, expression of *L-fng* is again downregulated, in particular within the posterior and anterior synencephalon (Fig. 14O). This leaves the boundaries and the dorsal aspect of the anterior synencephalon with stronger expression. The most ventral aspect of the posterior synencephalon has maintained expression from E 5, although at lower levels. The dorsal thalamus shows stronger expression closer to the zli at dorsal levels, whereas the more posterior and ventral aspects have low expression of *L-fng*. The ventral thalamus still exhibits high expression levels, although expression within ventral parts is lower. The stronger expression domains within the dorsal thalamus and the ventral thalamus appear to be continuous with each other across the zli and have the shape of an arrowhead. Apart from the strong expression just posterior to the zli, the entire *L-fng* expression domain has shifted ventrally, which leaves the dorsal aspect of the dorsal thalamus and the anterior synencephalon devoid of staining. The expression within the zli has returned to the anterior slope of the ridge at the ventral aspect.

The dynamic pattern of expression of *L-fng* is also reflected within the neural tissue in horizontal sections through a HH 20 embryo (Figs. 14P and Q). In a dorsal section (Fig. 14P), expression is strong within the narrow marginal layer and the basal part of the ventricular zone, although some expression is seen further apically. The ventral situated section (Fig. 14Q) is at the level of strong ventral expression and is marked by a black arrow in Fig. 14J. At this level, expression of *L-fng* within the dorsal thalamus and synencephalon has moved medially and is strong within the basal part of the ventricular zone, but is absent from the marginal layer. Within the ventral thalamic domain, expression is patchy throughout the ventricular zone, but is stronger towards the basal

part of the ventricular zone. At E 5 *L-fng* is confined to the ventricular zone, although some low-level expression may persist just lateral in the mantle layer (Fig. 14R). This suggests that *L-fng* is expressed in cells undergoing cell division, but is downregulated following differentiation.

4.5 Expression of *NeuroM*

NeuroM is a proneural helix-loop-helix transcription factor (Roztocil et al., 1997) and like *L-fng,* the expression pattern of *NeuroM* is very dynamic. In the diencephalon at HH 16, expression of *NeuroM* is patchy and confined to the ventral aspect of the presumptive dorsal thalamus. A few cells within the anterior and posterior parts of the ventral synencephalon are also seen at this stage (Fig. 15A). This leaves the majority of the synencephalon, the entire presumptive ventral thalamus, and the dorsal aspect of the presumptive dorsal thalamus devoid of expression. Expression within the basal plate is strong although patchy, extending upwards towards the presumptive zli, and continuing into the secondary prosencephalon. At HH 18, a line of *NeuroM* negative cells appears between the expression domains in the basal and alar plates (Fig. 15B). Expression within the presumptive dorsal thalamus extends dorsally and there is a small domain of expression within the ventral-most aspect of the synencephalon. There is also an area of patchy expression extending from the basal plate in the secondary prosencephalon up to the dorsal midline within the telencephalon, which probably demarcates the boundary between the telencephalon and the parencephalon.

At HH 20, the expression of *NeuroM* is more homogeneous (Fig. 15C). The line of *NeuroM* negative cells separating the alar and basal plate is maintained and the basal plate expression is still present, although downregulated more anteriorly. An area of *NeuroM* negative cells appears within the basal secondary prosencephalon, within the presumptive hypothalamus. Adjacent to this region, a line of strong expression extends toward the ventral thalamus in a manner similar to the *Dlx2* expression domain at a similar stage. There is no detectable expression in the ventral thalamus or the synencephalon, apart from the extreme ventral aspect of the latter. Within the dorsal thalamus, expression is stronger ventrally and appears to decrease towards the dorsal aspect, although it does not reach the dorsal midline.

Figure15

NeuroM

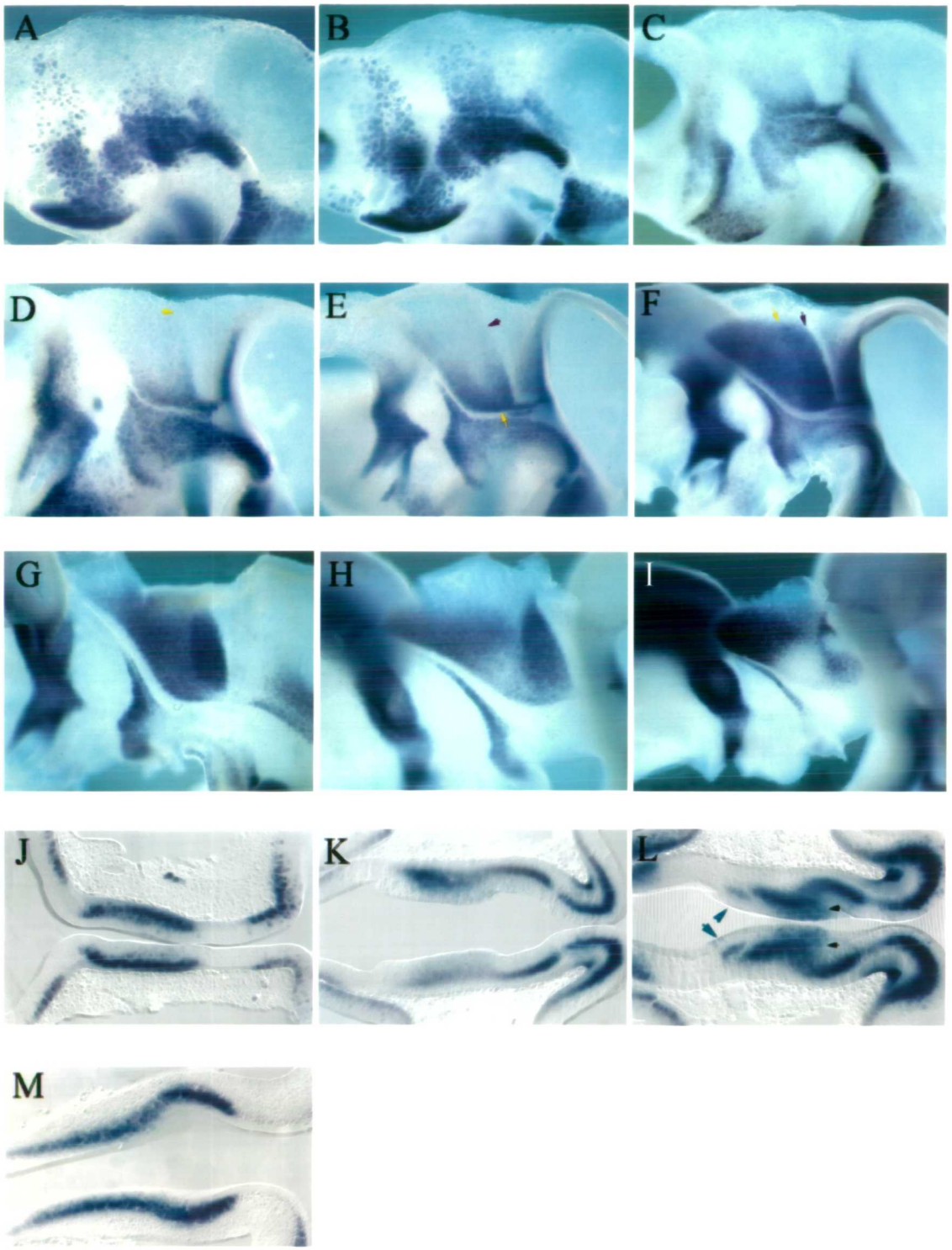

A stage later, the dorsal thalamic expression has extended further dorsally and appears to be graded with stronger expression at the ventral aspect (Fig. 15D). The synencephalon is still devoid of expression, apart from the extreme ventral domain, whereas strong expression is seen at the boundary between the synencephalon and the midbrain. The *NeuroM* negative line separating the alar and basal expression domains is wider at the posterior end of the diencephalon, and the expression within the basal plate is still patchy. Thus, the width of the expression in the basal plate seems to increase towards the zli. A small line of *NeuroM* expressing cells appears within the zli and is bordered anteriorly by a line of *NeuroM* negative cells. This line of *NeuroM* negative cells is continuous with the line separating the alar and basal expression domain.

At HH 23, the expression of *NeuroM* within the zli extends dorsally and is still separated from the dorsal thalamic expression domain by a line of *NeuroM* negative cells (Fig. 15E). Expression increases within the dorsal thalamus and is still graded, with the strongest expression in the ventral aspect. Expression is stronger towards the zli and decreases towards the anterior synencephalon. Within the anterior synencephalon, there is stronger expression at the ventral aspect compared to the dorsal aspect. However, there is a sharp boundary between the *NeuroM* expressing anterior synencephalon and the non-expressing anterior part of the posterior synencephalon. Expression begins to fill the posterior synencephalon, but stronger at the posterior part towards the boundary between the posterior synencephalon and the midbrain. Strong expression is maintained in the synencephalic-midbrain boundary and in a line of cells at the extreme ventral aspect of the posterior synencephalon dorsal to the *NeuroM* negative domain. A line of expression has appeared just ventral to the anterior and posterior synencephalon at the same location as the line of *Pax6* expression is seen at a similar stage (Fig. 13F). However, the line of *Pax6* expression is apparent before the line of *NeuroM* expression.

At HH 24, the entire dorsal thalamus expresses high levels of *NeuroM*, although it appears stronger towards the zli (Fig. 15F). Expression within the anterior synencephalon is slightly higher than in the dorsal thalamus. The posterior synencephalon also expresses high levels of *NeuroM,* apart from a line of *NeuroM* negative cells just adjacent and posterior to the boundary between the anterior and posterior synencephalon. The line of *NeuroM* expressing cells seen just ventral to the

alar expression domain is fainter, and expression has been downregulated throughout most of the basal plate. However, a line of strong expression still remains at the anterior limit of the basal plate and continues dorsally into the zli. At HH 25, expression of *NeuroM* is lost from the basal plate apart from the strong anterior expression domain, which has expanded a little posteriorly (Fig. 15G). The line of *NeuroM* negative cells next to the zli has widened compared to HH 24, whereas the rest of the dorsal thalamus expresses *NeuroM* strongly. There is increased expression in the anterior synencephalon, whereas the posterior synencephalon has lost all expression. The line of *NeuroM* expressing cells underneath the synencephalic domains has now disappeared.

At E5 *NeuroM* expression extends further dorsally within the zli, and now appears only in its anterior slope (Fig. 15H). The rest of the zli, as well as the line of cells adjacent to the zli, do not express *NeuroM*. Expression within the rest of the dorsal thalamus is stronger at the dorsal aspect, although extreme dorsal expression is absent. This is also the case for the extreme ventral aspect of the anterior synencephalon, which otherwise expresses *NeuroM* strongly. The posterior synencephalon is still devoid of staining. At E 6.5 strong expression remains at the anterior dorsal aspect of the dorsal thalamus, whereas the ventral aspect has lost most expression (Fig. 15I). The expression in the more ventral and dorsal aspects of the anterior synencephalon remains, and the posterior synencephalon does not exhibit detectable levels of expression. The staining anterior to the *NeuroM* negative ventral thalamus corresponds dorsally to the foramen of Monroi and ventrally to a region within the hypothalamus. The telencephalic vesicle now expresses *NeuroM* at high levels.

At HH 20, expression of *NeuroM* within the neuroepithelium is seen in the basal part of the ventricular zone as well as in some cells further apically (Fig. 15J). At dorsal levels at HH 24, the expression of *NeuroM* shifts medially within the neural tube, where the basal *NeuroM* negative domain probably corresponds to the mantle layer (Fig. 15K). The expression is fairly narrow throughout the two synencephalic domains, whereas it is broader in the dorsal thalamus. This section is slightly oblique, so that one side contains the stronger dorsally located domain within the thalamus, whereas the other side is more ventral where expression is not as strong. In a ventrally located section taken just dorsal to the basal plate, expression changes dramatically within the neural tube between the different areas (Fig. 15L).

Within the posterior synencephalon, the expression is still at the basal edge of the ventricular zone, but in the anterior synencephalon expression is now seen in cells within parts of the mantle layer as well. The expression follows the curvature of the pial surface, so that cells within the ventricular zone at the anterior part of the anterior synencephalon are not expressing *NeuroM*, which instead is expressed within the mantle layer. Upon entering the dorsal thalamus, cells begin to express *NeuroM* throughout the ventricular zone, marked by a black arrow, but expression is stronger at the basal part of the ventricular zone. The line of expression seen in the anterior synencephalon bends medially to join the area of higher expression within the dorsal thalamus. As expression moves further anterior, the cells at the medial part of the ventricular zone stop expressing *NeuroM*, which is also the case for the zli. At HH 25, expression is exclusively within the basal part of the ventricular zone irrespective of dorso-ventral position (Fig. 15M).

4.6 Expression of *Wnt3*

Wnt3, a member of the *Wingless* family of secreted molecules (Nusse, 1992), has previously been described to demarcate the dorsal thalamus, however as shown in Figs. 16A-C, this is not the case. At HH 17, expression is seen in the dorsal part of the presumptive dorsal thalamus in a triangular shape (Fig. 16A). This expression domain almost reaches the synencephalon posteriorly, but does not span the entire presumptive dorsal thalamic domain. Furthermore, there is strong expression along the dorsal midline in the midbrain. At HH 19, the *Wnt3* expression domain extends posteriorly, but retains its shape (Fig 16B). Thus, dorsally both the dorsal thalamus and the synencephalon express *Wnt3*, whereas the expression narrows ventrally so that most of the synencephalon is *Wnt3* negative. The anterior boundary of the expression domain is parallel to the forming zli. At HH 24 expression disappears from the dorsal thalamus, whereas low levels are maintained in the posterior synencephalon (Fig. 16C). Expression is now also apparent in the zli. From sections through an HH 20 embryo, it is clear that *Wnt3* is expressed throughout the ventricular zone (Fig. 16D).

Figure 16

Wnt 3

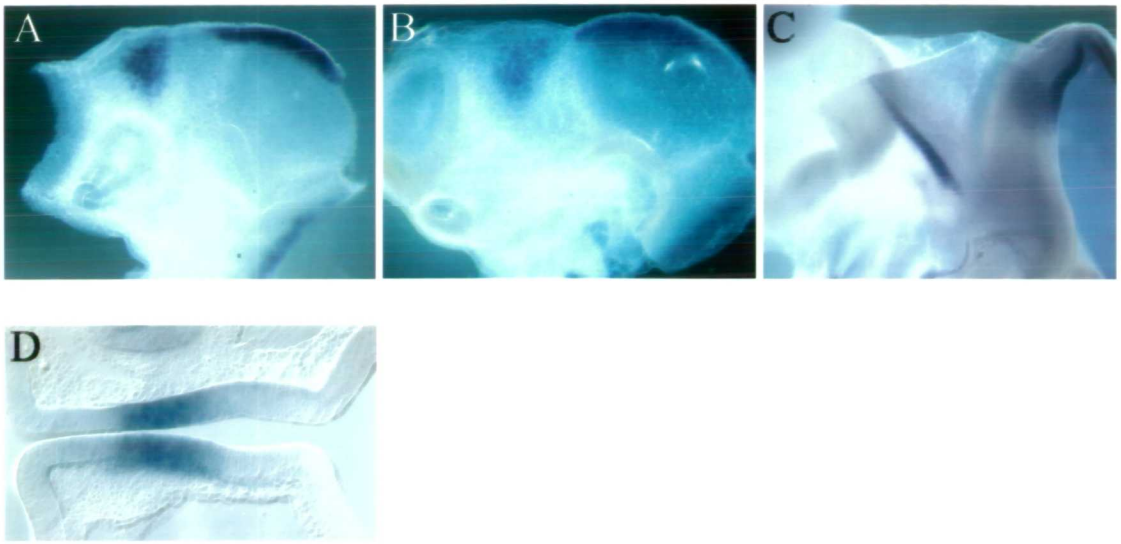

Prox

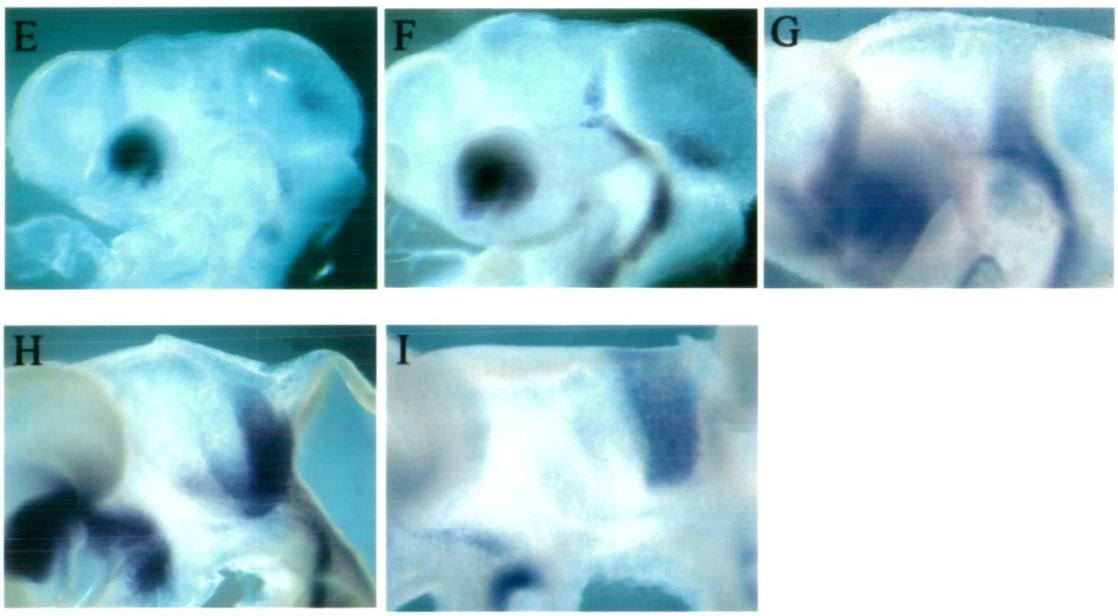

Double In-Situ

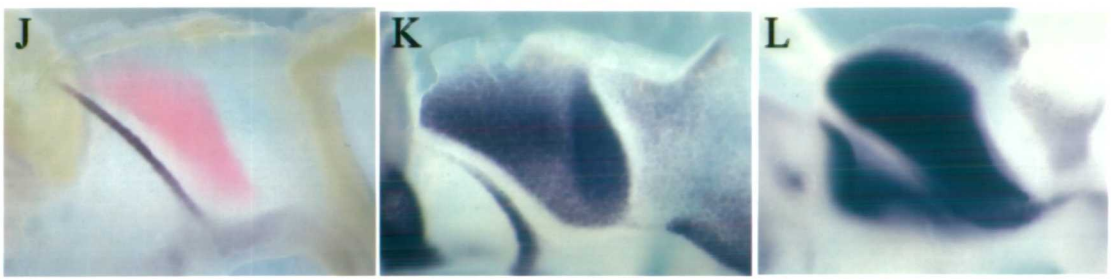

Shh+Gbx2 NeuroM+Prox Gbx2+Pax6

4.7 Expression of *Prox*

Prox is a homeobox containing transcription factor homologous to *Drosophila prospero* (Oliver et al., 1993). Throughout development until E 7, *Prox* is primarily expressed within the synencephalon and like both *Dlx2* and *Gbx2,* its expression is initiated ventrally and expands dorsally as development proceeds. Expression is first detected at HH 16 in a narrow domain at the ventral aspect of the synencephalon (Fig. 16E). This domain extends dorsally at HH 19, and a line of stronger expression also delineates the ventral limit of the neuromere (Fig. 16F). This line of expression extends into the midbrain posteriorly. At HH 21, the expression fills the ventral part of the synencephalic neuromere and appears to decrease in a gradient towards the dorsal aspect (Fig. 16G). At HH 24, the expression domain of *Prox* expands to fill the posterior synencephalon, apart from the extreme dorsal aspect (Fig. 16H). There is also a line of expression at the boundary between the dorsal thalamus and the anterior synencephalon, as well as some expression at the extreme ventral aspect of the anterior synencephalon. By E 5, the expression in the anterior synencephalon has disappeared, and *Prox* is now exclusively expressed within the posterior synencephalon (Fig. 16I).

4.8 Double ISH

Figs. 16 J-L show the expression patterns of two genes simultaneously in a double ISH. The *Gbx2* domain does not meet the zli, marked by *Shh* (Fig. 16J). This *Gbx2* negative area seems to correspond to the *NeuroM* negative area, which is also seen caudal to the zli at the same developmental stage (Fig. 15G). When the expression domains of *Prox* and *NeuroM* are compared at E 5.5, a line of negative cells is seen between the *Prox* positive posterior synencephalon and the *NeuroM* positive anterior synencephalon (Fig. 16K). This probably reflects the lack of expression of *NeuroM* in the posterior and anterior synencephalon. This indicates that *NeuroM* expression is downregulated within the anterior synencephalon at E 5.5 in a posterior to anterior fashion until it is practically gone by E 6.5 (Fig. 15I). Fig. 16L shows a comparison of the expression domains of *Gbx2* and *Pax6* at E 6, when the expression of *Pax6* is confined to parts of the ventral thalamus and the posterior synencephalon. The negative area between the two domains is broad, indicating that neither meets the zli

4.9 Summary

1) The expression domains of *Dlx2* and *Gbx2* demarcate the ventral and dorsal thalamus respectively. The expression of both genes is initiated at HH 19 at the ventral aspect of their respective area adjacent to the zli, and this corresponds to the developmental stage when the parencephalon is subdivided into the dorsal and ventral thalamus, as described in Chapter 3. Both genes extend dorsally over a period of development until the entire domain expresses the gene. The expression of both genes follows the morphological changes, which occur in later stages of development.

2) The expression of *Prox* demarcates initially the synencephalon and then the posterior synencephalon. The expression is initiated at HH 16, corresponding to the developmental stage when the diencephalon is divided into the synencephalon and the parencephalon. Like *Gbx2* and *Dlx2,* its expression is initiated ventrally and slowly expands dorsally. After the subdivision of the synencephalon, the expression of *Prox* is initially present in the anterior synencephalon but is then confined to the posterior synencephalon.

3) The levels of expression of *NeuroM* and *L-fng* vary between different domains, and this corresponds to the progressive subdivision of the diencephalon. This is particularly clear within the synencephalon, which after subdivision exhibits differential levels of expression of both genes within the anterior synencephalon compared to the posterior synencephalon. However, the level of expression of both genes between the anterior synencephalon and the dorsal thalamus is often similar and sometimes continuous. The expansion of the anterior synencephalon can clearly be followed by comparing the width of expression demarcating this neuromere just after subdivision to later in development. Finally, both gene expression patterns within the dorsal thalamus are stronger closer to the zli and the width of expression runs parallel to the zli.

4) The expression pattern of *Pax6* is very dynamic during development and is expressed throughout the diencephalon before being restricted to the ventral thalamus and posterior synencephalon from HH 24 onwards. *Pax6* does not demarcate the entire ventral thalamus, since the expression stops some distance from the zli. Also, it does not seem to demarcate the entire posterior synencephalic neuromere, since its expression

appears to be confined to the posterior commissure only. However, at HH 16, when the synencephalon and parencephalon are subdivided, the two *Pax6* expression domains are clearly separated by a line of *Pax6* negative cells. This line disappears by HH 18 and the two domains seem continuous.

5) *Wnt3* is expressed within the dorsal thalamus and pretectum, but does not demarcate the borders of these neuromeres.

6) For all of the genes analysed, the expression domains in the alar and basal plate are separated or the gene is not expressed in the basal plate.

Chapter 5

Specialised boundary morphology

Segmentation and compartmentalisation in the vertebrate hindbrain are associated with the generation of a unique boundary morphology (Lumsden and Krumlauf, 1996). Compared to the hindbrain, little is known about the boundary regions in the vertebrate diencephalon, although some studies have proposed that boundaries are populated by axon tracts (Keyser, 1972; Chedotal et al., 1995; Figdor and Stern, 1993), in a manner similar to the boundaries in the hindbrain (Lumsden and Keynes, 1989). Regardless of the number of diencephalic divisions, it is likely that a specialised boundary morphology could be identified within this region. The close similarity between the four segment model proposed by Figdor and Stern (1993) and hindbrain organization, further suggests that these two systems display similar boundary morphology.

The next step was therefore to carry out an extensive analysis in the diencephalon for a boundary phenotype similar to that seen in the hindbrain. The purpose of this analysis was twofold. First, a diencephalic boundary morphology similar to that in the hindbrain would provide evidence that these two systems are patterned in a similar manner. Second, from the anatomical and molecular analysis it had not been possible to determine whether the boundary between the posterior and anterior synencephalon was similar to the other boundaries identified. The discovery of specific boundary markers would enable an independent verification of the phenotypic similarity to the other boundaries.

This analysis included BrdU pulse labeling to establish whether the arrangement of S-phase cells is similar to that seen at the hindbrain boundaries. In the hindbrain boundaries, interkinetic movement is disrupted so that S-phase cells are located apically as opposed to their normal position close to the pial surface (Guthrie et al., 1991). This particular phenotype in the hindbrain has been associated with the generation of compartments, and should therefore be present in all diencephalic boundaries, since these have been associated with cell lineage restriction (Figdor and Stern, 1993). BrdU

is a thymidine analog and is incorporated into DNA during S-phase DNA duplication. Survival for 30 min after BrdU injection preferentially labels cells in S-phase, after which their distribution can be assessed by using a BrdU specific fluochrome-conjugated antibody, together with ISH with molecular markers for diencephalic neuromeres. The embryos were sectioned horizontally to reveal the specific location of BrdU incorporated cells within the neural epithelium. Within each developmental stage from HH 14 to E 6.5, six embryos were labeled and the labeling was repeated once for each stage. From HH 26 to E 6.5 a set of embryos were allowed to survive for 4 hours, approximately half the cell cycle.

An analysis of the localisation of several cell adhesion and extracellular matrix molecules was performed, using immunocytochemistry on wholemount embryos and sectioned material. These included NgCam, the heavily polysialated form of NCAM (embryonic NCAM), Laminin, CSPG and Vimentin, which all localises to the hindbrain boundaries. Ng-Cam and Laminin are thought to be associated with preferential growth of axons within the hindbrain boundaries, whereas the lack of the heavily polysialated form of NCAM represents a more adhesive nature of boundary cells (Lumsden and Keynes, 1989). Vimentin, on the other hand is an early marker of radial glial, and CSPG is thought to promote neurite outgrowth in the hindbrain boundaries (Heyman et al., 1995). A similar pattern of localisation of these molecules to diencephalic boundaries would suggest a similarity between the two systems. However of these molecules, only CSPG and Vimentin localised to some of the diencephalic boundaries. Furthermore, the localisation of a range of other molecules was analysed, including fibronectin, NrCAM, β-catenin, P-Cadherin, Connexin-32 and Tenascin. Only Tenascin and NrCAM were localised to boundaries, and then only to some boundaries.

For each of the candidate boundary markers, immunocytochemistry was carried out with three embryos of each stage between HH 14 to E 5.5 in the same experiment. Each experiment contained two controls and was repeated twice. One set of control embryos did not include primary or secondary antibody, which controlled for any non-specificty of the DAB reaction. Primary antibody was omitted from another set of controls to exclude any non-specific binding of the secondary antibody. In general the DAB reagent did not produce non-specific staining, but the secondary-anti mouse antibody

Figure 17

HH 14

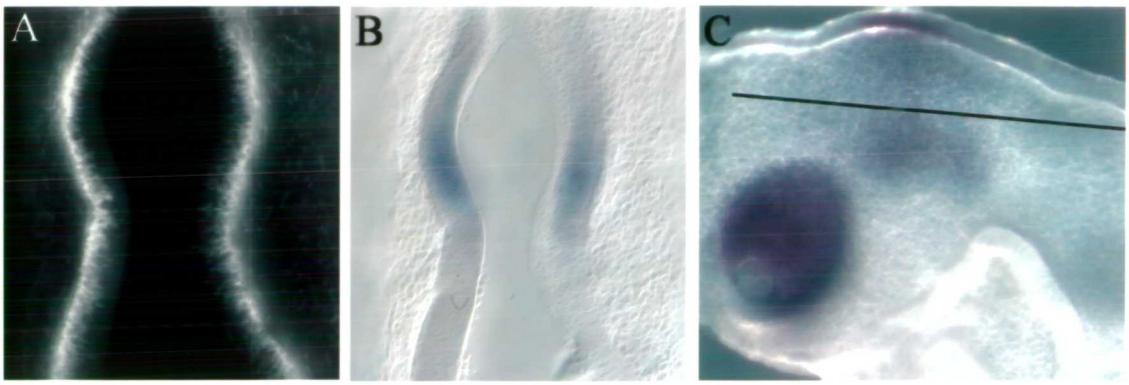

HH 17

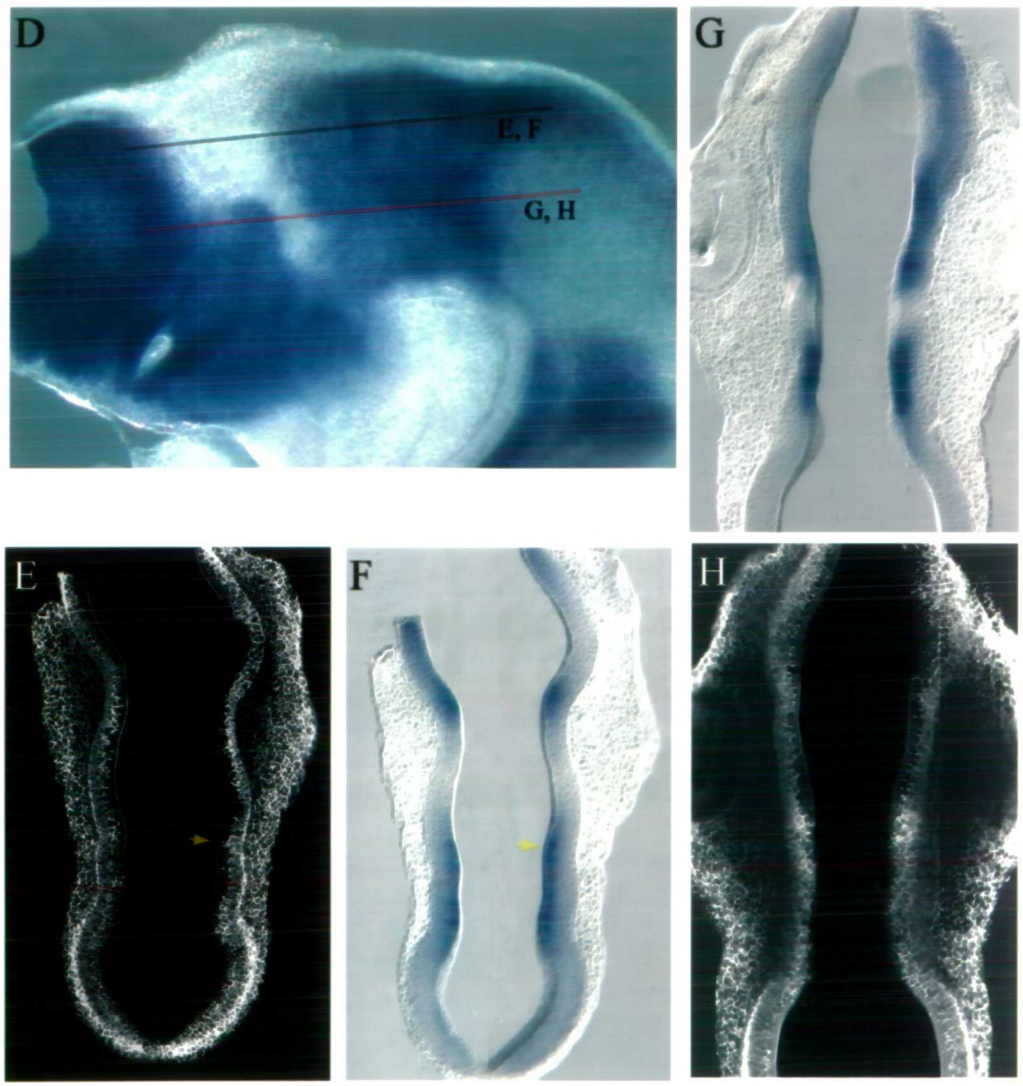

Figure 18

HH 16

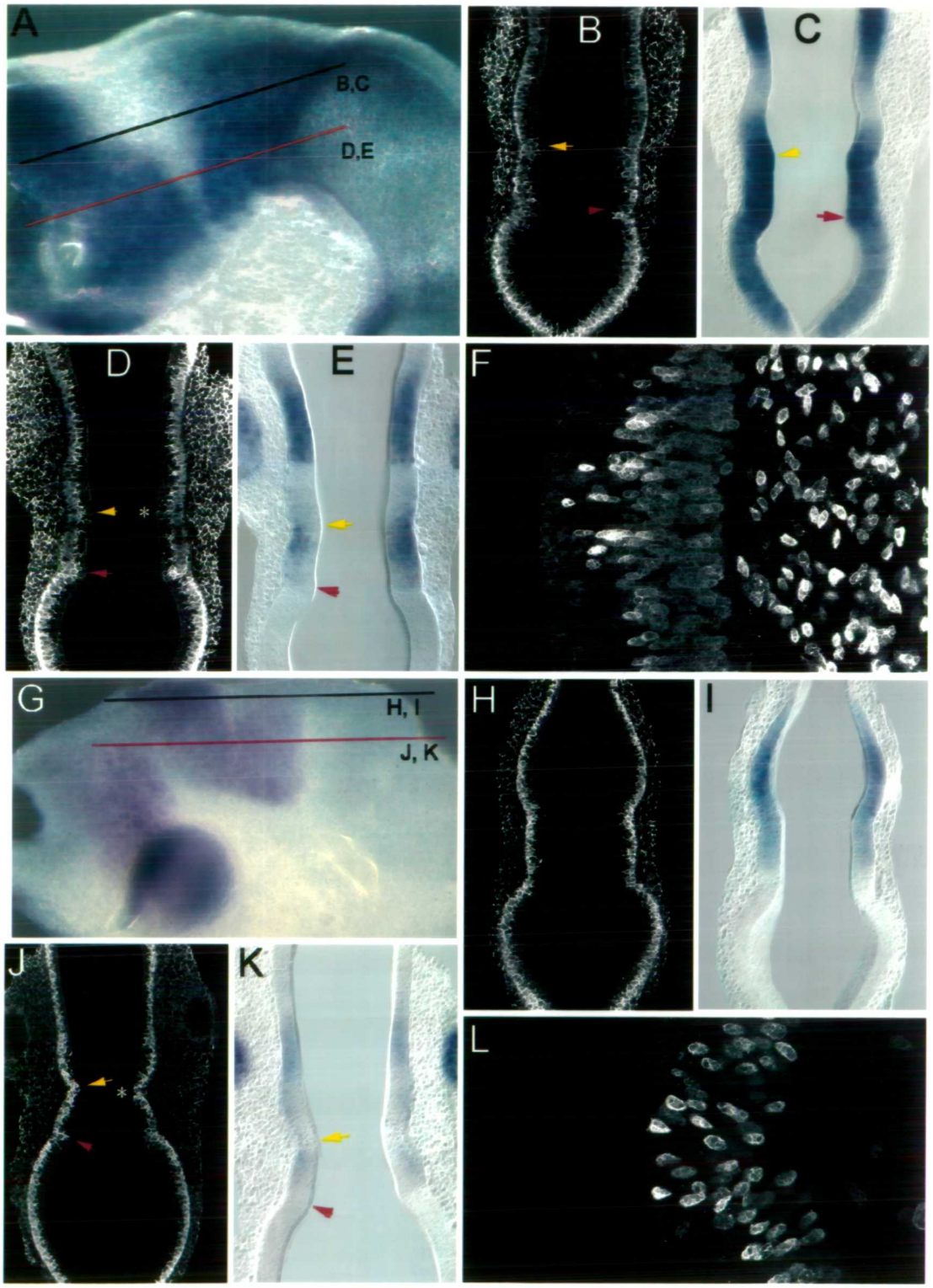

exhibited some low-level non-specific binding. To verify the wholemount staining, vibratome-sectioned material was also immunostained. This was carried out for NrCAM, CSPG and Tenascin antibodies, which all worked on vibratomed material. However, the Vimentin antibody did not show any specific staining on vibratome sections and this data is not shown.

Diencephalic boundaries were also examined for an increase in extracellular spaces utilising TEM, at HH 16 and HH 24. Since radial cells display a fan shaped morphology at hindbrain boundaries, DiI labeling at HH 18, 22 and 24 assessed morphology of radial cell structures in the diencephalic boundaries.

5.1 Apical-Basal position of cells during S-phase

At HH 14, S-phase nuclei are predominantly located at the pial side of the ventricular layer, although more apically located nuclei can be found randomly distributed within the entire neuroepithelium (Fig 17A). However, at HH 16 cells in S-phase are found near the ventricular surface in areas corresponding to boundary regions (Fig. 18). In coronal sections taken approximately from the middle of the embryo, S-phase cells are situated apically at the midbrain-diencephalic boundary and at the synencephalic-parencephalic boundary (Figs. 18D, J and L). The brightfield image (Fig. 18E) of the section shown in Fig. 18D shows that strong *L-fng* staining decreases just anterior to the synencephalic-parencephalic boundary and just posterior to the synencephalic-midbrain boundary. Comparison of the darkfield and brightfield images reveals that the apical S-phase cells are located exclusively within the area of strong expression.

In a ventrally located section taken just above the basal plate, apically localised S-phase cells are only observed at the synencephalic-midbrain boundary,as well as a few in the synencephalic-parencephalic boundary (Fig. 18B). In embryos horizontally sectioned at extreme dorsal levels, BrdU labeled cells are located predominately at the pial side throughout the diencephalon (Fig. 18H). Fig 18D and E also shows that there is no visible difference in the number of BrdU labeled cells in the *L-fng* positive and negative areas within the parencephalon. The BrdU studies indicate that apically located S-phase cells are not found within the two boundaries at extreme dorsal and ventral levels.

Figure 19

HH 19

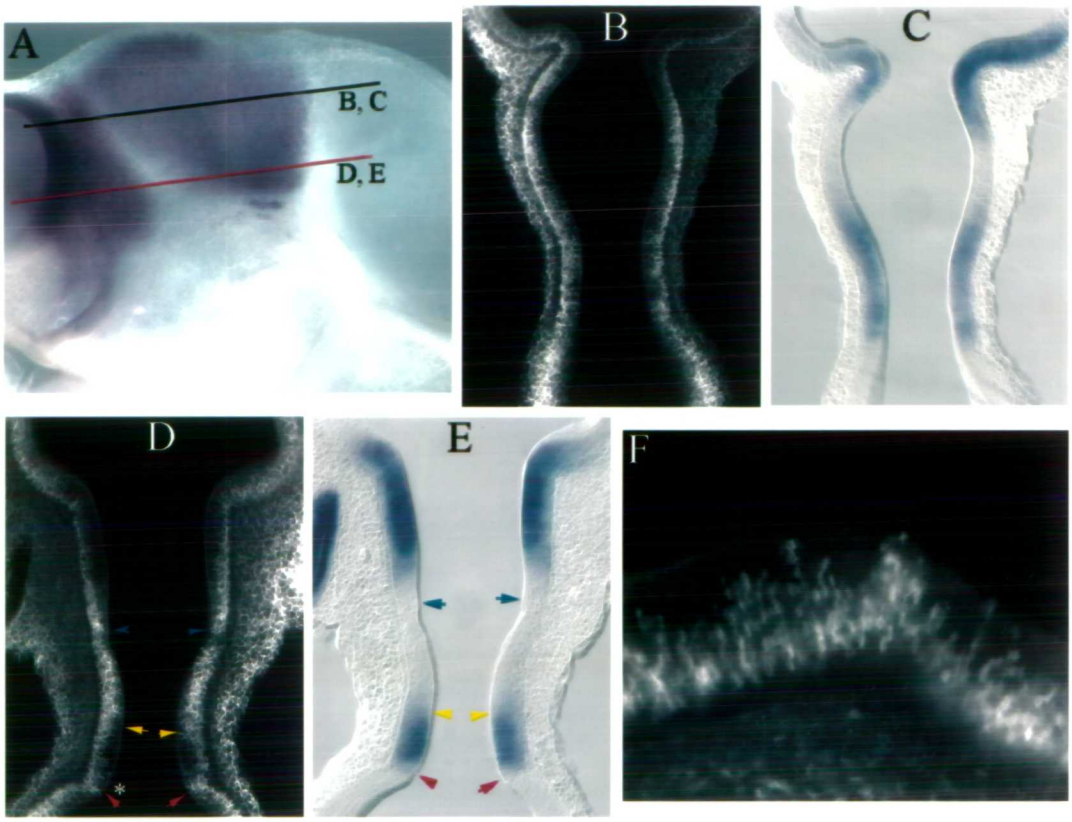

HH20

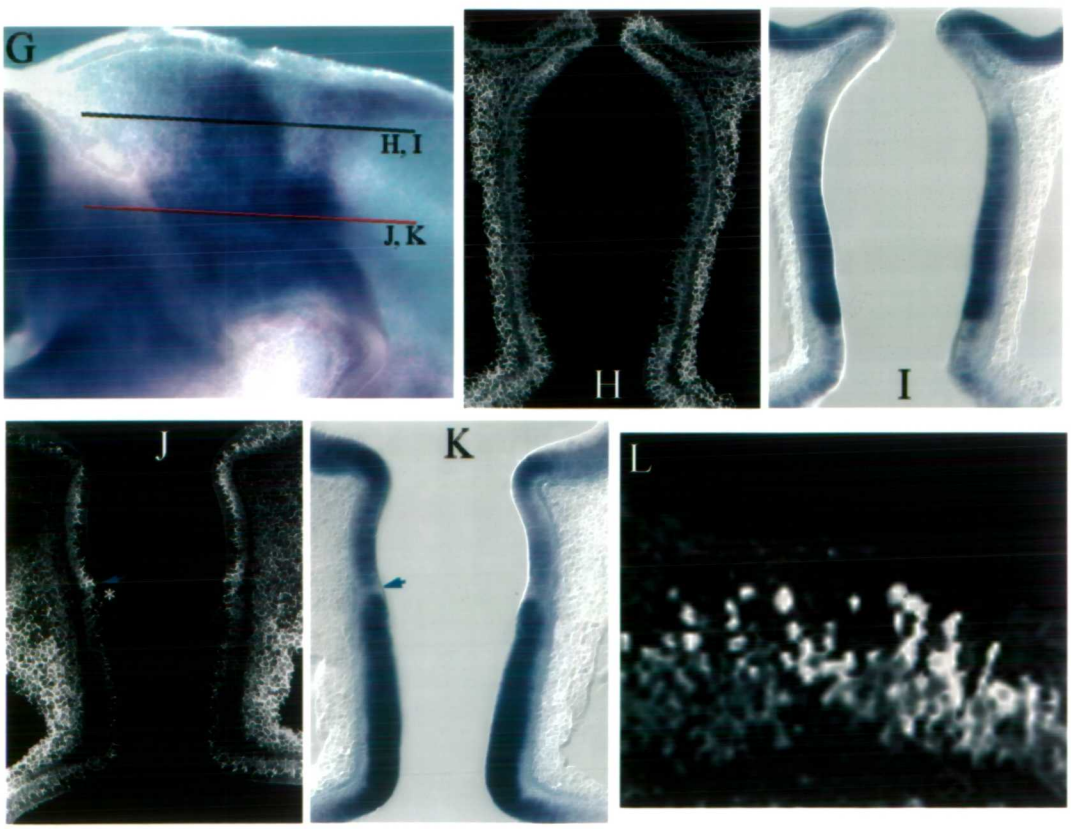

Figure 20

HH 21

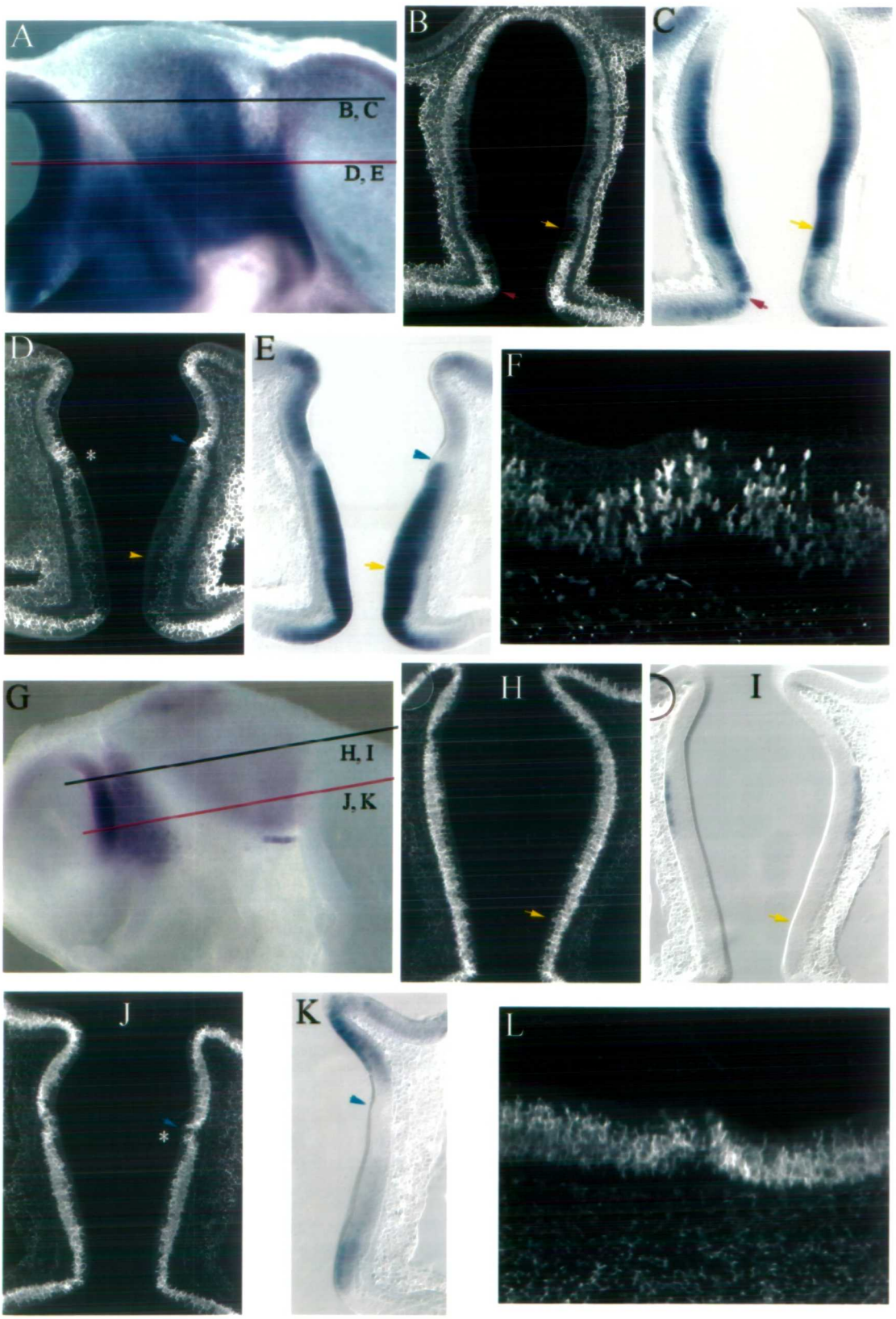

Furthermore the appearance of apical S-phase cells is not due to the angle of the section since embryos horizontal and coronal sections were obtained.

At HH 17 apically situated S-phase cells are still observed in both the midbrain-synencephalic boundary and the synencephalic-parencephalic boundary (Fig 17G-H). This is also the case for the midbrain-synencephalic boundary at HH 19, whereas S-phase cells are now predominantly located towards the pial side at the boundary between the parencephalon and the synencephalon, (Fig. 19B and D). At this stage the arrangement of S-phase cells in the dorsal thalamic neuroepithelium appears uniform. At HH 20 S-phase cells are located exclusively within the basal half of the neuroepithelium at dorsal levels (Fig. 19H) but aggregate apically in the area corresponding to the forming zli at ventral levels (Fig. 19J).

At HH 21 S-phase cells are observed close to the apical surface within the zli (Fig. 20D). At dorsal levels of the neural tube, S-phase cells are located predominantly towards the pial side throughout the diencephalon (Fig. 20B and H). However, at more ventral levels S-phase cells are seen both apically and basally within the neuroepithelium (Fig. 20D and J). S-phase cells appear to aggregate at the apical side within the rostral part of the zli ridge, whereas just posterior within the caudal aspect of the zli there is a line where there are few S-phase cells (Figs. 20D,F, J and L). Just posterior to the ridge another area of apically located S-phase cells can be seen, whereas S-phase cells are located towards the pial side throughout the rest of the diencephalon. At this developmental stage, S-phase cells are located primarily in the pial side of the neuroepithelium both at the parencephalic-synencephalic boundary and at the midbrain-synencephalic boundary. The apical position of S-phase cells at dorsal levels is observed immediately caudal to the posterior boundary of *Pax6* expression, which marks the midbrain-synencephalic boundary (Figs. 20J and K).

At HH 22 apically positioned BrdU labeled cells within the zli are observed at dorsal as well as ventral levels (Figs. 21B and D). S-phase cells are located towards the ventricular surface throughout the ridge and the area of few S-phase cells seems to have gone (Fig. 21F). In the remainder of the diencephalon S-phase cells are located towards the pial side of the neuroepithelium. Apically located S-phase cells are no longer seen at the synencephalic/midbrain boundary. Furthermore the distribution of S-phase cell in

Figure 21

HH 22

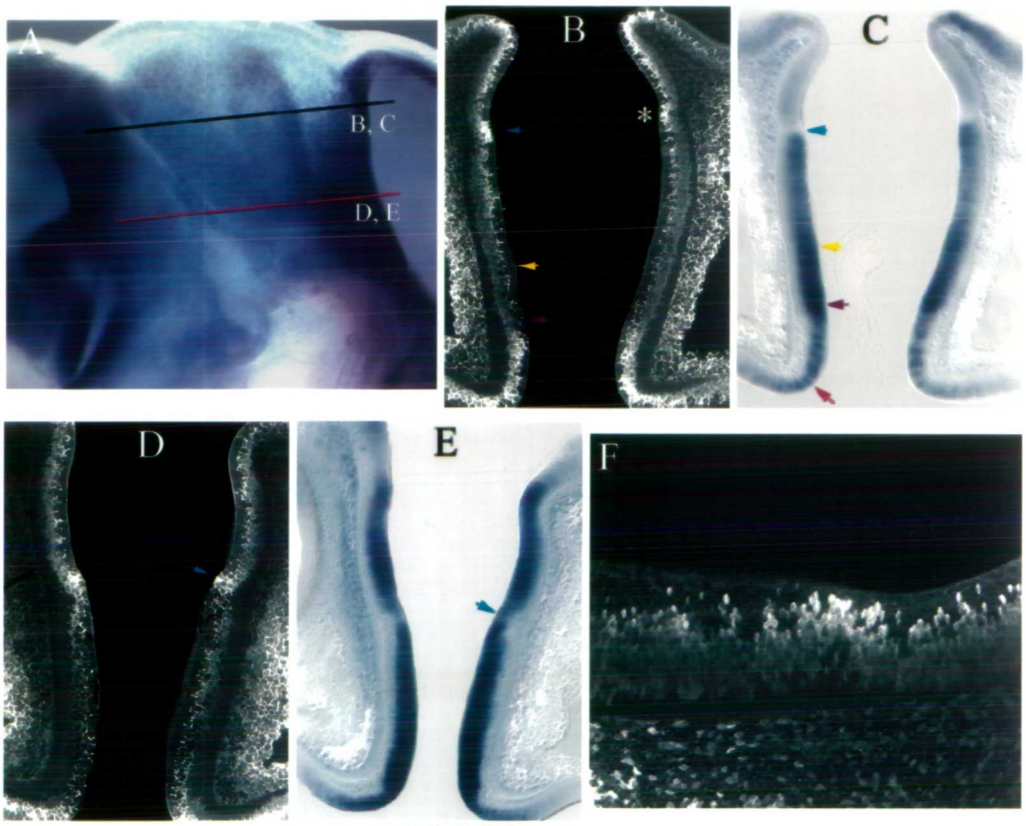

HH 24

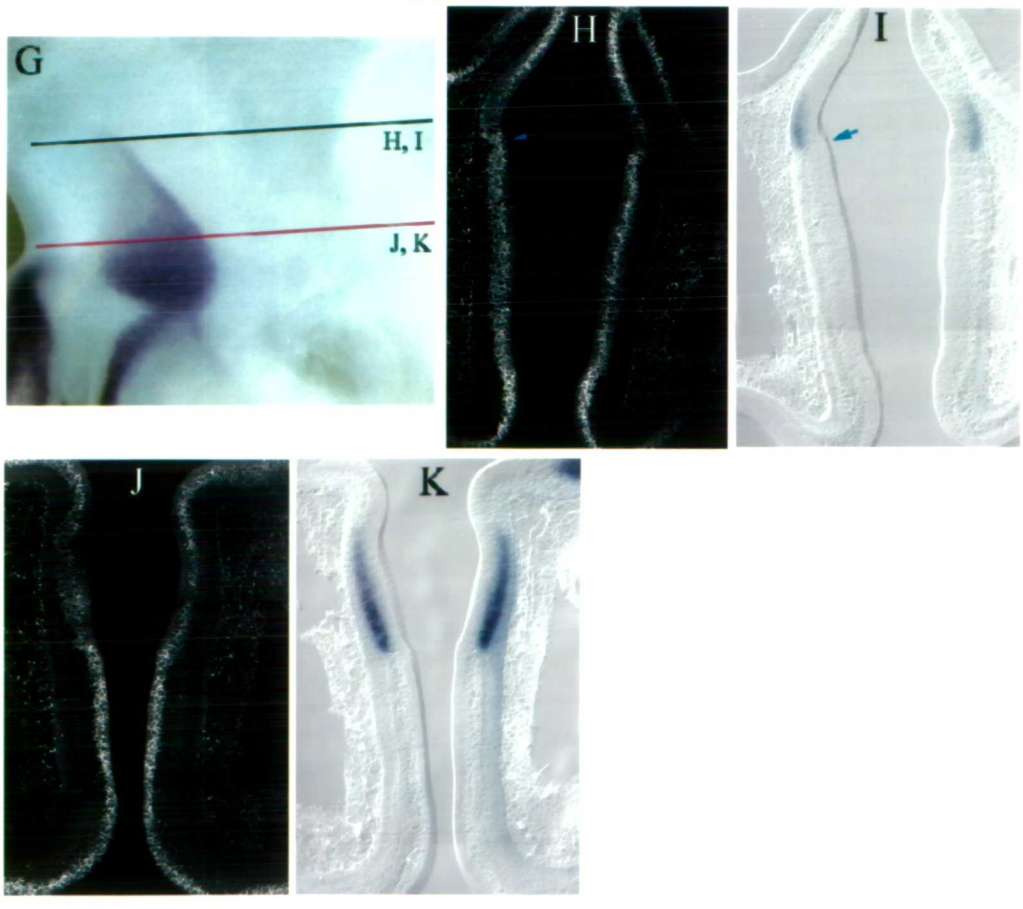

Figure 22

HH 26

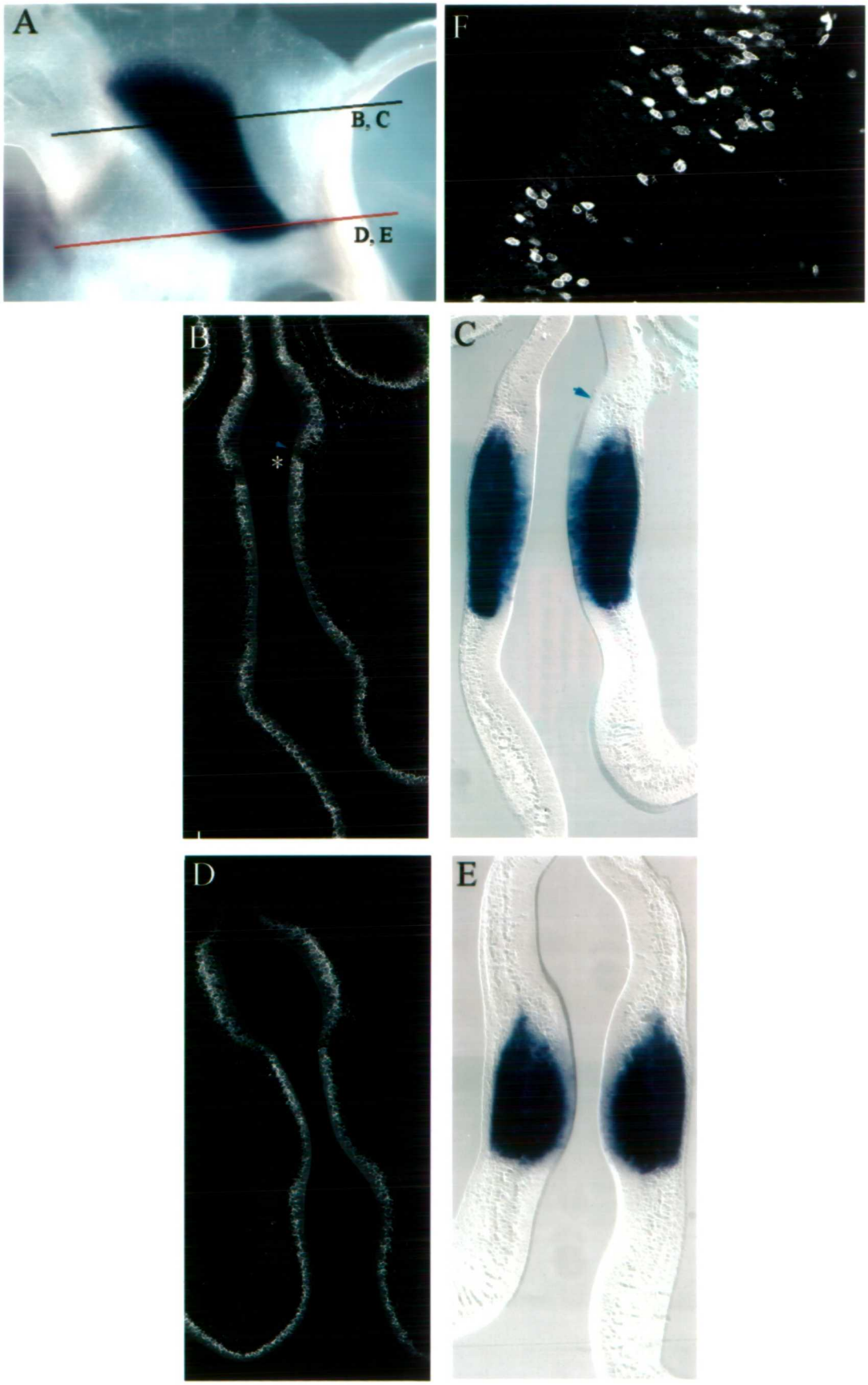

Figure 23

E 5.5

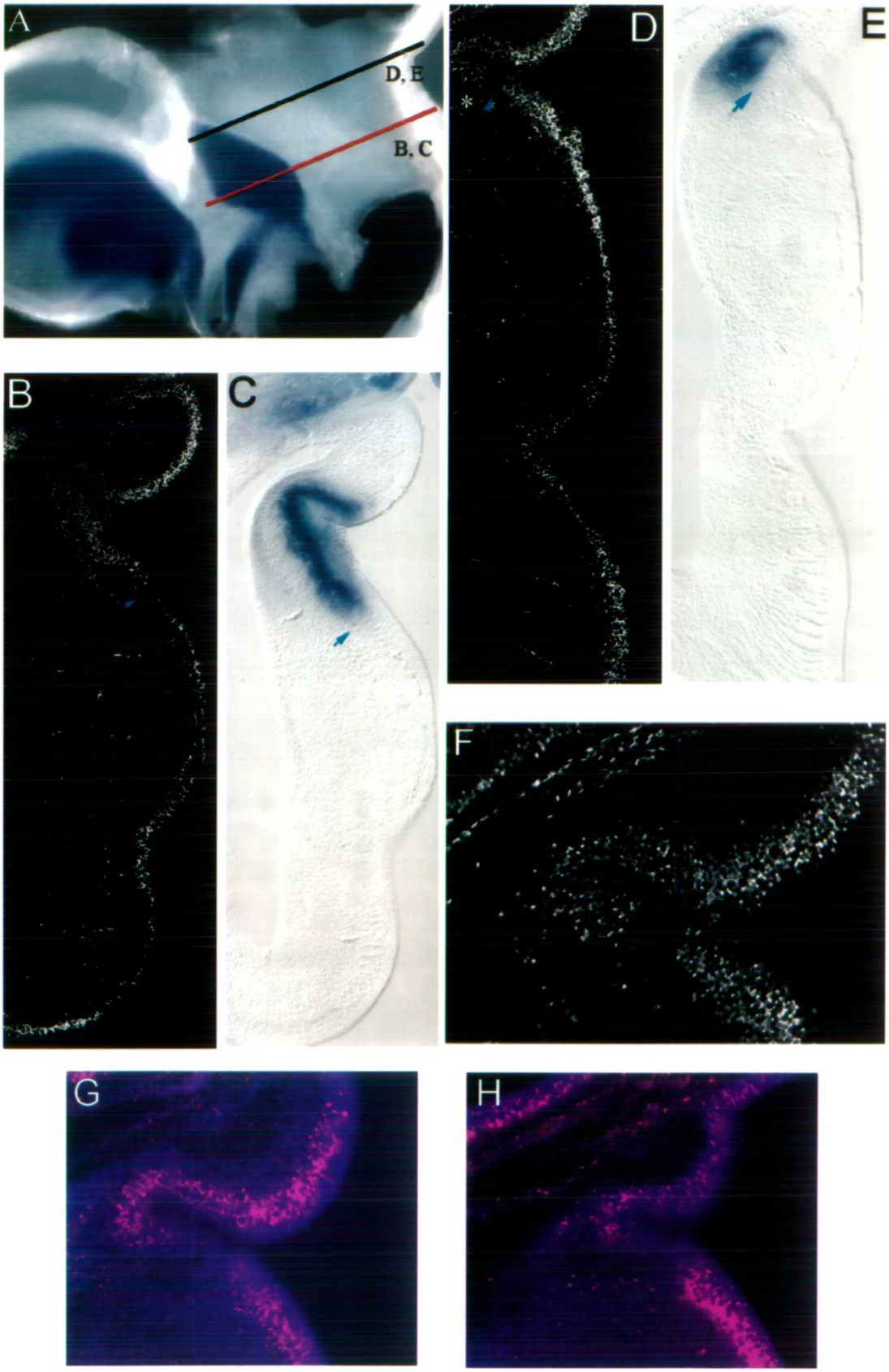

the intrasynencephalic boundary is identical to the adjacent neuromeres. At HH 23 (data not shown) and HH 24, the distribution of S-phase cells is similar to that seen at HH 22 (Fig. 21G-K). In the basal plate, S-phase cells are seen throughout the neuroepithelium.

The distribution of S-phase cells at HH 26 is similar to that seen at HH 22 and HH 24, except that cells in the zli have not taken up BrdU (Fig. 22B). BrdU labeled cells are absent from the apical and pial sides of the neuroepithelium at the zli, and this appears to extend through the whole ridge. However on both sides of this area, S-phase cells seem to extend towards the ventricular surface (Fig. 22F). The lack of S-phase cells within the zli is also apparent in embryos that have been labeled for four hours (data not shown). This may suggest that the rate of cell division has slowed down in the zli or perhaps stopped altogether. At ventral levels, S-phase cells are still present within the zli and exhibit the same distribution as those within the dorsal thalamus. In the rest of the diencephalon, S-phase cells are predominantly located towards the pial side, although the distribution appears to be more random with some cells located towards the ventricular side. However, these are individual cells and do not correspond to any of the other boundaries present at this developmental stage.

At E 6, BrdU labeled cells are still absent from the zli, adjacent and posterior to the caudal boundary of the *Dlx2* expression domain (Figs. 23D, E and F). S-phase cells are evenly distributed throughout the rest of the diencephalon, including the tissue adjacent to the zli (Figs. 23B and D). The distribution of S-phase cells reveals the extent of matrix exhaustion within the different neuromeres, particularly at more ventral levels. The ventricular zone within the posterior synencephalon only has a few S-phase cells, whereas there are comparatively more within the anterior synencephalon (Fig. 23B).

The dorsal thalamus appears to have fewer S-phase cells than both the anterior synencephalon and the ventral thalamus, whereas the latter exhibits a broad band of tightly packed BrdU labeled cells. At dorsal levels, the anterior part of the dorsal thalamus seems to have more S-phase cells than more posterior parts (Fig. 23D). The labeled cells seen within the mantle layer are located within blood vessels and may be blood cells that have taken up the BrdU, since birds have nucleated erythrocytes. The distribution of S-phase cells is similar in an embryo labeled for four hours (data not shown). DAPI staining, which labels all nuclei, in conjunction with anti-BrdU

Figure 24

CSPG

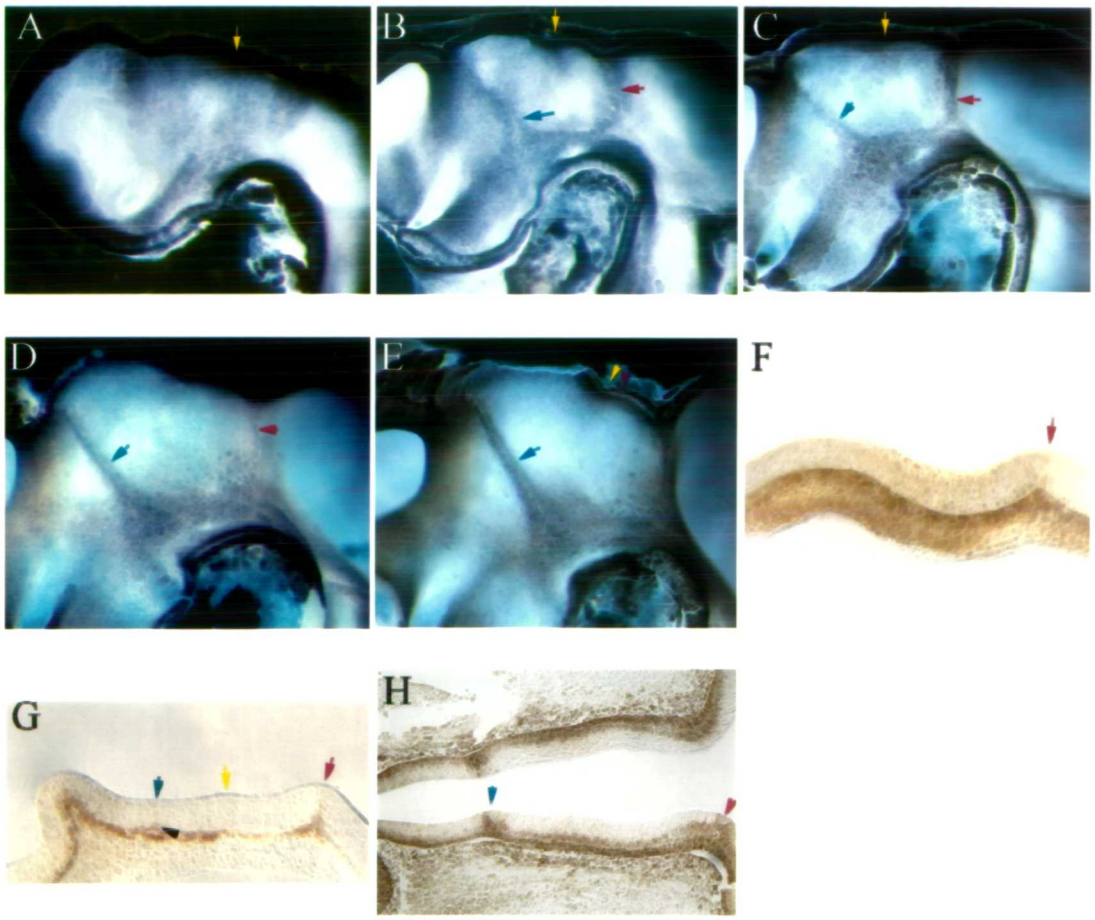

Tenascin

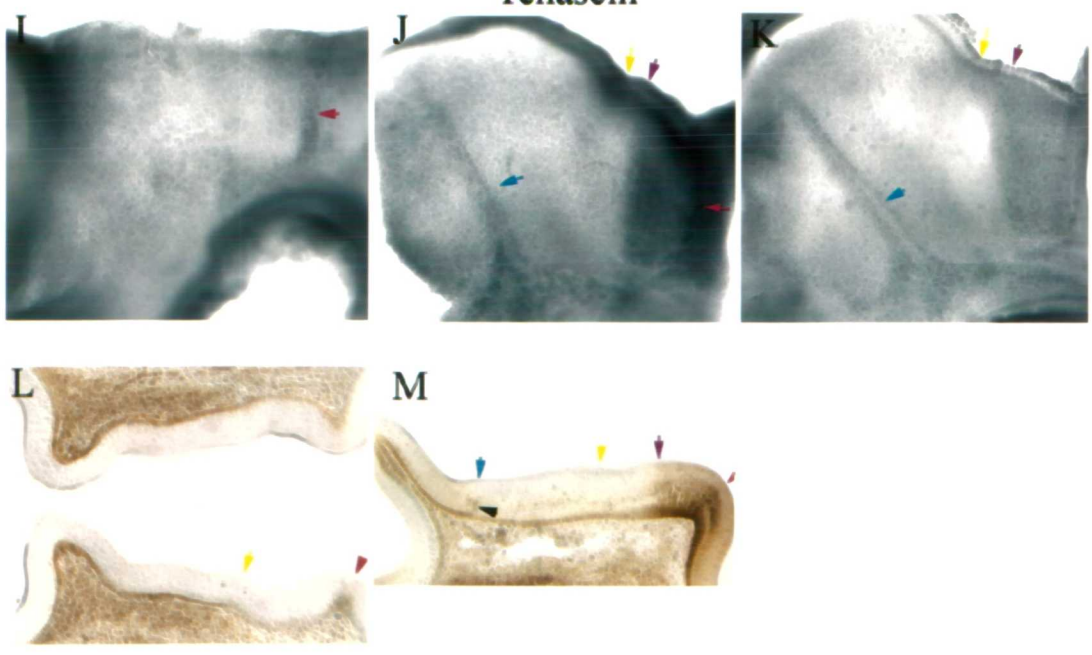

immunohistochemistry demonstrates that the lack of S-phase cells within the zli is not due to a lack of cells within the zli per se (Figs. 23G and H).

5.2 Localisation of cell adhesion and extracellular molecules

5.2.1 CSPG

CSPG is a secreted extracellular molecule, which is expressed throughout the nervous system in several species (Herndon and Lander, 1990; Kiang et al., 1981). In the chick diencephalon, CSPG immunolocalises to distinct regions at all the developmental stages analysed. As early as HH 16, CSPG staining is seen throughout the diencephalon (Fig. 24A), both within the mesenchyme and the neuroepithelium. From HH 16 to HH 19, CSPG immunolocalisation disappears from the neuroepithelium within the synencephalon and parencephalon and is found predominantly in boundaries (data not shown). By HH 19, CSPG is found in the zli and in the boundary between the synencephalon and midbrain as well as the basal plate (Fig. 24B).

CSPG immunolocalisation is seen along the entire dorso-ventral extent of the zli, although this domain is broader than the zli ventrally. The domain at the synencephalic-midbrain boundary is broad and appears to include some midbrain tissue as well. At the boundary between the synencephalon and the dorsal thalamus, CSPG is only found at the extreme dorsal aspect. CSPG is detected at the junction between the mesenchyme and the neural tube, and it extends towards the ventricular side of the ventricular zone at the boundary between the synencephalon and the midbrain (Fig. 24G). Immunostaining at this stage is seen within the ventricular zone in the ventral thalamus, but is absent in the zli, apart from a small area next to the mesenchyme, marked by a black arrow. .

At HH 20, the domains of CSPG immunostaining in the area of the zli and the synencephalic-midbrain boundary are narrower and appear exclusively within the boundary regions (Fig. 24C). The dorsal immunostaining at the dorsal thalamic-synencephalic boundary has disappeared. Over the next two stages, immunostaining becomes stronger at the zli and appears to be localised within the ridge (Figs. 24D and E). In contrast, immunostaining decreases at the synencephalic-midbrain boundary and by HH 22 only a thin line of immunostaining remains within the boundary. Patchy

expression of CSPG is also apparent in the ventral aspect of the posterior commissure as well as the extreme ventral aspect of the dorsal thalamus. Immunostaining is still seen in the basal plate. Horizontal sections reveal that CSPG staining is present throughout the marginal and mantle layers (Fig. 24G and H). There may also be some staining at the lateral part of the ventricular zone, whereas most of the ventricular zone does not exhibit any staining, except at the zli, and the synencephalic-midbrain boundary, where immunolocalisation is seen throughout the ventricular zone. CSPG is also found in the mesenchyme in a band next to the neural tube. The reason for the discrepancy between the wholemount staining and that seen in the section is likely to be due to a permeability of the tissue at these developmental stages in wholemount immunostaining. Antibodies may reach CSPG protein localised near the ventricular surface, but may not reach the marginal layer in the wholemounts. This emphasises the importance of performing immunocytochemistry on sectioned material as opposed to sectioning immunostained embryos.

5.2.2 Tenascin

Tenascin is an extracellular matrix glycoprotein (Chiquet-Ehrismann et al., 1986) and is expressed in the CNS during development (Erickson and Bourdon, 1989). In the diencephalon, Tenascin is found in the mesenchyme and in restricted areas of the ventricular zone. Immunolocalisation of Tenascin is not observed until HH 18 where a band of staining appears at the synencephalic-midbrain boundary (Fig. 24I). Immunostaining within the ventricular zone is exclusively seen at this location, whereas the rest of the neuroepithelium was devoid of staining (Fig. 24L).

By HH 22, low amounts of Tenascin are also seen at the zli, whereas stronger staining is observed within the posterior synencephalon as well as at the synencephalic-midbrain boundary (Fig. 24J). In ventral sections, the staining seen in the posterior synencephalon spreads throughout the ventricular zone, whereas the ventricular zone within the anterior synencephalon and the dorsal thalamus is devoid of staining (Fig. 24M). Within the latter two regions a line of faint immunostaining can be seen at the border between the ventricular zone and the mantle layer. Stronger staining is seen within the mantle layer of the zli. Tenascin is also detected in the basal plate at HH 22. By HH 24, immunolocalisation of Tenascin has decreased in all domains.

Figure 25

NrCAM

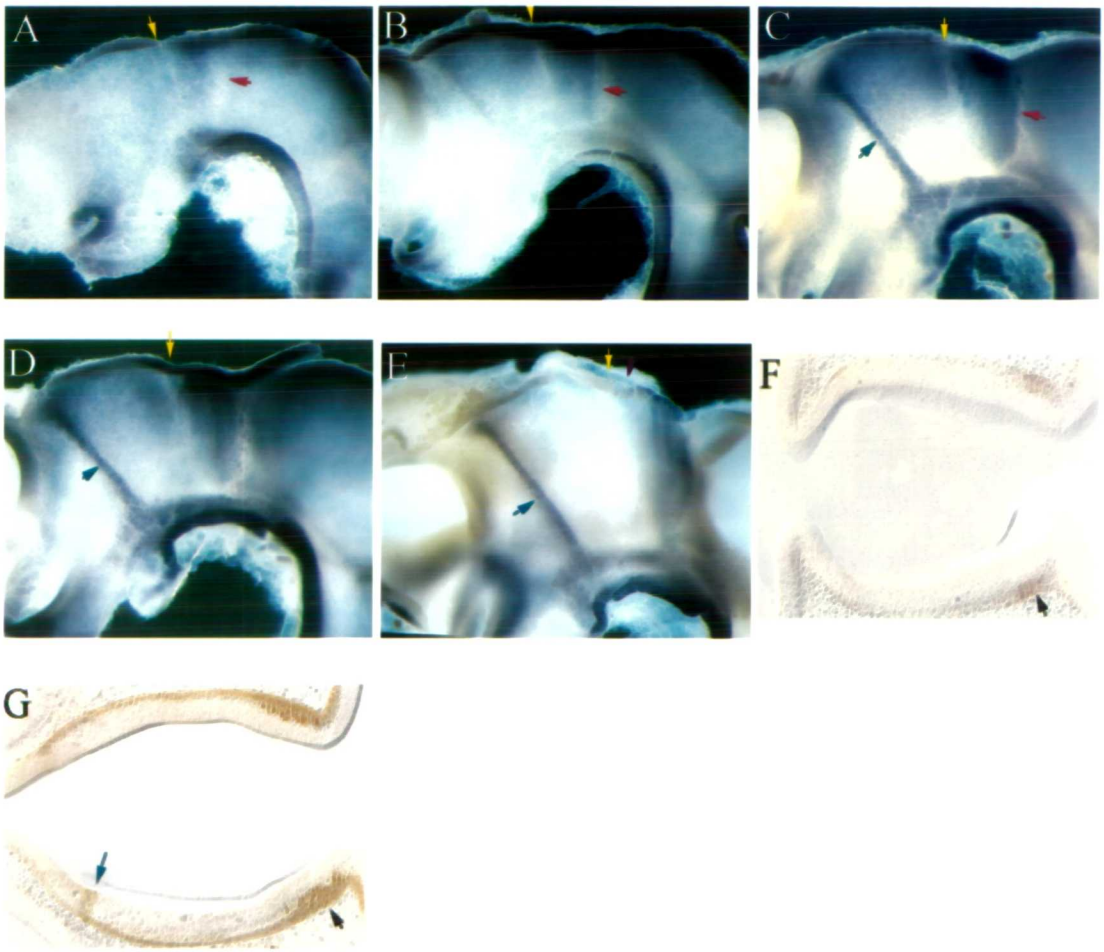

Vimentin